AFCRL-65-877

DEVELOPMENT OF BALLUTE FOR RETARDATION OF ARCAS ROCKETSONDES

J.J. Graham, Jr.

GOODYEAR AEROSPACE CORPORATION
AKRON, OHIO

CONTRACT AF-19(628)-4194
PROJECT NO. 6682
TASK NO. 668206

FINAL REPORT
DECEMBER 1965

PERIOD COVERED: MAY 1964 TO DECEMBER 1965

Prepared for

AIR FORCE CAMBRIDGE RESEARCH LABORATORIES
OFFICE OF AEROSPACE RESEARCH
UNITED STATES AIR FORCE
BEDFORD, MASSACHUSETTS

ABSTRACT

Goodyear Aerospace Corporation has completed a design and development program for a BALLUTE[a] retardation system for Arcas rocket-launched meteorological instruments. Various BALLUTE configurations were fabricated, tested, and evaluated in four stages: airdock drop tests; low-altitude helicopter drop tests; high-altitude balloon-borne drop tests; and rocket-launched flight tests at Cape Kennedy. The program culminated in three successful rocket-launched flights of the final configuration which, because of the high stability of the system, yielded telemetered temperature data of unprecedented quality. The BALLUTE system that meets the design goals of reliability, stability, descent rate, and cost will be made of fractional mil plastic film, will be about 16-1/2 ft in diameter, and will weigh about two pounds. Further development and system qualification testing are recommended prior to incorporation of the BALLUTE into the operational sounding system.

[a]TM, Goodyear Aerospace Corporation, Akron, Ohio.

TABLE OF CONTENTS

LIST OF ILLUSTRATIONS

LIST OF TABLES

SECTION I

INTRODUCTION

1. GENERAL

Under Contract AF19(628)-4194 to Cambridge Research Laboratories, Office of Aerospace Research, Goodyear Aerospace Corporation (GAC) has designed and tested a new retardation device for an Arcas rocket-launched meteorological telemetry payload. This rocketsonde meteorological sounding system is currently used operationally as part of the Meteorological Rocket Network (MRN) and constitutes the primary source of high-altitude atmospheric data obtained on a continuing basis.

The mission of the rocketsonde system is (1) to measure the temperature of the atmosphere between 220,000 ft and 80,000 ft and to transmit these data to a ground station and (2) to define the ambient winds by the lateral motions of the descending system recorded by skin-tracking radar or by the GMD-2 tracking set when a transponder is included in the radiosonde. Temperature data are used to define the density profile of the atmospheric segment sampled.

The Arcas rocket is capable of boosting a meteorological instrument to an apogee altitude of about 220,000 ft. At apogee, the instrument is separated from the rocket motor and begins a sampling mission decelerated and stabilized by the retardation device.

2. PERFORMANCE

For accurate temperature readings, the descent must be as slow as possible to eliminate aerodynamic-heating effects on the thermistor sensor. Since the air temperature is affected by the sensor's thermal mass, that the thermistor be exposed only to air that has not been preheated or

otherwise disturbed is extremely important. This requires a stable, nonoscillating descent.

In addition to thermal accuracy, stability is mandatory for the proper operation of the telemetry module. Signal dropout and excessive RF noise have been related to unstable flight.

High-altitude wind sensing has long been a problem in meteorological technology because of two related inadequacies of the sensing devices - that is, instability and slow response.

In the Arcas rocketsonde system, the wind data obtained are based on the premise that lateral excursions of the descending instrument are identical to the magnitude and velocities of the winds. The wind data are, therefore, only as valid as this premise is accurate.

If the radiosonde system is not stable at zero angle of attack and descends in an oscillating, coning, or gliding manner, the efficiency of the system as an aerodynamic drag body varies according to its angle of attack, introducing variables both in vertical-descent rate and in lateral-wind response. If the radiosonde system descends in a gliding manner, the error is cumulative.

Since winds usually are variable in both velocity and direction rather than constant for even short periods, the system's ability to respond to these shifts in speed and direction is also critical. If the system is unstable and at an angle of attack, the effect of lateral-wind acceleration can appear as both lifting and as drag forces. Even if the system is stable, a lag between the acceleration or deceleration of the wind and the resultant motion of the system exists. It is obvious, therefore, that a system of minimum mass presenting maximum drag area to the composite airflow would minimize the error-causing lag.

The retardation device in current use on the operational rocketsonde is a conventional parachute. Because of effective instability at varying degrees of inflation at the flight's upper portions, a new deceleration and stabilization device was required.

The performance of the retardation device to be developed by GAC is defined contractually in four design goals:

1. Reliability - performance in 98 percent of all flights
2. Stability - oscillations less than ±3 deg
3. Descent rate - less than 300 fps at 180,000 ft
4. Cost - less than $200 per unit in lots of 500

3. RESULTS

The development effort has been completed and was culminated by three successful operational flights at Cape Kennedy. In each case the BALLUTE[a] performance was as anticipated. Stability was excellent, resulting in temperature data of a far better quality than any previously recorded at high altitudes. The feasibility of meeting the descent rate requirements was clearly established. The opportune recovery, intact, of two of the three systems verified the adequacy of the structural integrity of all components. The work in the area of materials and fabrication techniques indicates that the target unit costs in production lots can be achieved by using proper tooling and semiautomated production techniques.

[a]TM, Goodyear Aerospace Corporation, Akron, Ohio.

SECTION II

SYSTEMS ANALYSIS

1. AERODYNAMIC ANALYSIS

a. General

The first step in designing the decelerator is to establish the ballistic coefficient W/C_DA, which yields a terminal descent velocity of 300 fps at an altitude of 180,000 ft.

Since W/C_DA = q (dynamic pressure) at terminal velocity and

$$q = \frac{\rho V^2}{2},$$

by substituting the desired velocity of 300 fps and the value of ρ at 180,000 ft,

$$q = \frac{1.2 \times 10^{-5} \times (300)^2}{2}$$

$$= 0.054 \text{ psf}$$

and W/C_DA = 0.054 psf.

The weight of the payload as defined in the contract is seven pounds. Assuming the decelerator weighs two pounds, the effective drag area is determined, as follows:

$$\frac{W}{C_DA} = \frac{7 + 2}{C_DA}$$

$$= 0.054$$

and

$$C_D A = \frac{9}{0.054}$$

$$= 167 \text{ sq ft}$$

The decelerator for the Arcas radiosonde system was to be one of several types of BALLUTEs, each with its own drag coefficient value. For this reason, the size of the BALLUTE was indefinite at this time.

For this report, the reference area (A) used in the drag formula is the hydraulic area of the inflated BALLUTE, that is, the area of a sectional plane at the maximum diameter.

The BALLUTE configurations under consideration for this application had been tested previously for other missions. Configuration C_D values had been established from 0.8 to 1.2. If, therefore, the $C_D A$ required is 167 sq ft, approximate BALLUTE sizes can be determined:

where $C_D = 0.8$,

$$A = \frac{167}{0.8}$$

$$= 209 \text{ sq ft, or } 16.3\text{-ft diam;}$$

where $C_D = 1.0$,

$$A = 167 \text{ sq ft, or } 14.6\text{-ft diam;}$$

where $C_D = 1.2$,

$$A = \frac{167}{1.2}$$

$$= 139 \text{ sq ft, or } 13.1\text{-ft diam}$$

b. Weight and Volume Requirements

An examination of the weight and volume requirements for a BALLUTE system about 15-ft diam now showed that the assumed two pounds should be adequate and that the BALLUTE could be packaged in the

existing parachute container. The target $W/C_DA = 0.054$ would provide the acceptable descent rate, but the goal was to descend as slowly as possible. Slightly larger BALLUTEs and consequently lower W/C_DA values seemed at this time practicable; therefore, computer analyses for system trajectories with $W/C_DA = 0.049$ psf and 0.037 psf were run. The initial, or apogee, conditions used were furnished by the Air Force Cambridge Research Laboratories (AFCRL) and represent the minimum, maximum, and nominal deployment altitudes.

In each case, inflation time is assumed to be six seconds. The drag area of the BALLUTE increases linearly from zero at time zero to maximum at T + 6 sec. Programs were run for ballistic coefficients of 0.049 psf and 0.037 psf.

Initial conditions for the analyses are given below:

Case I

Weight = 9 lb
Altitude = 214,000 ft
Mach no. = 0.71
Horizontal velocity = 711 fps
Vertical velocity = 0
C_DA = 185 sq ft (at T + 6 sec)

Case II

Weight = 9 lb
Altitude = 214,000 ft
Mach no. = 0.71
Horizontal velocity = 711 fps
Vertical velocity = 0
C_DA = 241 sq ft

Case III

Weight = 9 lb

Altitude = 197,000 ft
Mach no. = 0.70
Horizontal velocity = 737 fps
Vertical velocity = 0
C_DA = 185 sq ft

Case IV

Weight = 9 lb
Altitude = 197,000 ft
Mach no. = 0.70
Horizontal velocity = 737 fps
Vertical velocity = 0.
C_DA = 241 sq ft

Case V

Weight = 9 lb
Altitude = 194,000 ft
Mach no. = 0.84
Horizontal velocity = 886 fps
Vertical velocity = 0
C_DA = 185 sq ft

Case VI

Weight = 9 lb
Altitude = 194,000 ft
Mach no. = 0.84
Horizontal velocity = 886 fps
Vertical velocity = 0
C_DA = 241 sq ft

The significant characteristics of the six trajectories are presented in Figures 1, 2, and 3.

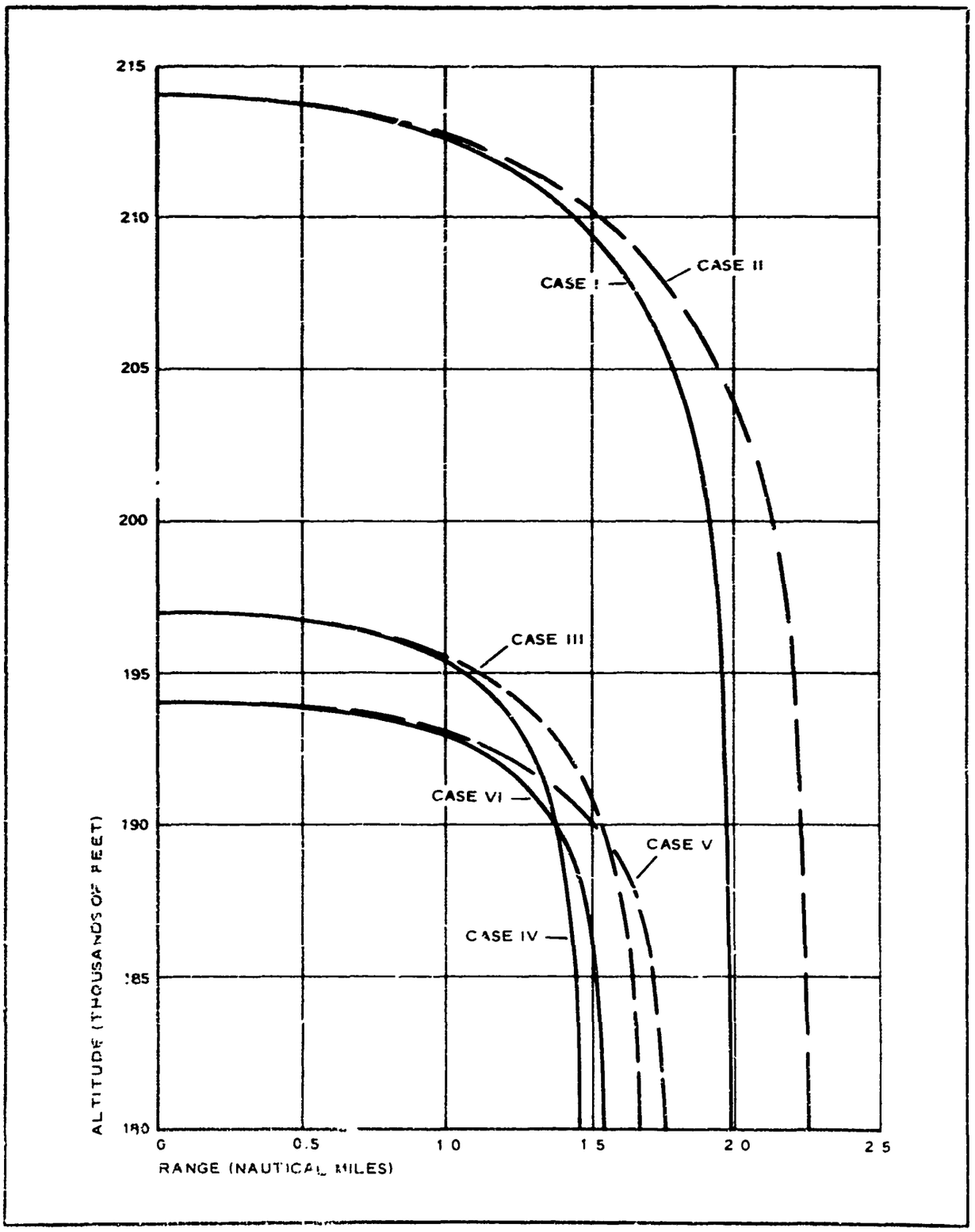

Figure 1 - Analysis of Trajectories (Altitude versus Range)

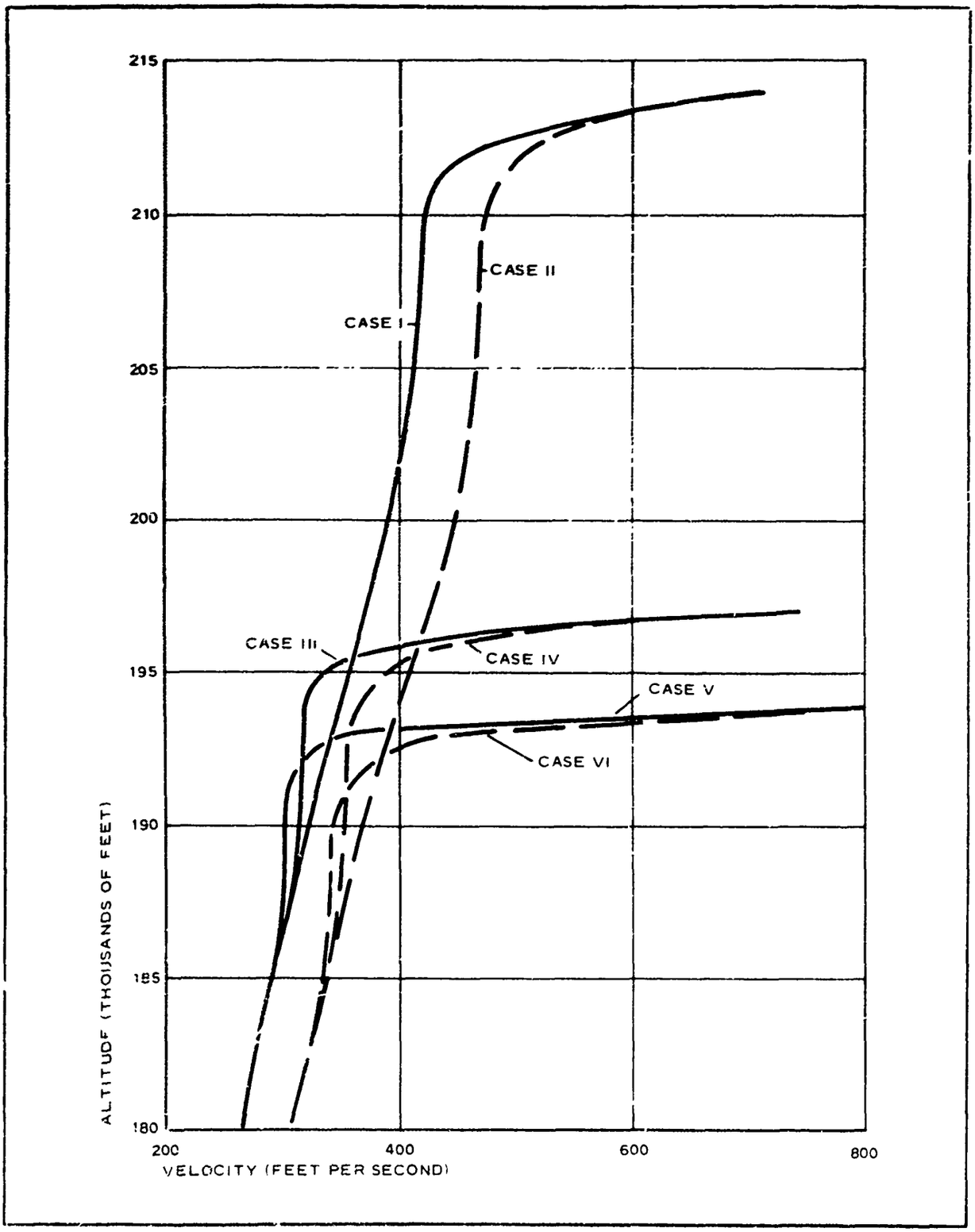

Figure 2 - Analysis of Trajectories (Altitude versus Vertical Velocity)

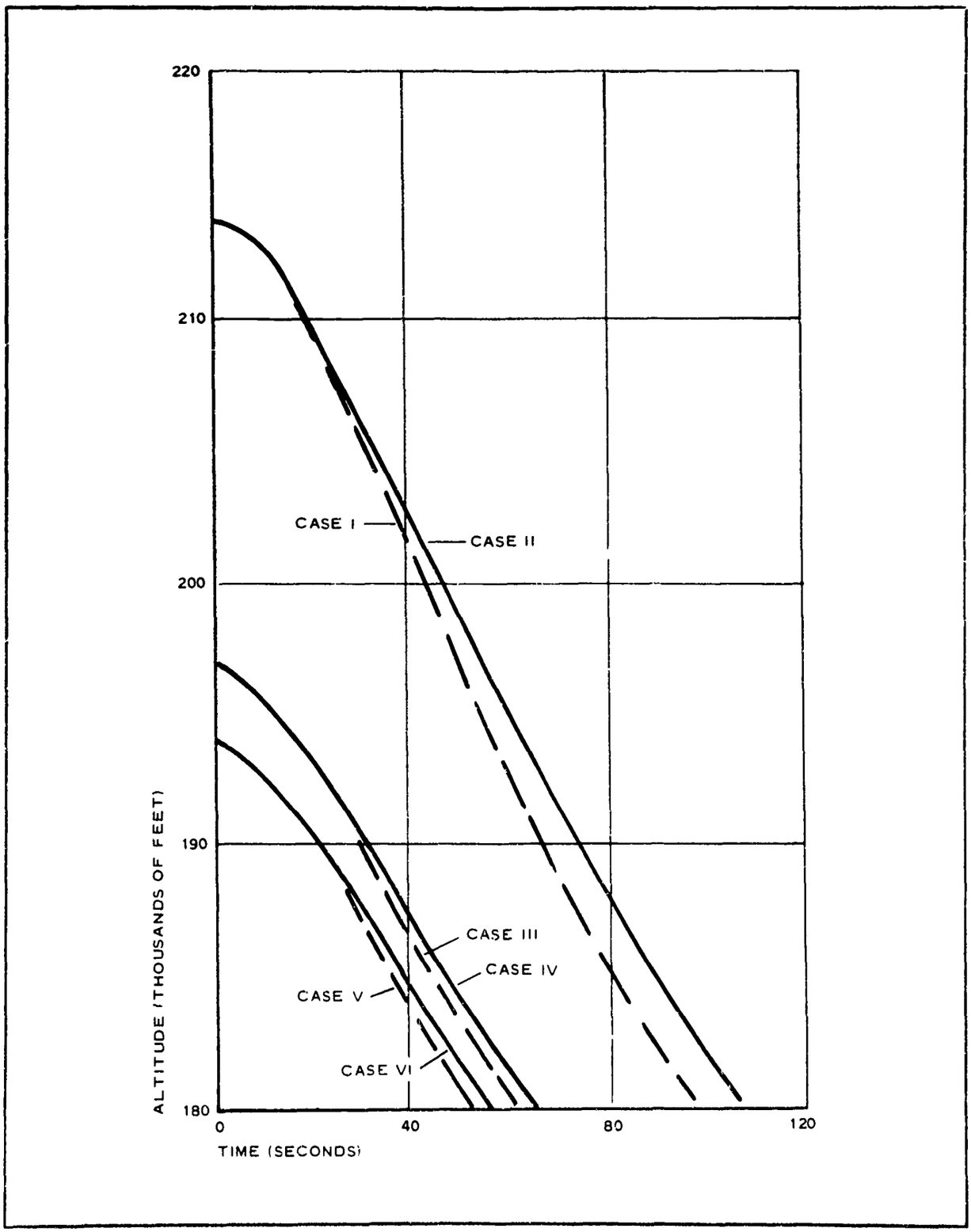

Figure 3 - Analysis of Trajectories (Altitude versus Time)

2. DESIGN ANALYSIS

For development purposes, minimum modification to the existing rocketsonde system and maximum use of the parachute system's hardware components were to be the guidelines in the physical design of the system. The preliminary design, therefore, used the existing forward closure plate as the basic BALLUTE-instrument interface.

To ensure reliable performance, the following design criteria were established:

1. **Positive mechanical erection and orientation of the ram-air inlet into the air stream**
2. **Structural coupling of the BALLUTE and instrument to eliminate a relative pendulum action**
3. **Sufficiently small inlet size to reduce initial inflation stresses on the BALLUTE material**
4. **Use of high-tensile-strength materials that were suited to economic fabrication techniques**
5. **Gore pattern sizes compatible with standard material stock widths**
6. **Arranging components to allow the use of conventional BALLUTE-packing techniques**

The major components of the prototype design for the burble-fence BALLUTE are shown in Figure 4.

The second design goal was stability. In most BALLUTE work preceding this effort, the aerodynamic environment was either supersonic or in the upper subsonic levels. At these higher velocities, the stability of the BALLUTE was within the ±3-deg oscillation envelope. For the rocketsonde application, however, testing of the various types of BALLUTEs at low ballistic coefficients and Reynolds numbers appeared mandatory to confirm stability.

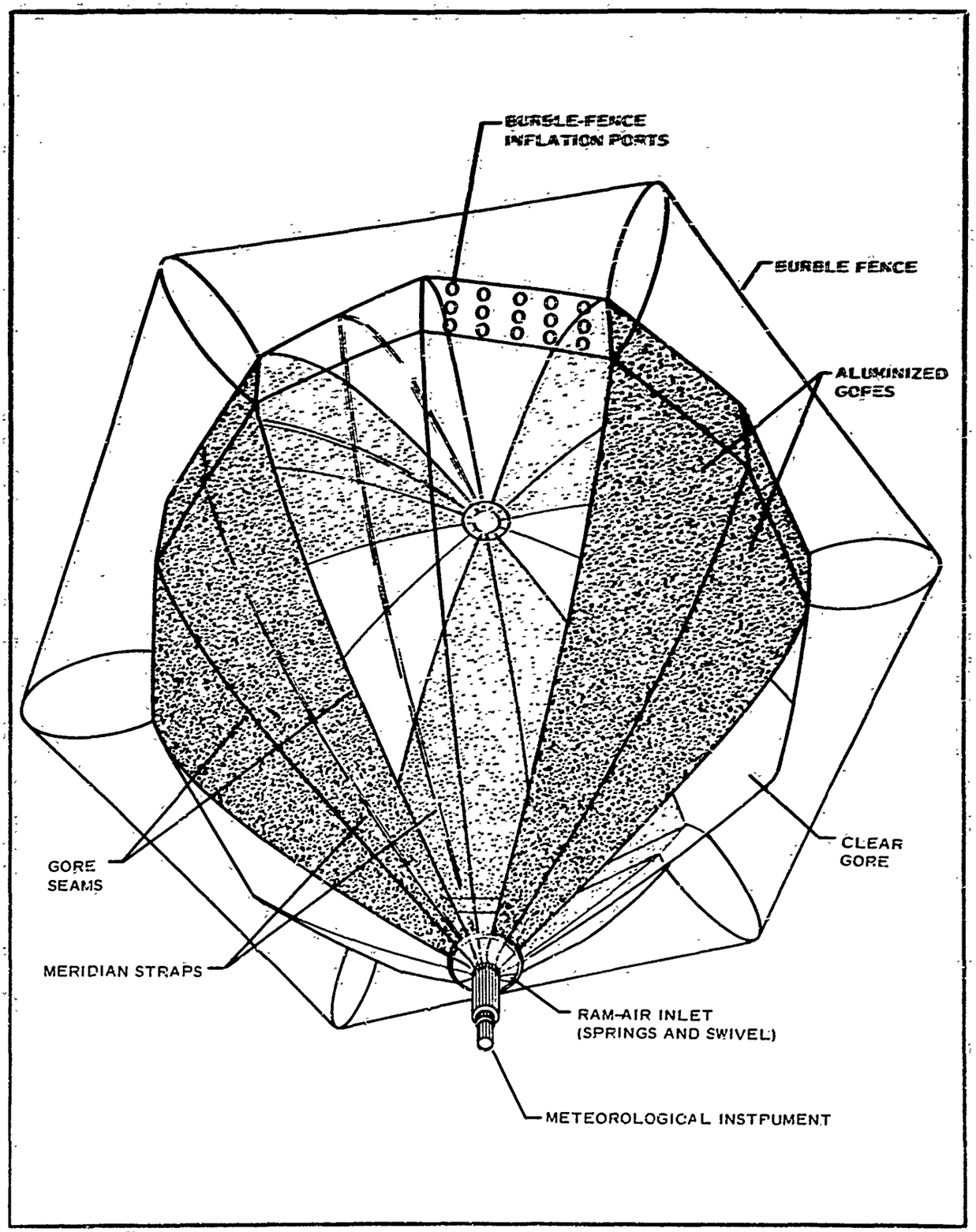

Figure 4 - BALLUTE Schematic with Nomenclature of Major Components

The three basic BALLUTE types chosen as candidates for the mission at hand were the tucked-back, burble-fence, and partitioned BALLUTEs shown in Figures 5 through 7.

3. ENVIRONMENTAL ANALYSIS

To ensure reliability of the BALLUTE, a review was made of the critical environmental conditions to be encountered during the logistic and operational cycles. The BALLUTE must be capable of withstanding these conditions:

1. Humidity and temperature changes resulting from normal transportation and storage
2. Long periods packaged and folded under high pressure
3. Compression loading of BALLUTE material at launch
4. Aerodynamic heating of BALLUTE canister section during ascent and resulting conductive heating of BALLUTE material
5. Burning of BALLUTE material at deployment, which results from flash of the pyrotechnic separation device
6. Rapid temperature change of BALLUTE material at deployment, from canister temperatures to low temperature of the atmosphere at apogee altitudes
7. The effects of the residual-trapped air within the BALLUTE and the amount of initial inflation due to this phenomenon

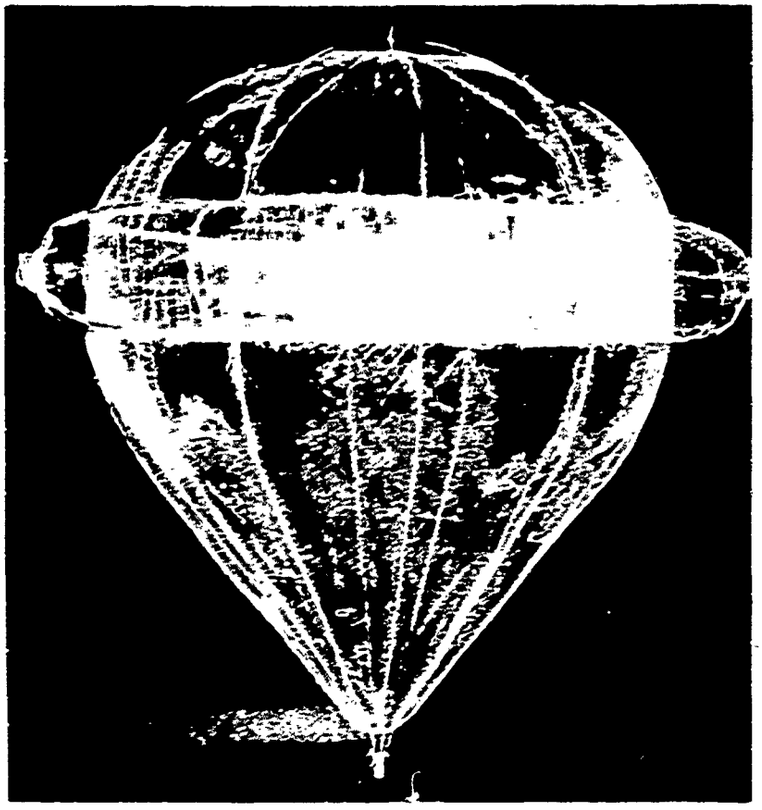

Figure 5 - Four-Foot-Diameter Isotensoid BALLUTE with 10-Percent Toroidal Burble Fence

Figure 6 - Five-Foot-Diameter Partitioned BALLUTE

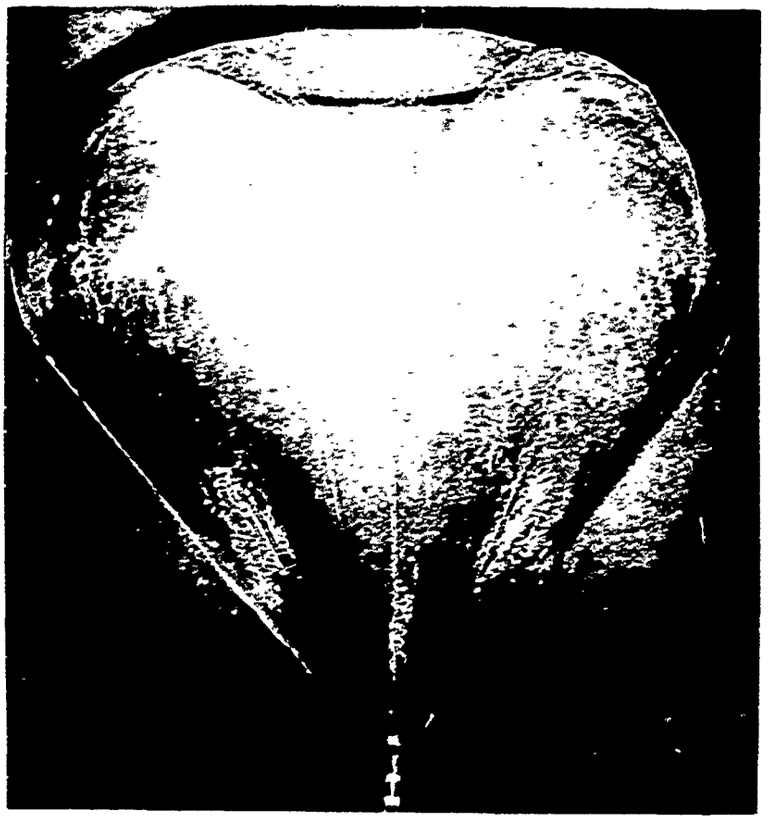

Figure 7 - Four-Foot-Diameter Tucked-Back BALLUTE

4. STRUCTURAL ANALYSIS

a. Preliminary Stress Analysis

(1) General

The BALLUTE is designed to decelerate a seven-pound payload traveling at high altitude but at a velocity slightly below Mach 1. The dynamic pressure has a low value of 0.2 psf, which results in a large (16-ft-diam) lightweight device. Preliminary estimates of the drag load and the resulting meridian stress at the nose attachment circle indicate that the thinnest nylon film available has more than adequate strength, and that no reinforcement is necessary in the meridian direction. At all other locations, stresses are lower still. The problem, therefore, is to

obtain a device with the least-possible surface area and one that can be fabricated at a minimum cost.

(2) Plain-Back Model

For simplicity, no center cord is used in the plain-back model; the rear of the BALLUTE is a constant pressure surface that has no axial load at the center. The minimum area surface is one that has zero hoop stress throughout. This surface is the curve for k = 1 in Figure 5 of an AIAA paper by N. E. Houtz.[a] The BALLUTE is formed by an 80-deg cone tangent to a spherical surface. The loads and dimensions are shown in the sketch below:

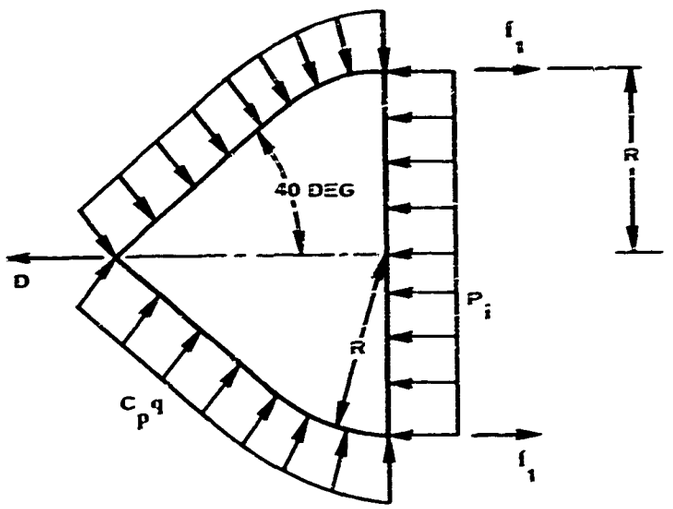

The drag coefficient is estimated to be 0.9, which gives $D = 0.9qR^2$. C_P is approximated by a constant value of 0.4 and P_1 is estimated to be 1.3q. Summing forces horizontally gives

$$2\pi Rf_1 + 0.4q\pi R^2 = 0.9qR^2 + 1.3q\pi R^2$$

or

[a]Houtz, N. E.: "Optimization of Inflated Drag Devices by Isotensoid Design," AIAA paper No. 64-437, 1st Annual AIAA Meeting, Washington, D.C., June 29 to July 2, 1964.

$$\frac{2f_1}{qR} = 1.8 .$$

The membrane equation gives

$$\frac{f_1}{R} + \frac{f_2}{R} = q(1.3 - 0.4) .$$

Substituting for f_1 gives,

$$\frac{f_2}{R} = 0 .$$

The radius, R, of the arc is therefore the smallest radius that will allow a wrinkle-free surface under load.

The burble fence has a height of 10 percent of the nominal diameter, 2R. The fence should be firmly inflated to function most effectively; the fence, therefore, is assumed to have a uniform stress in both directions throughout its surface. For analysis, the fence's external loading is approximated by one constant value of 0.4q from the equator forward and another constant value of -0.2q from the equator aft. The fence can be formed by two of the constant pressure isotensoid curves of Mr. Houtz's Figure 7.[a] The curve for $\rho_r = 0.8$ for the rear of the fence gives approximately the desired height. Equation 23 from N. E. Houtz's AIAA paper[a] gives

$$\frac{2f}{1.5qR_b} = 1 - 0.8$$

$$= 0.2$$

or

$$\frac{2f}{qR_b} = 0.3 ,$$

[a] Op. cit.

where R_b is the radius to the top of the fence. Equation 24 from N. E. Houtz gives

$$\frac{2f}{0.9qR} = 1 - \rho_f .$$

Substituting $2f/qR_b = 0.3$ and solving for ρ_f gives $\rho_f = 0.667$.

The burble-fence curves are closely approximated by circular arcs near the equator. The radius of the arc for each curve is given by

$$r_1 \text{ at } x = R_b = \frac{R_{b(1-\rho)}}{(1+\rho)} .$$

Substituting $R_b = 115.2$ in. for the respective values of ρ gives a radius of 12.8 in. for the rear of the fence and 23.04 in. for the front. These values are sufficiently accurate to construct the entire fence profile with these circular arcs.

(3) Tucked-Back Model

The rear contour chosen is the curve for $k + \rho = 0.6$ in Figure 5 from the cited reference. For this curve, $k = 0.3$ and $\rho = 0.3$. From the definition of ρ, the center table load is $0.3P\pi R^2$. This surface has a constant hoop stress, f_2, equal to f_1, which is given by N. E. Houtz's Equation 23 as

$$f = \frac{PR}{2}(1 - k - \rho_r) .$$

The meridian stress, f_1, is given by Equation 2b from N. E. Houtz as

$$f_1 = f + \frac{nT_m}{2\pi X} ,$$

where $nT_m = kP\pi R^2$. Thus, at the equator,

$$f_1 = \frac{PR}{2}(1 - k - \rho) + \frac{kPR}{2}$$

$$= \frac{PR}{2}(1 - \rho) .$$

The tucked-back design has no burble fence, which results in a different drag coefficient and pressure distribution. The pressure difference over the front is estimated to be 0.9q - the same as the burble fence - but the drag coefficient is reduced to 0.6 and the pressure difference, P, is 1.5q. The meridian radius of the BALLUTE's front at the equator is 0.583R, and the hoop radius is R.

The membrane equation gives

$$\frac{f_1}{0.583R} + \frac{f_2}{R} = 0.9q$$

or

$$\frac{f_2}{R} = 0.9q - \frac{0.525}{0.583}q$$

$$= 0 .$$

Thus, the value 0.583R is the smallest radius that allows full inflation.

(4) Deployment Stress

Experience has shown that, during deployment and inflation, BALLUTEs undergo a flagging that produces dynamic fabric stresses considerably higher than the calculated static stresses. Testing has indicated that the maximum stress is approximately 2qR, where q is the dynamic pressure at deployment and R is equatorial radius of the BALLUTE proper. Substituting q = 0.0015 psi and R = 96 in. gives a stress of 0.288 psi. The material (Capran 77C[a]) has a minimum yield stress of 3000 psi.

[a]Capran Polyamide Film Technical Data, Allied Chemical Corp., General Chemical Division, Morristown, N. J.

With a thickness of 0.0025 in., the strength is 0.75 lb/in. and the safety factor is 0.75 = 2.6.

(5) Attachment-Spring Analysis

The nose of the BALLUTE is attached to the payload by eight cantilever springs, which provide a positive opening at deployment. When the BALLUTE is packaged, the springs are deflected inward toward the center. The springs should be straight in the deflected position and have predetermined curvature in the free condition.

Each spring's length is 8.5 in. In the deployed condition, the ends move outward 4 in. Since some load should remain in the spring at this point, the free shape is given to be deflected so $P\ell 3/3EI = 5$ in. The figure below shows the loading and dimensions in the closed position:

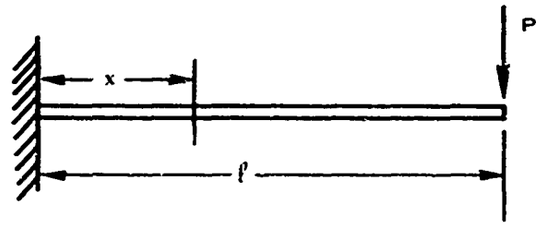

The moment at any point, x, is $P(\ell - x)$. The bending equation gives $1/r = M/EI$, where r is the radius of curvature, E is the modulus of elasticity, and I is the cross section moment of inertia. Substituting for M gives $r = EI/P(\ell - x)$. Substituting $P\ell 3/3EI = 5$, or $P = (3)(5)EI/3$, and $\ell = 8.5$ gives

$$r = \frac{1}{1.763\left(1 - \frac{x}{\ell}\right)}.$$

This relationship gives the following values of r/ℓ for various values of x/ℓ.

$\frac{x}{\ell}$	$\frac{r}{\ell}$
0	0.568
0.1	0.630
0.2	0.71
0.3	0.811
0.4	0.945
0.5	1.134
0.6	1.42
0.7	1.89
0.8	2.84
0.9	5.68
1.0	∞

r/ℓ is plotted versus x/ℓ in Figure 8. For each increment of $\ell/10$, an average radius is taken from the curve. Beginning with the fixed end, the spring's free shape is approximated by laying out these average radii in series for arc lengths of $\ell/10$ each. Each arc is tangent to the x axis at x = 0. The resulting curve is also shown in Figure 8, along with the estimated deployed shape of the spring.

The following values are given: $E = 30 \times 10^6$ psi, t = 0.033 thickness, and w = 0.50 width. The moment of inertia is given by

$$I = \frac{wt^3}{12}$$

$$= \frac{(0.5)(0.033)^3}{12}$$

$$= 1.498 \times 10^{-6} \text{ in.}^4$$

and $EI = 30 \times 1.498 = 44.9$ psi.

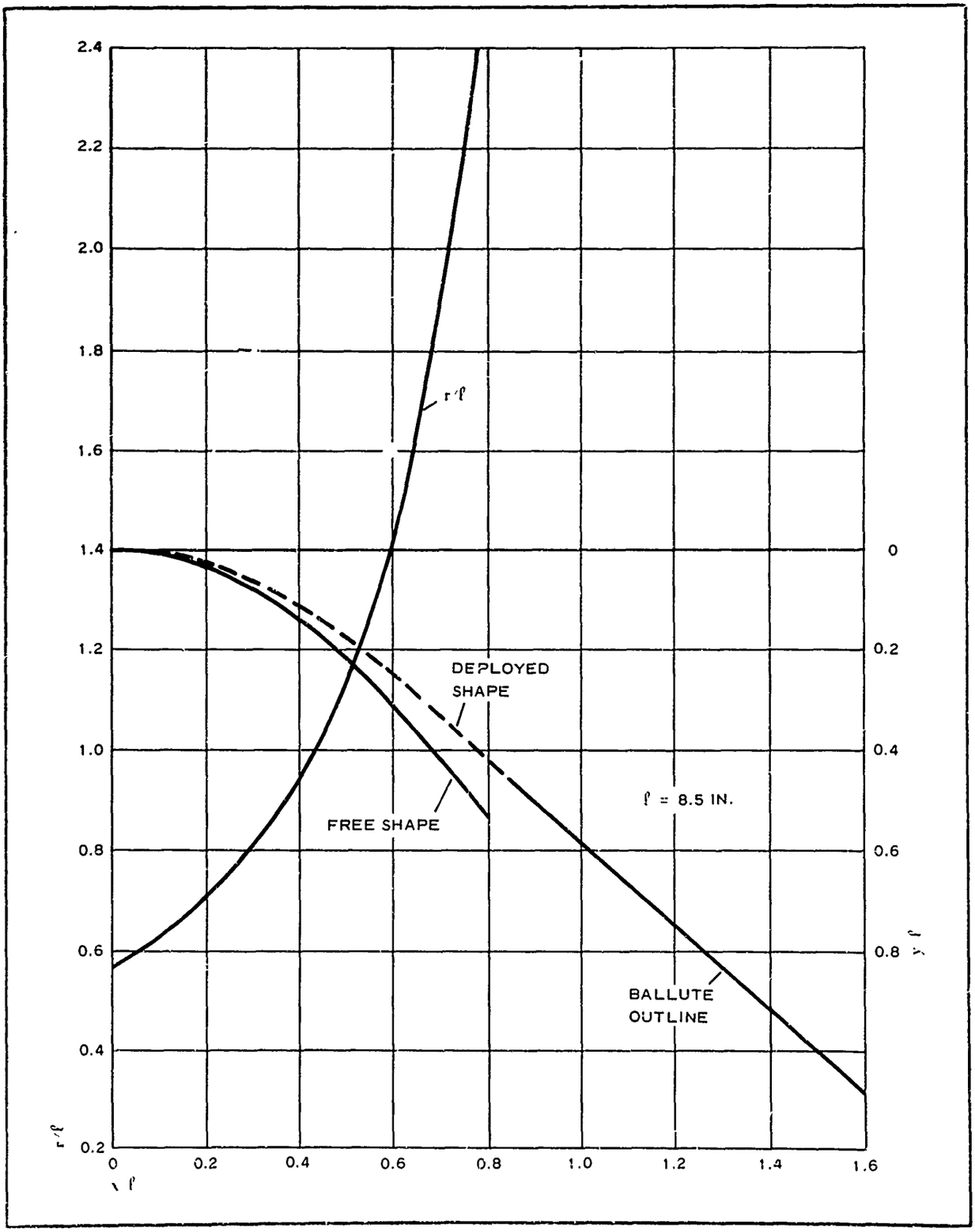

Figure 8 - Spring Analysis

The maximum load, P, is equal to $15EI/3 = (15)(44.9)/(8.5)^3 = 1.1$ lb.

The maximum moment is $(1.1)(8.5) = 9.32$ in./lb, and the bending stress is given by

$$S = \frac{(9.32)\left(\frac{0.033}{2}\right) \times 10^6}{1.498}$$

$$= 102,900 \text{ psi}.$$

The material is 1095 steel heat treated to 200,000 psi strength, giving a safety factor of 1.95.

(6) Inlet Hoop Analysis

At deployment, the eight inlet springs are released suddenly and snap outward to the deployed position. The springs are then restrained by the inlet hoop. This inlet hoop analysis assumes that the energy released is all absorbed by the hoop.

The load deflection for each inlet spring is as follows:

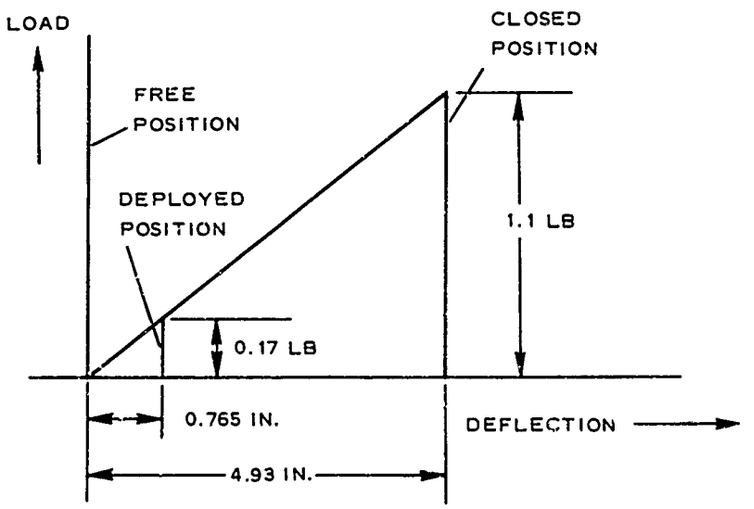

The energy released by each spring is equal to the area under the above curve, assuming the hoop's strain allows the springs to extend from their free shape during the impact. This energy is

equal to (1.1)/2 (4.93) = 2.71 in./lb. For all eight springs, the energy is 21.7 in./lb.

The inlet hoop is 1/2 in. wide, 0.005 in. thick, and is approximately 12 in. in diam, which gives a cross-section area of 0.0025 sq in. and a length of 37.7 in. The material has a minimum yield strength of about 3000 psi at a strain of 20 percent. The load is (3000)(0.0025) = 7.5 lb and the elongation is (0.2) (37.7) = 7.54 in. The strain energy (conservatively assuming a linear stress-strain curve) is (7.5)(7.54)/2 = 28.3 in./lb, which is more than the calculated input from the springs. In view of the conservative assumptions made in the inlet hoop analysis, the inlet hoop is believed adequate.

5. MATERIALS INVESTIGATION

a. General

As a result of the structural analysis, the anticipated loading of the BALLUTE requires an essentially impermeable material. The obvious material category is plastic films.

The major criteria used in the selection of an appropriate plastic film are:

1. The capacity to withstand the environment without deterioration
2. The highest tensile strength for the least film thickness and weight
3. Fabrication requirements compatible with low-cost production methods

Many films are capable of exposure to environmental extremes without physical deterioration or embrittlement resulting.

b. Polyester Films

Of the films exhibiting high tensile strength in fractional mil gages, polyester is outstanding, with ultimate results of 17,000 to 40,000 psi. Because they are not thermoplastic, however, polyester films required adhesive resin or resin-faced tape for seam construction. This construction has proved extremely reliable in many applications, and the weight penalty resulting from the addition of tapes is not prohibitive. The deterrent factor is the relatively high man-hour burden involved in seam construction, compared with a heat-sealed or fused-seam construction that lends itself more readily to semiautomated production techniques.

Films that can be heat sealed, although they differ in temperature-pressure-dwell requirements, are generally equal in fabrication ease.

In all cases, seam reliability is a function of the ability to control temperature tolerances, pressure, and dwell-time values. The accuracy required is inversely proportionate to the film gage.

c. Polyamide Films

The most promising of the heat-sealable films were the polyamides, with tensile strengths of 9000 to 12,000 psi - roughly one-third the strength of the polyesters. This tensile capability was not considered sufficient to rule out the use of a polyamide film, since neither the polyesters nor the polyamides is readily available in gages less than 1/4 mil. This thickness appears adequate - even with the polyamide - based on the preliminary structural analysis.

During the fabrication study, test-sample seams of polyamide film of four different gages (0.25 mil, 0.3 mil, 0.4 mil, and 0.75 mil) were made using five separate sealing methods.

d. Test Data

(1) Group 1 Specimens - 1/8-In.-Wide Band Seams (Figure 9)

The Group 1 specimens were made with a roller-type sealer that

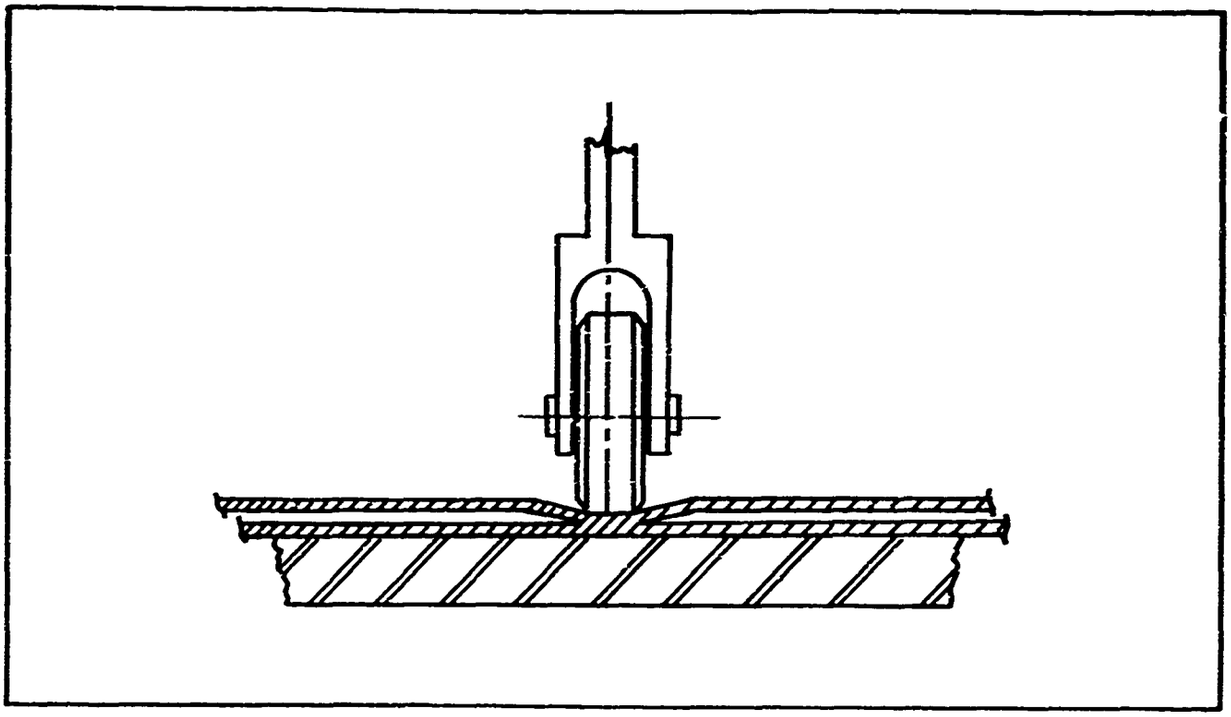

Figure 9 - Band Seaming (1/8 In. Wide)

was held by hand. The operator controled the pressure and the rate of travel. The Teflon-coated roller was electrically heated, and its temperature was controlled by a variac. The seams obtained in Group 1 had an average strength of 53 percent of the parent material ultimate (see Table 1).

(2) Group 2 Specimens - Weld-Bead Seams (Figure 10)

The tool for the Group 2 specimens was different from that used for Group 1 only in the roller's shape. This Teflon-coated wheel was sharply pointed and performed the dual function of cutting and of sealing. Because the heated roller cuts through both layers of film, pressure was not critical in this operation.

Cutting was accomplished by melting the material that came in contact with the edge of the tool. Because of the roller's sharpness, the implement cut through a line of molten film and made contact with the working surface, which resulted in separation to

TABLE 1 - POLYAMIDE FILM SEAM SPECIMEN TEST DATA

Specimen no.	Width (in.)	Thickness (in.)	Seam type	Ultimate load (lb)	Average (lb)	Type failure
1	2.0	0.00075	None	6.59		At jaw
2	2.0	0.00075	None	8.01	6.80	At jaw
3	2.0	0.00075	None	6.09		At jaw
4	2.0	0.00075	None	6.50		At jaw
5	2.0	0.00075	Weld bead	5.86		Seam
6	2.0	0.00075	Weld bead	6.09		Seam
7	2.0	0.00075	Weld bead	5.93	5.72	Seam
8	2.0	0.00075	Weld bead	5.78	(84 percent)	Seam
9	2.0	0.00075	Weld bead	4.95		Seam
10	2.0	0.00075	1/8-in. band	1.66		Seam
11	2.0	0.00075	1/8-in. band	3.14		Seam
12	2.0	0.00075	1/8-in. band	5.49	4.01	Seam
13	2.0	0.00075	1/8-in. band	4.60	(59 percent)	Seam
14	2.0	0.00075	1/8-in. band	5.15		Seam
15	2.0	0.0004	None	4.11		Field
16	2.0	0.0004	None	3.39	3.96	Field
17	2.0	0.0004	None	4.35		At jaw
18	2.0	0.0004	None	3.99		Field
19	2.0	0.0004	Weld bead	3.30		Seam
20	2.0	0.0004	Weld bead	3.19		Seam
21	2.0	0.0004	Weld bead	2.86	3.11	Seam
22	2.0	0.0004	Weld bead	3.14	(79 percent)	Seam
23	2.0	0.0004	Weld bead	3.08		Seam

TABLE I - POLYAMIDE FILM SEAM SPECIMEN TEST DATA (Continued)

Specimen no.	Width (in.)	Thickness (in.)	Seam type	Ultimate load (lb)	Average (lb)	Type failure
24	2.0	0.0004	1/8-in. band	2.96		Seam
25	2.0	0.0004	1/8-in. band	2.06		Seam
26	2.0	0.0004	1/8-in. band	2.04	1.94	Seam
27	2.0	0.0004	1/8-in. band	1.43	(49 percent)	Seam
28	2.0	0.0004	1/8-in. band	1.22		Seam
29	2.0	0.0003	None	2.41		Field
30	2.0	0.0003	None	2.96	2.70	At jaw
31	2.0	0.0003	None	2.72		Field
32	2.0	0.0003	1/8-in. band	1.40		Seam
33	2.0	0.0003	1/8-in. band	1.38		Seam
34	2.0	0.0003	1/8-in. band	2.40	1.93	Seam
35	2.0	0.0003	1/8-in. band	2.26	(72 percent)	Seam
36	2.0	0.0003	1/8-in. band	2.20		Seam
37	2.0	0.0003	Weld bead	2.26		Seam
38	2.0	0.0003	Weld bead	2.40		Seam
39	2.0	0.0003	Weld bead	2.02	2.25	Seam
40	2.0	0.0003	Weld bead	2.42	(83 percent)	Seam
41	2.0	0.0003	Weld bead	2.14		Seam
42	2.0	0.00025	None	2.20		Field
43	2.0	0.00025	None	2.80	2.55	Field
44	2.0	0.00025	None	2.64		Field
45	2.0	0.00025	1/8-in. band	0.80		Seam
46	2.0	0.00025	1/8-in. band	0.40		Seam
47	2.0	0.00025	1/8-in. band	1.04	0.84	Seam
48	2.0	0.00025	1/8-in. band	0.64	(33 percent)	Seam

TABLE 1 - POLYAMIDE FILM SEAM SPECIMEN TEST DATA (Continued)

Specimen no.	Width (in.)	Thickness (in.)	Seam type	Ultimate load (lb)	Average (lb)	Type failure
49	2.0	0.00025	1/8-in. band	1.30		Seam
50	2.0	0.00025	Weld bead	1.96		Seam
51	2.0	0.00025	Weld bead	1.93		Seam
52	2.0	0.00025	Weld bead	1.72	1.83	Seam
53	2.0	0.00025	Weld bead	1.68	(72 percent)	Seam
54	2.0	0.00025	Weld bead	1.84		Seam

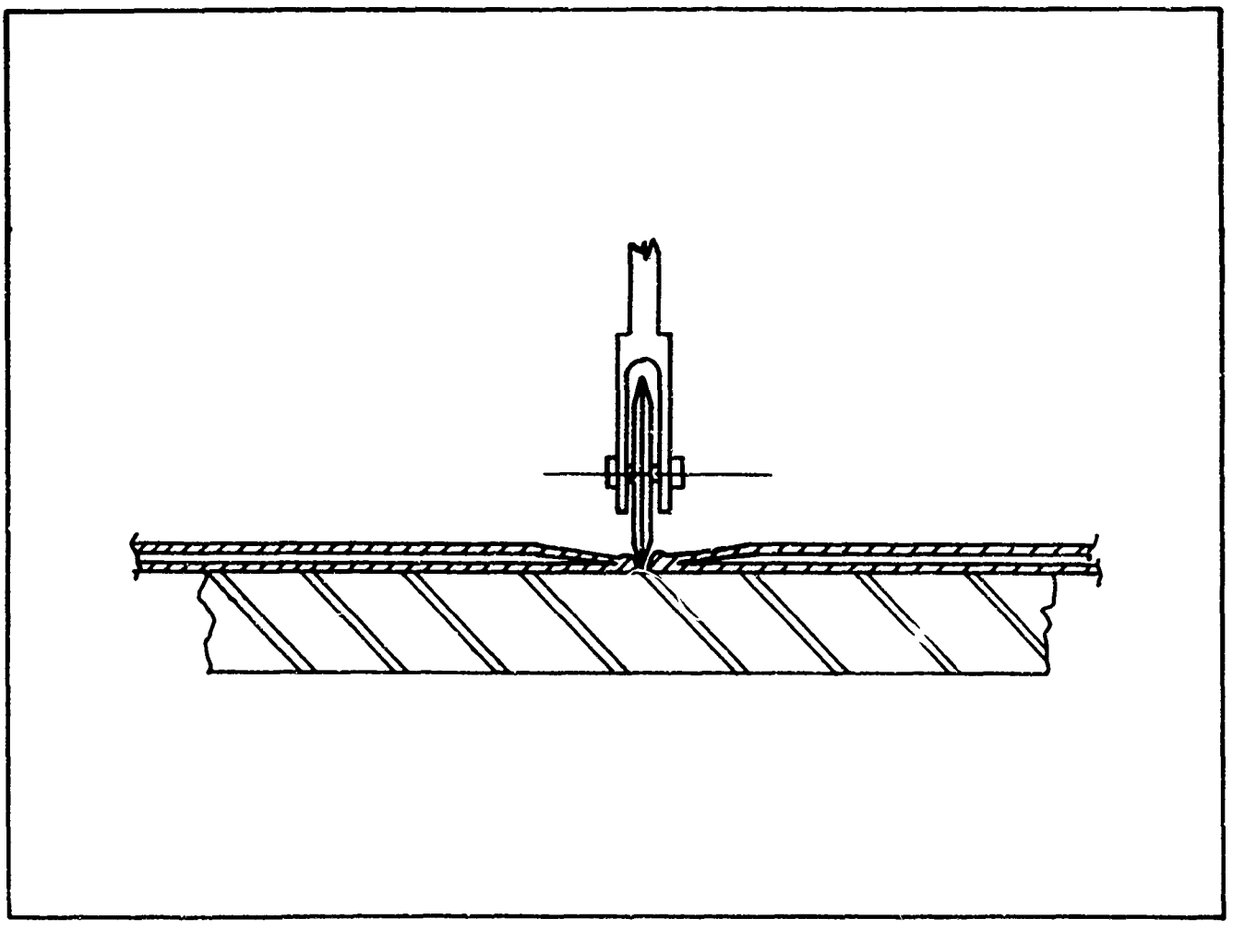

Figure 10 - Weld Bead Seaming

either side of the tool. The cohesive properties of the molten edges of the film's upper and lower layers caused formation of a continuous bead joining the adjacent films. The strength of the weld-bead seam averaged 80 percent of the parent material, as shown in Table 1. The weld-bead seam was the most promising of the types investigated and will be considered in any production assembly effort.

(3) Group 3 Specimens - Hot Air Welding (Figure 11)

A weld-bead seam similar to the weld-bead seam of Group 2 is accomplished by a hot-air jet. Both temperature and flow rate are controllable. Although temperature is controlled more easily with this tool, the air jet causes material flutter, which disturbs the bead during the cooling period. Because the material is difficult to handle, this method was eliminated, and tensile specimens were not made.

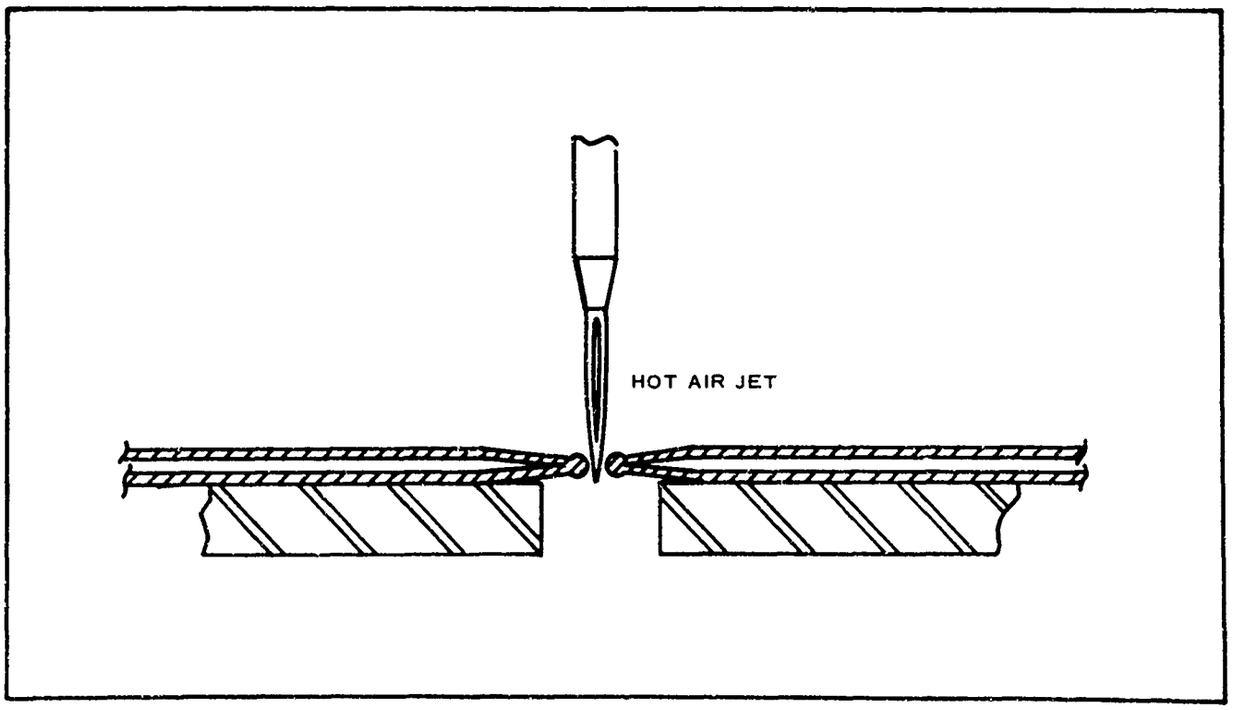

Figure 11 - Hot Air Jet Seaming

(4) Group 4 Specimens - Ultrasonic Band Seam (Figure 12) and Group 5 Specimens - Dielectric Band Seam (Figure 13)

The Group 4 and Group 5 methods of film bonding, although widely used in the packaging industry, were unable to yield a continuous reliable seam with fractional mil films. No tensile test specimens were fabricated.

The results of the tensile tests conducted on Groups 1 and 2 specimens are given in Table 1.

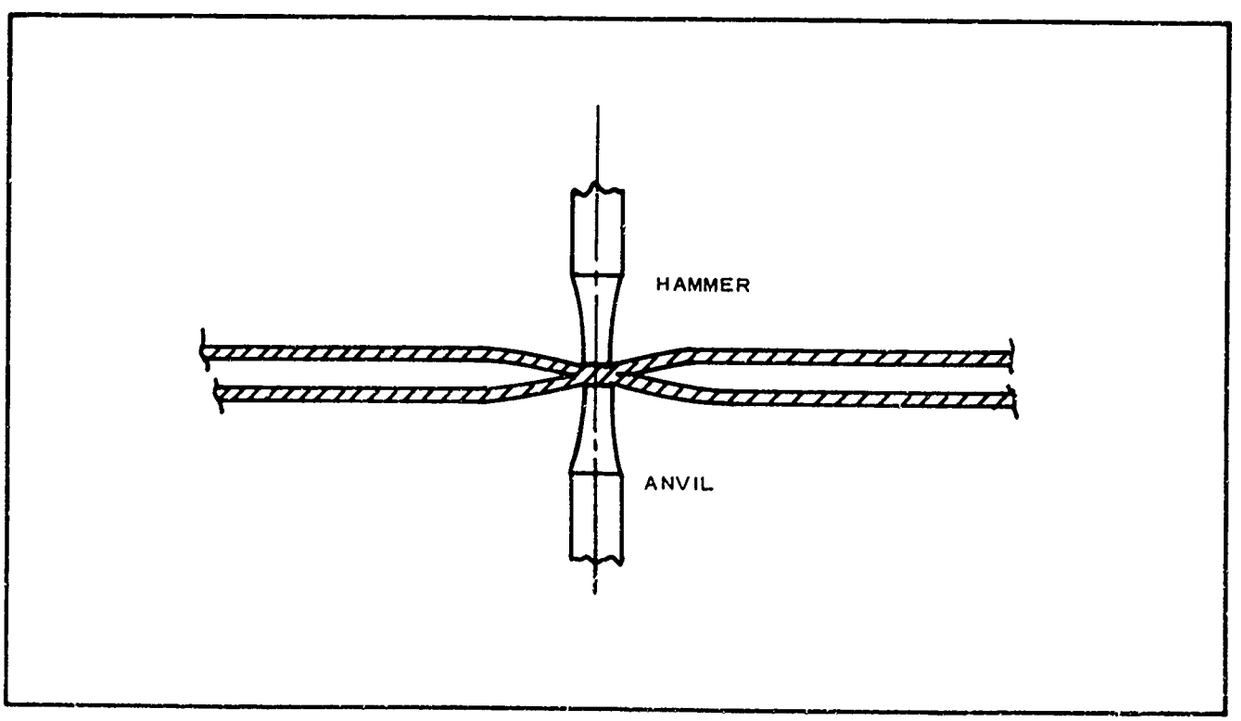

Figure 12 - Ultrasonic Seaming

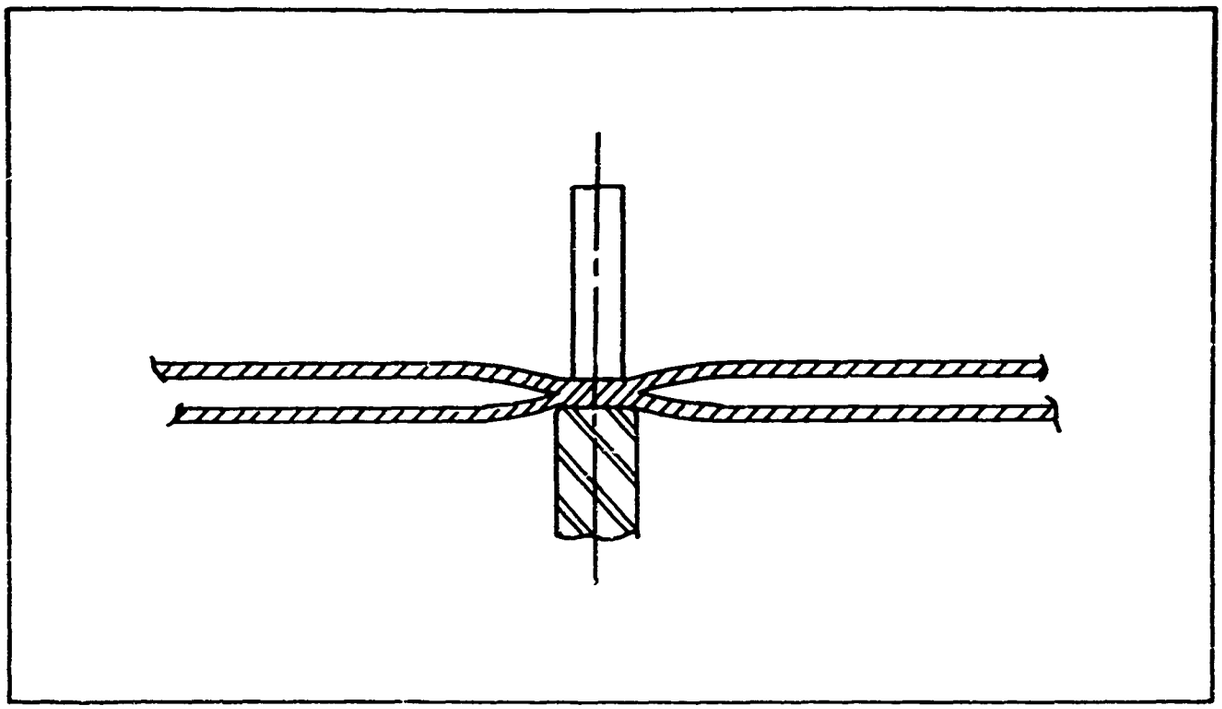

Figure 13 - Dielectric Seaming

SECTION III

AIRDOCK DROP TEST PROGRAM

1. PURPOSE

As a result of the trajectories study, the W/C_DA required to perform the airdock drop test program is 0.05 psf, or a BALLUTE about 15 ft in diameter.

In solving for Reynolds number at 180,000 ft, where

$$\rho = 1.11 \times 10^{-5},$$

$$v = 300 \text{ fps},$$

$$d = 15 \text{ ft},$$

$$\mu = 3.62 \times 10^{-7},$$

then

$$RN = \frac{\rho v d}{\mu}$$

$$= \frac{1.11 \times 10^{-5} \times 300 \times 15}{3.62 \times 10^{-7}}$$

$$= 1.38 \times 10^{4}.$$

Since this Reynolds number value is in the subcritical regime for a sphere, the drag and stability characteristics of the BALLUTE were assumed significantly different from available subsonic data at higher Reynolds numbers.

The purpose of the airdock drop test program was to compare in free flight the performance of the three candidate BALLUTE configurations by

measuring drag and stability at simulated Reynolds numbers and at equivalent W/C_DA values.

The GAC airdock was used for the drop tests. The BALLUTEs were suspended from a point on the uppermost central catwalk 178 ft above the floor, as shown in Figure 14.

The sequence of the airdock drop tests was as follows:

1. A low-velocity air supply was injected into the ram-air inlet until the BALLUTE inflated to its fully pressurized shape.
2. At T - 10 sec, a pivoting bank of 20 floodlights was trained on the test item from release to the floor.
3. At T - 7 sec, the motion picture camera No. 1 was started to follow the BALLUTE during descent (see Figure 14).
4. At T - 5 sec, camera No. 2 was started to record any lateral excursions during the flight.
5. At T - 1 sec, the inflation hose was removed from the ram-air inlet.
6. At T = 0, the vertically suspended system was released, and the stop watch at the floor-control station was actuated. Portable transceivers were in operation at four positions - topside, floor control, and at two of the three catwalk elevations used as intermediate monitoring stations.
7. As the test item passed the sighting plane of each monitoring station, the stop watch at that point was started.
8. At the instant of impact, the floor station transmitted the signal to stop all watches. The point

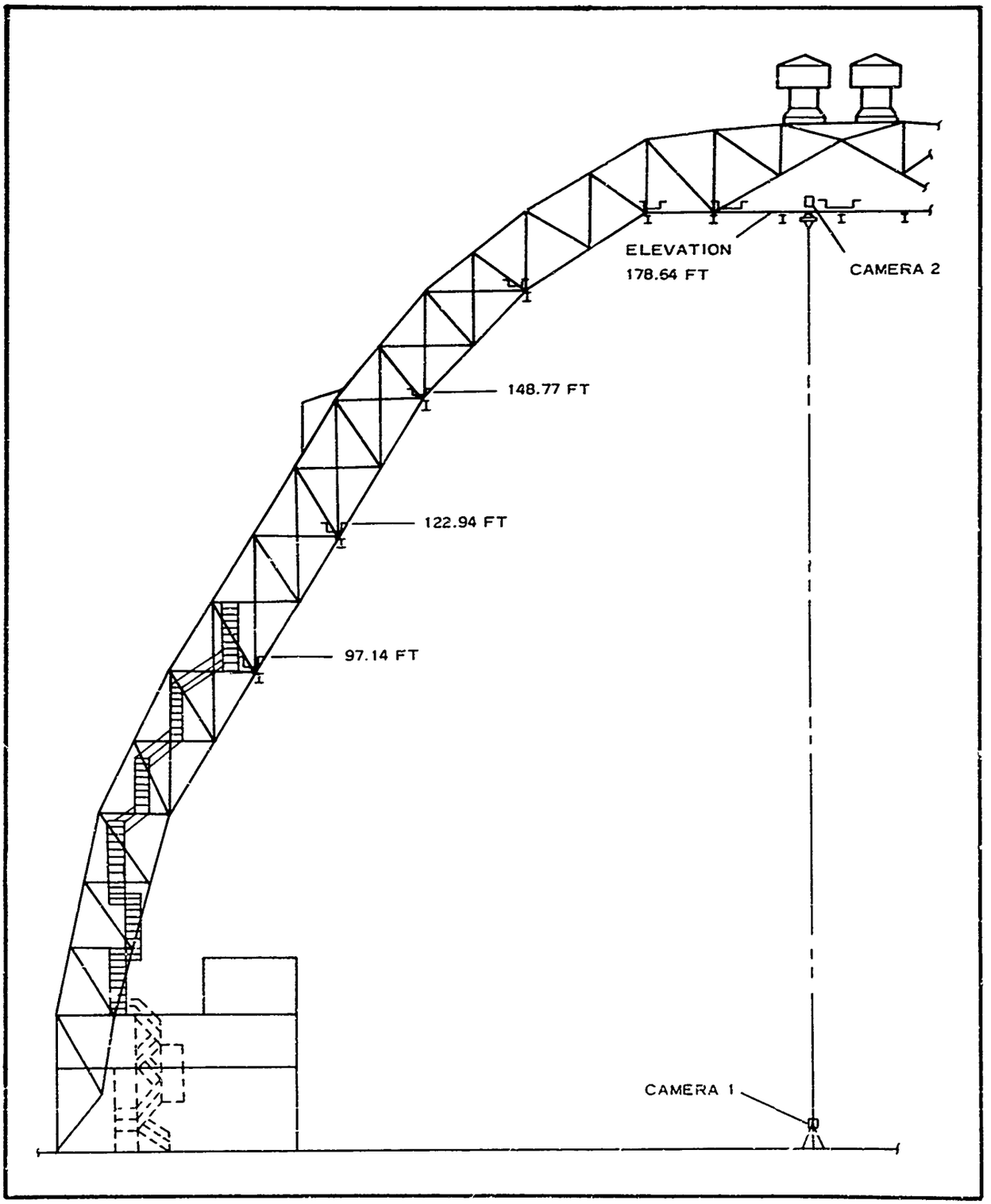

Figure 14 - Airdock Cross Section Showing Monitoring Stations and Camera Installations

of impact and the distance from the target center were recorded in feet.

9. Both motion picture cameras were synchronous motor driven at 24 frames per second. To calculate velocities more accurately, a tape of white webbing - with every ninth foot blackened - was suspended vertically in view of camera No. 1, 15 ft behind the release point of the test items. The theoretical error in this method of calculating velocities is one frame, or 1/24 sec. In terms of distance at a nominal velocity, 10 fps is 10 fps/24 frames per second, or 0.42 ft per frame. This error in a 100-ft sounding is 42/100, or 0.4 percent.

The three BALLUTEs used for the airdock drop tests are shown in Figures 5, 6, and 7. By varying the weight of the simulated payload, a variety of ballistic coefficients was achieved.

2. TEST DATA

a. General

The airdock drop test results are discussed here in groups for each major BALLUTE type. Test data are given in Appendix I.

b. Series 1 - Toroidal Burble Fence BALLUTE (see Figure 15)

The toroidal burble fence BALLUTE is the most common of the BALLUTE types and has proved to be a reliable drag device for many other applications. This BALLUTE is basically an 80-deg cone angle, isotensoidal pressure vessel, with the burble fence located at the station of maximum diameter. The burble fence's height is 10 percent of the diameter of the isotensoid shape.

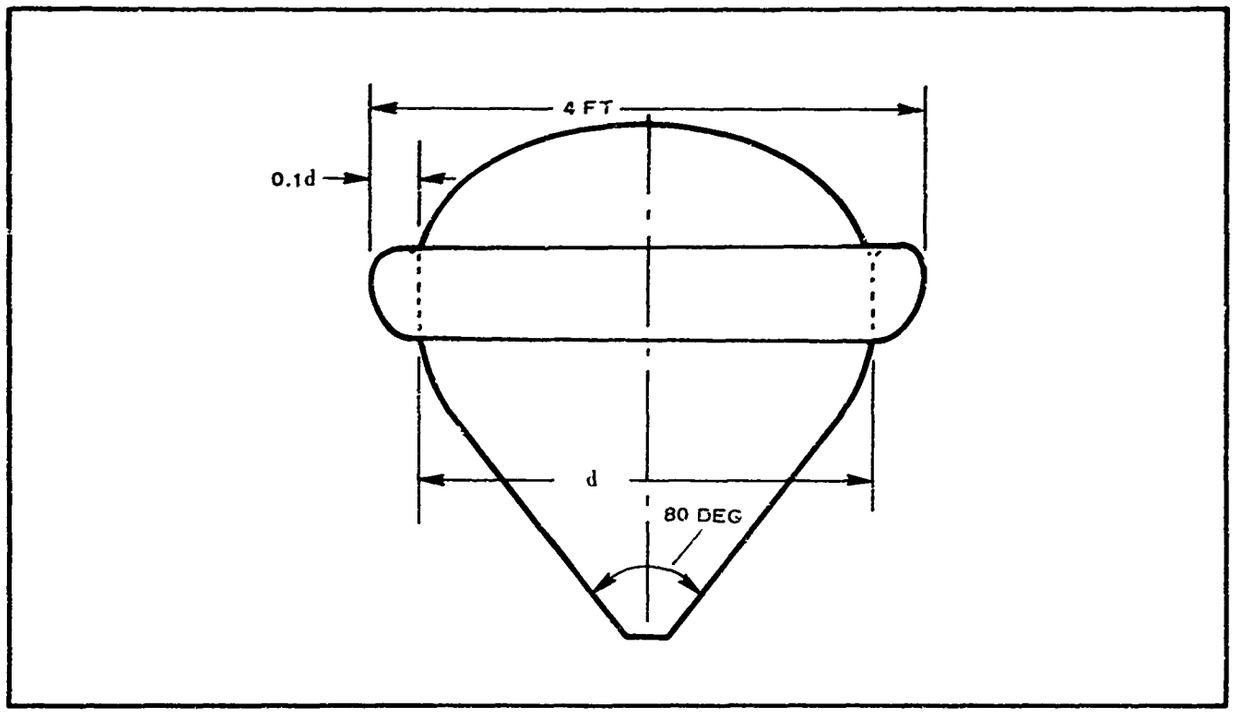

Figure 15 - Toroidal Burble Fence BALLUTE

The variation of C_D apparently is related to stability, with C_D increasing when stability worsens and when velocities decrease.

c. Series 2 - Tucked-Back BALLUTE (see Figure 16)

The tucked-back BALLUTE, because of its construction simplicities, was a desirable configuration costwise. The tucking of the aft surface results in a reduction of the radius of curvature, which effects separation control of the boundary layer like the burble fence. Although effective at some velocities, this configuration proved extremely unstable at low velocities for the airdock drop test program.

d. Series 3 - Sixty-Degree Partitioned BALLUTE (see Figure 17)

The partitioned BALLUTE had its inception in a decelerator requirement that included a corner reflector for radar tracking. The exceptionally fine stability previously noted in this configuration was reconfirmed in the airdock drop tests. The C_D was constant but significantly lower than the C_D value for Series 1.

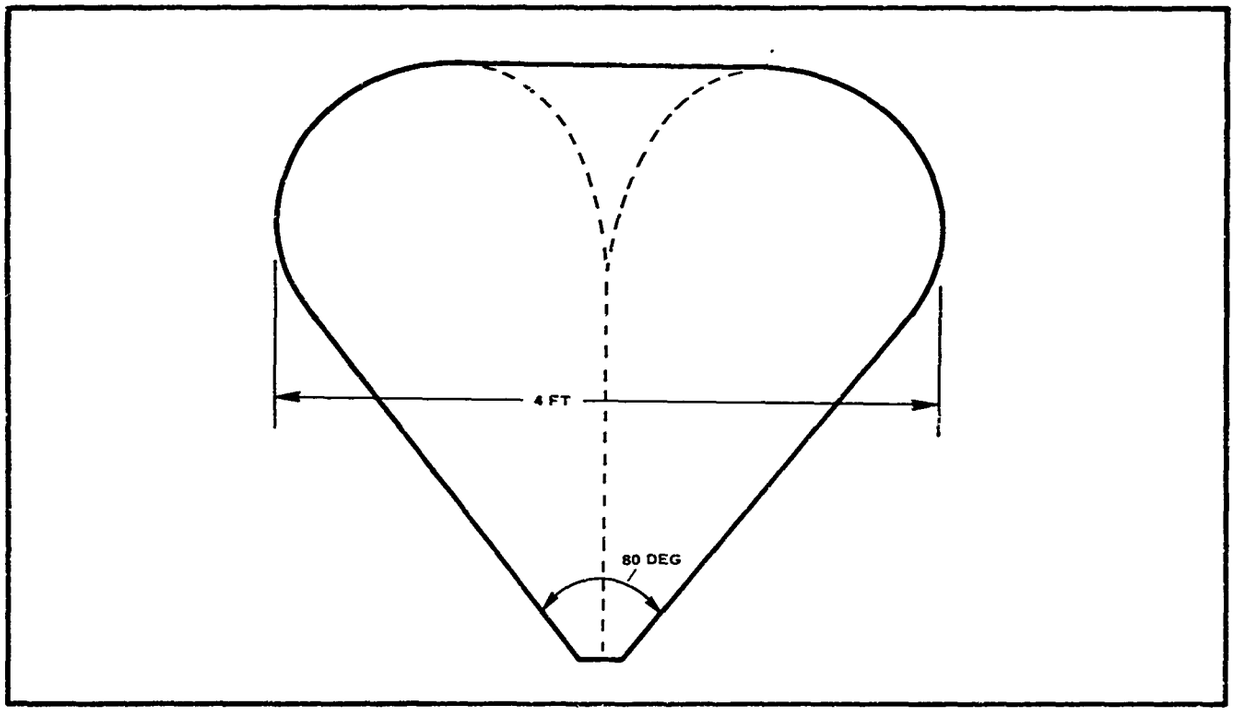

Figure 16 - Tucked-Back BALLUTE

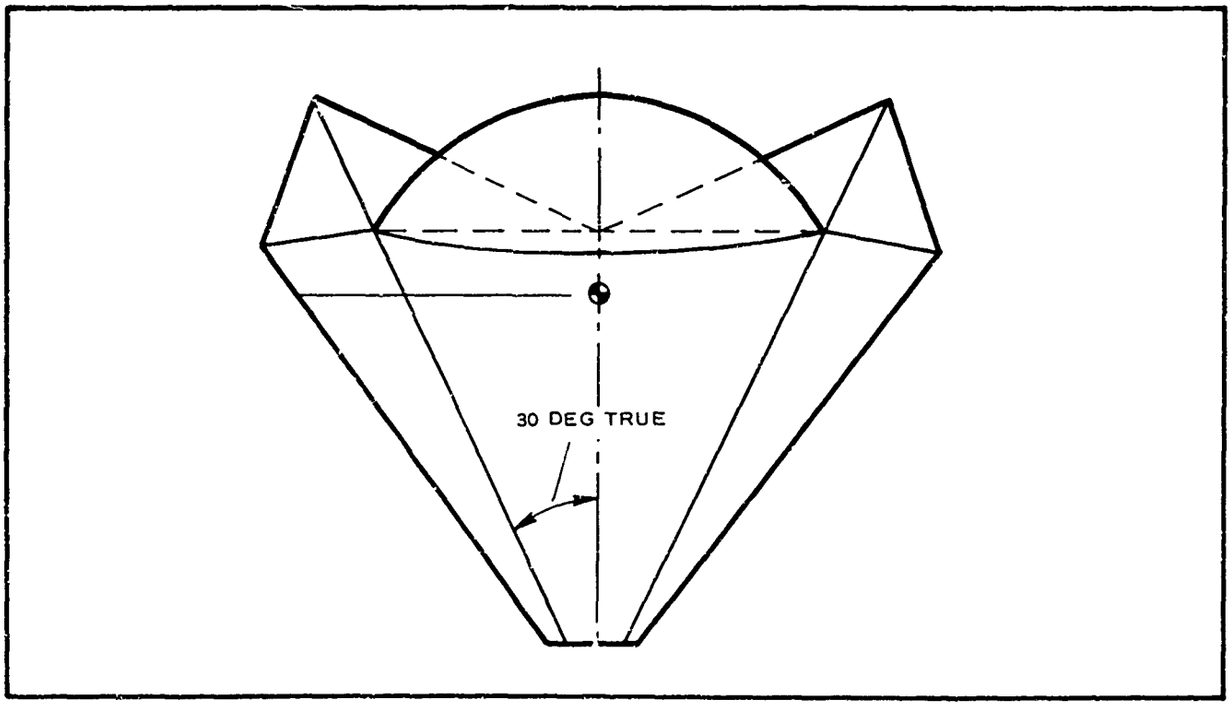

Figure 17 - Sixty-Degree Partitioned BALLUTE

At this point, the very stable Series 3 configuration yielded too low a drag coefficient, while a high drag shape of Series 1 was excessively unstable. The challenge was to make appropriate geometric modifications while attempting to combine the best characteristics of each.

e. Series 4 - Eighty-Degree Partitioned BALLUTE (see Figure 18)

The first modification attempted was a partitioned BALLUTE with a more obtuse cone angle. This modification demonstrated good stability, but no increase in drag efficiency. A 12-in. model of the same shape was constructed to determine whether the drag coefficient increased at lower Reynolds numbers. Tests revealed no increase of drag coefficient.

f. Series 5 and 6 - Tucked-Back BALLUTE with Intermittent Fence and Isotensoid BALLUTE with Intermittent Burble Fence (see Figures 19 and 20)

With no increase in the drag of the stable-partitioned shape, effort was now directed toward stabilizing the high-drag, burble-fence

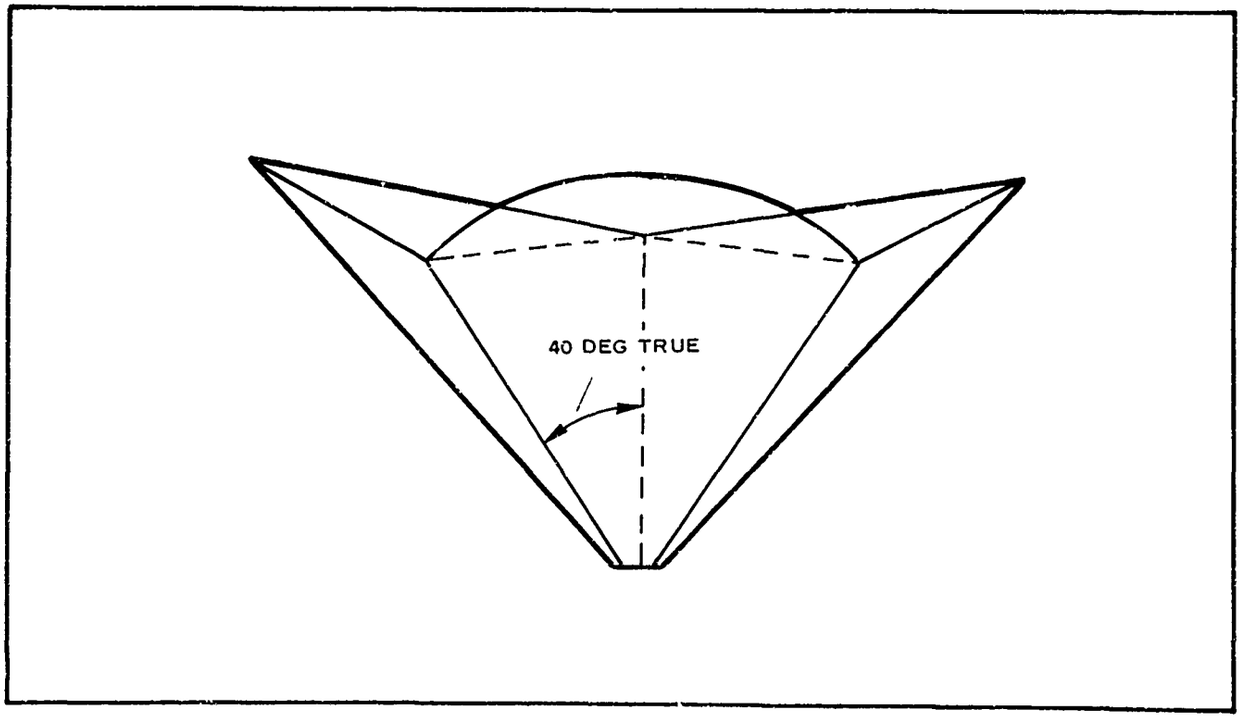

Figure 18 - Eighty-Degree Partitioned BALLUTE

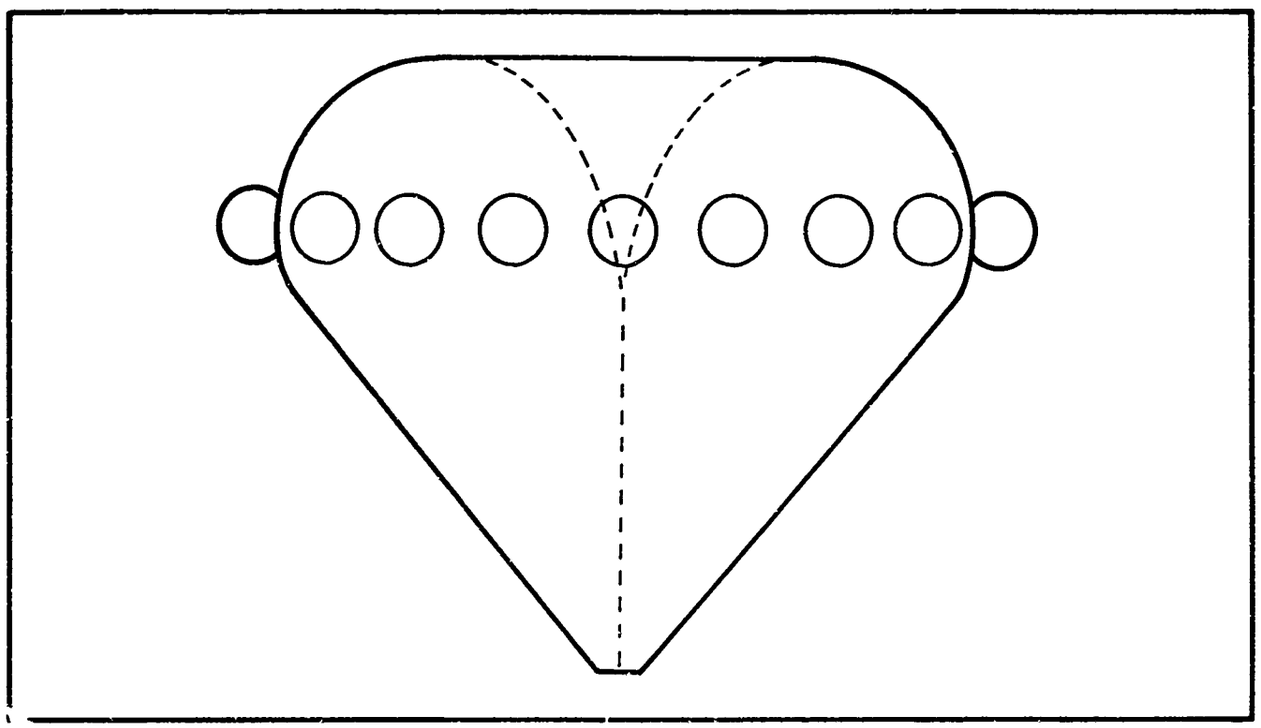

Figure 19 - Tucked-Back BALLUTE with Intermittent Fence

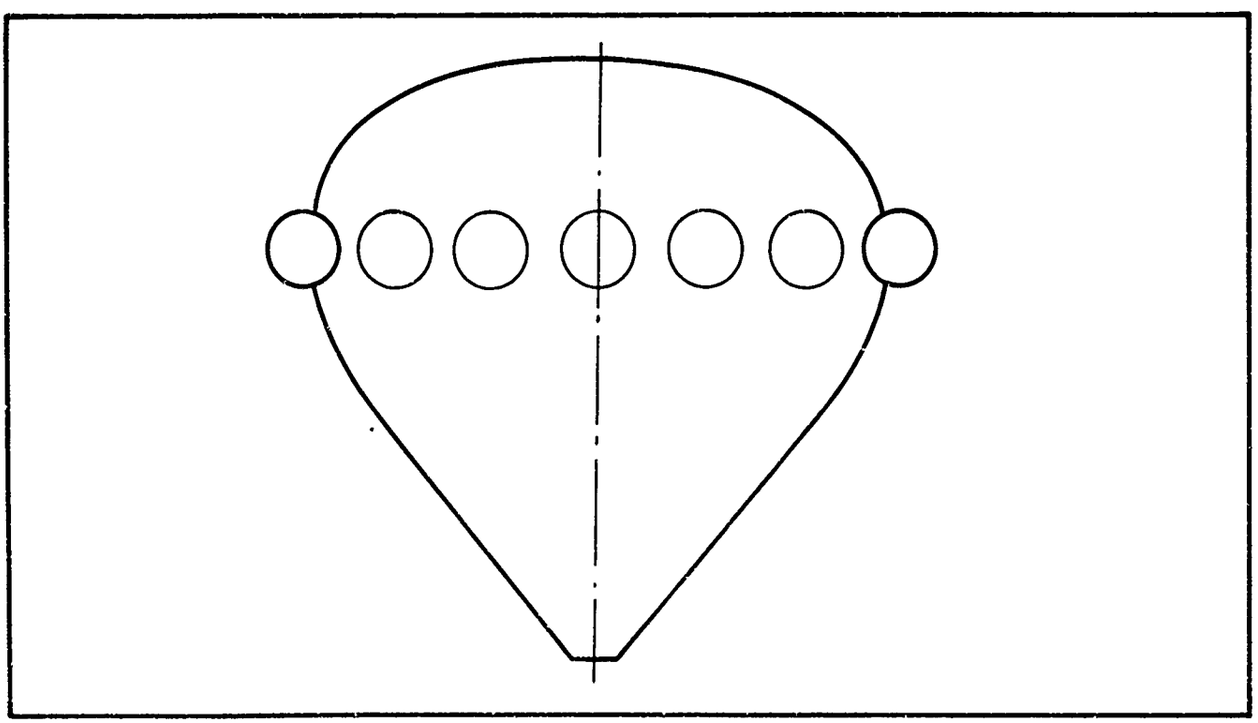

Figure 20 - Isotensoid BALLUTE with Intermittent Burble Fence

BALLUTE. The first step toward stabilizing the burble-fence shape was using an interrupted or noncontinuous burble fence. Both the tucked BALLUTE and the standard 80-deg BALLUTE were so modified. A series of inflated toy balloons about 1/10 the size of the basic BALLUTE were attached in a symmetrical pattern and replaced the normal burble fence. The theory was that, although the burble fence was probably performing its job of causing flow separation at a given station, no positive control for symmetrical generation of vortexes in the plan view existed. This circumferential sectioning of the fence would provide this control.

In both Series 5 and 6, stability was improved somewhat, but the drag coefficients were lower. Although the primary function of the burble fence is to ensure symmetrical flow separation, the burble fence also constitutes a large portion of the total drag area. The fence area reduction described above in effect removed part of the most effective drag surface on the BALLUTE.

g. Series 7 - Isotensoid BALLUTE with Dodecagonal Fence (see Figure 21)

To effect the symmetrical generation of vortixes in the plane normal to the flight path, the burble fence was modified to a series of 12 intersecting cylinder segments rather than a torus. It was hoped that the intersections would initiate the vortexes in a symmetrical pattern. The stability was somewhat improved but not satisfactorily.

h. Series 8 - Isotensoid BALLUTE with Hexagonal Burble Fence and Cones (see Figure 22)

The next modification was to preserve the burble-fence drag while providing for symmetrical circumferential vortex generation. Trailing conical appendages were added to the burble fence for this purpose in Configurations 57 through 61 (see Appendix I). To obtain the greatest effect from the cones, the fence geometry was changed from toroidal to an annular hexagon of intersecting cylinders.

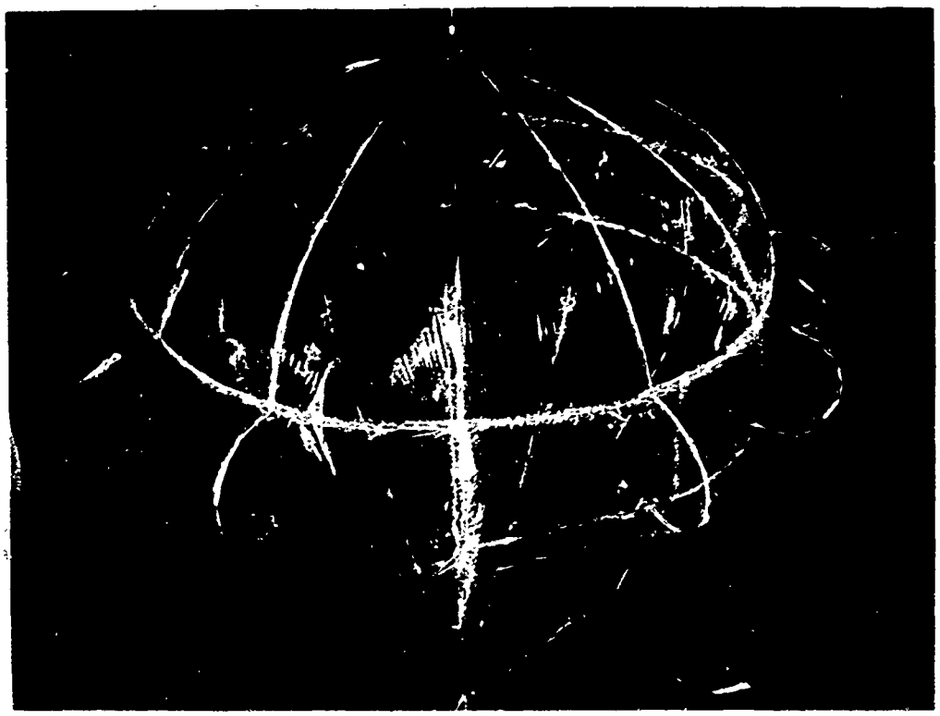

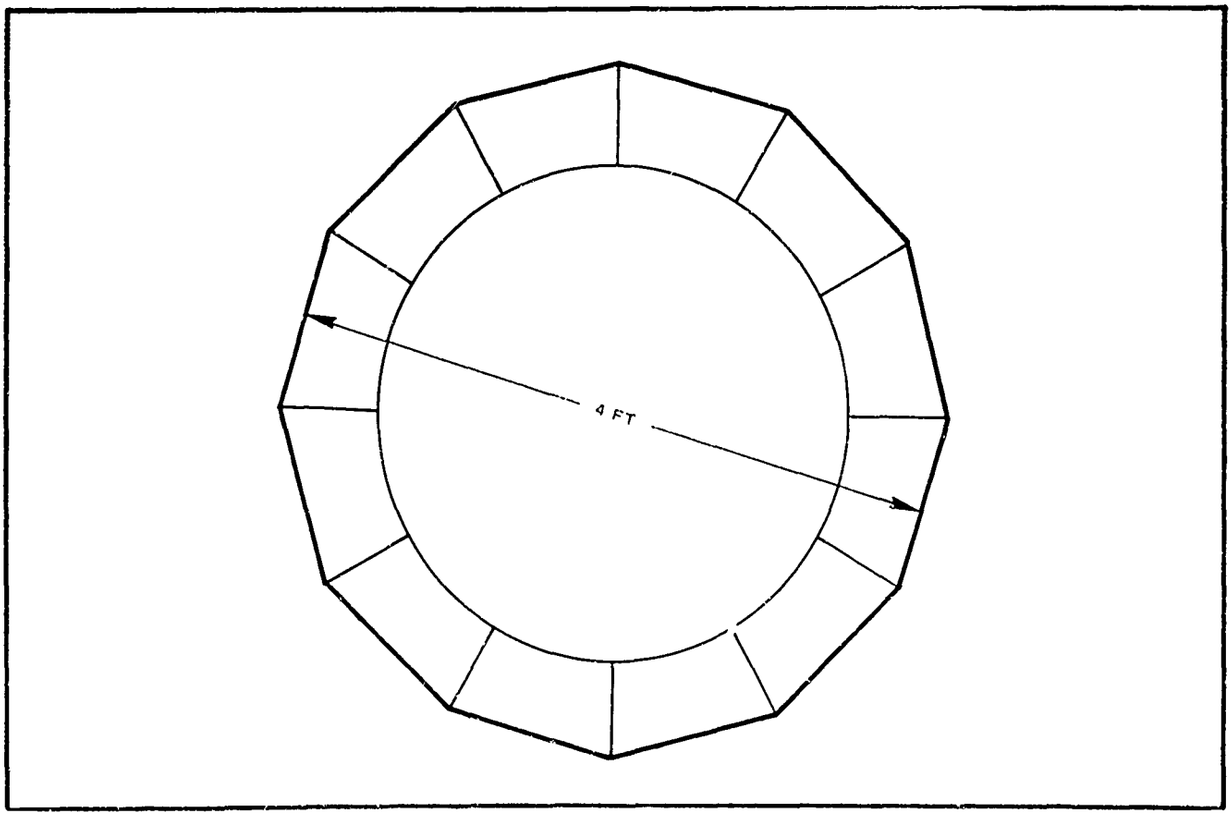

Figure 21 - Isotensoidal BALLUTE with Dodecagonal Fence

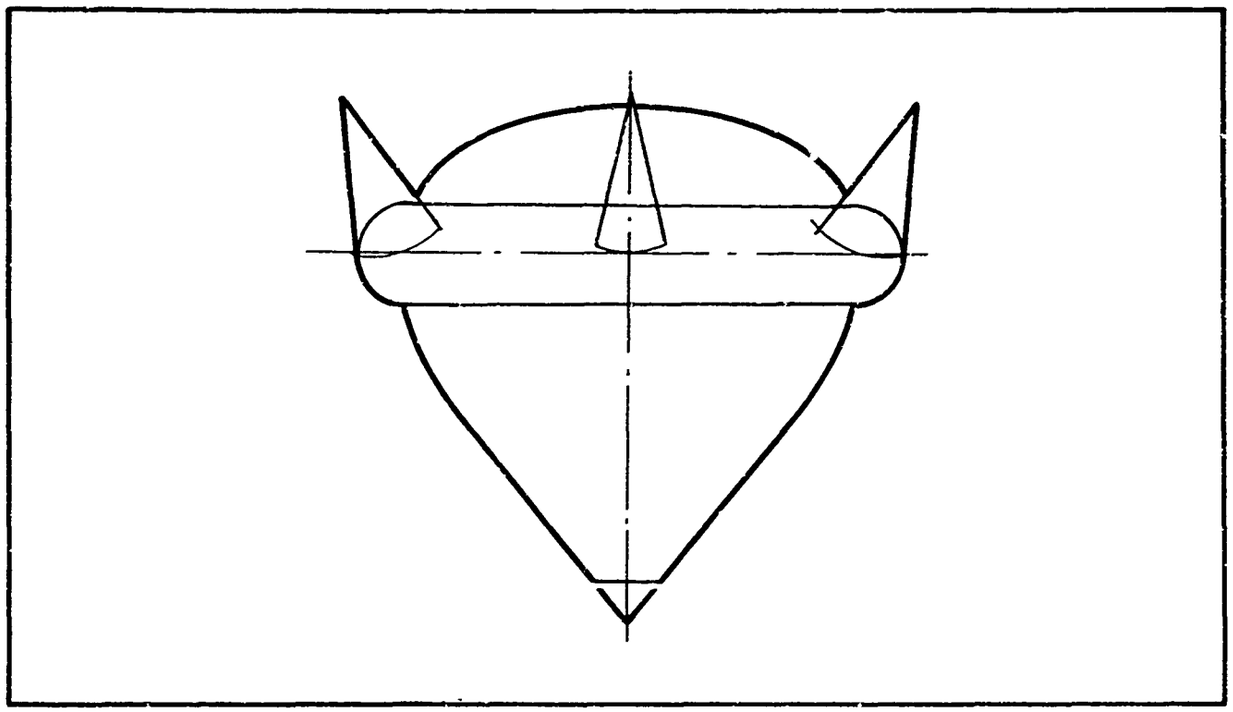

Figure 22 - Isotensoidal BALLUTE with Hexagonal Burble Fence and Cones

Locating the cones at the cylinder intersections reduced the influence of the main body.

Excellent stability and high drag were repeatedly recorded in the testing of these latest configurations.

i. Series 9 - Hexsymmetric BALLUTE (see Figure 23)

Because two variables were incorporated in the hexsymmetric BALLUTE tests (the hexagonal fence and the cones), it was necessary to retest and isolate the contribution of each. The six conical appendages, therefore, were removed, and the hexagonal fence configurations were tested. Stability was excellent and was unchanged. Drag coefficient values were lower but adequate.

j. Series 10 - Vented Hexsymmetric (see Figure 24)

Since the last two series of tests were different only in the presence of the cones - the frontal profile remaining the same - the variation

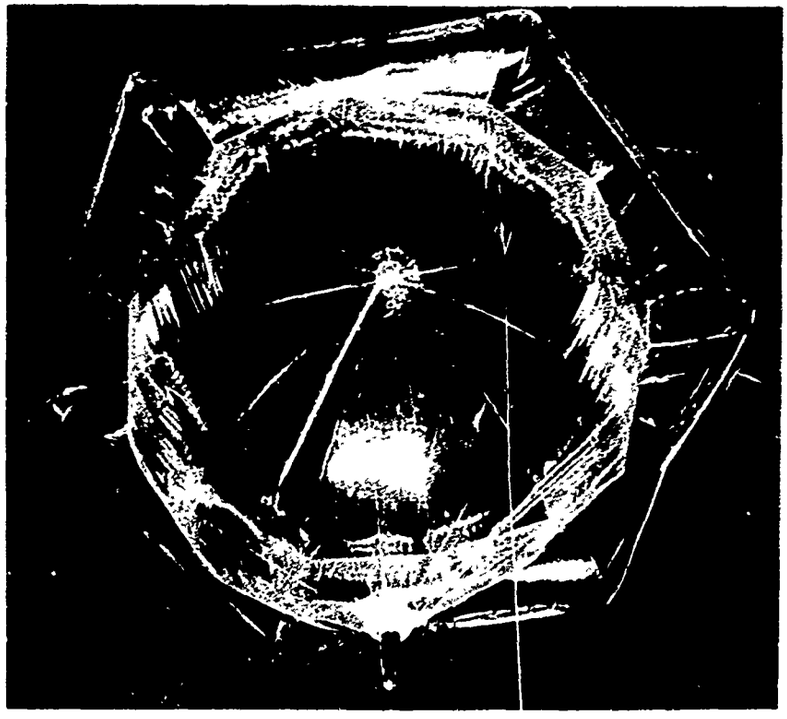

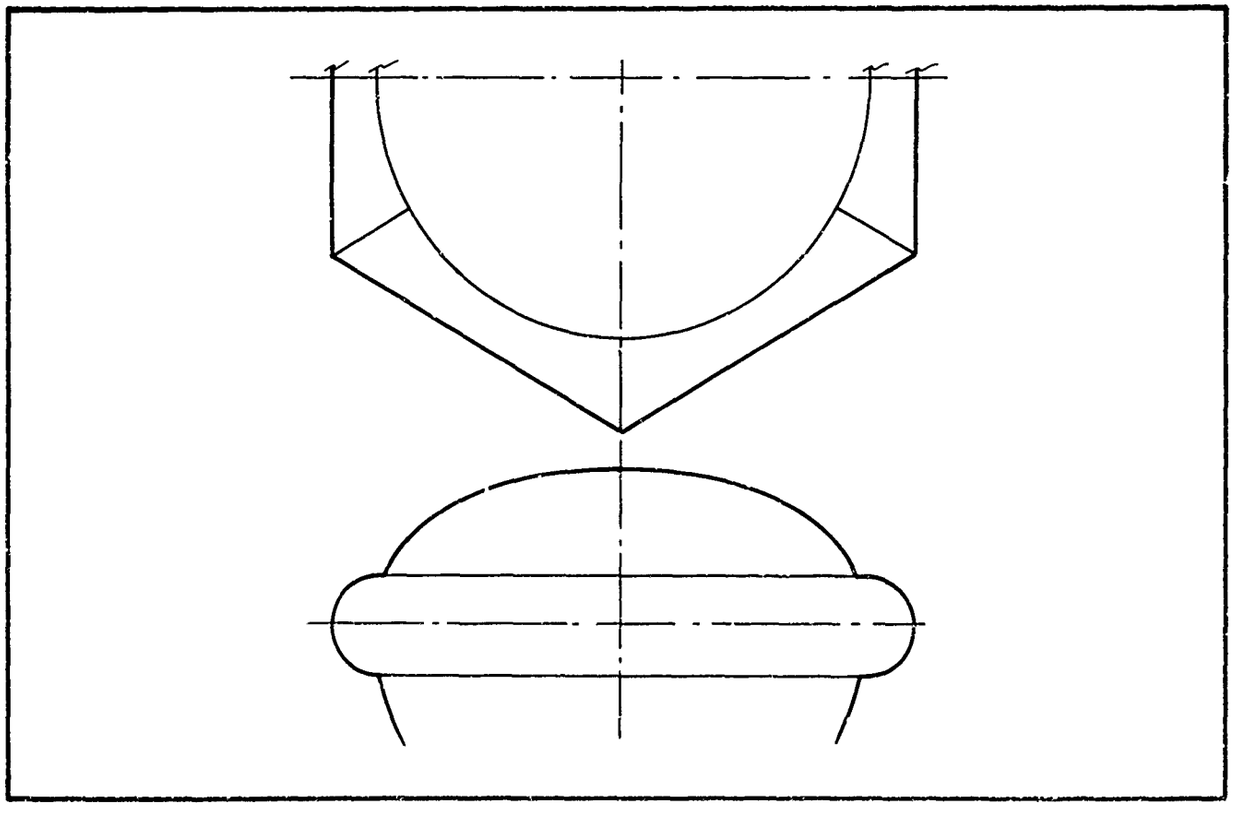

Figure 23 - Hexsymmetric BALLUTE

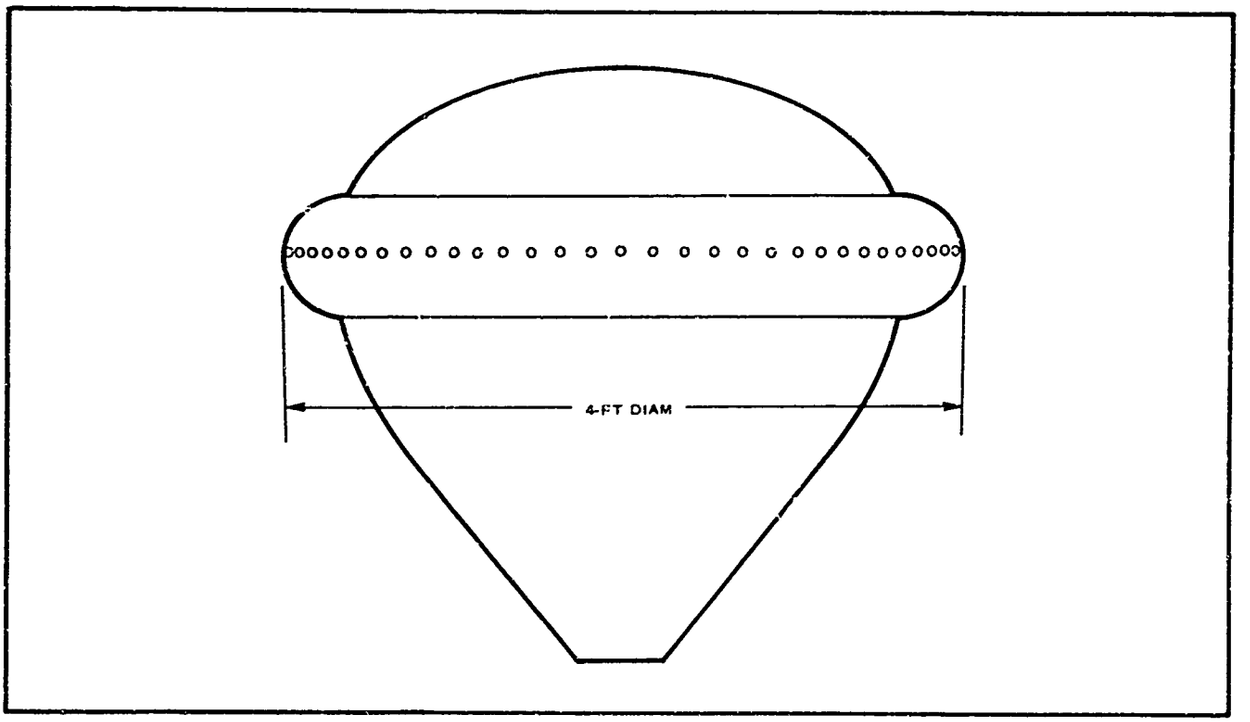

Figure 24 - Vented Hexsymmetric BALLUTE

of drag coefficient must be attributed to a change of base drag characteristics and not pressure drag. In an attempt to increase the wake divergence, a series of 1/8-in.-diameter holes 1-in. apart were cut in the burble fence's outer surface at its maximum diameter. The purpose was to direct the separating flow away from the BALLUTE by introducing the lateral force of the exhaust jets into the normal flow pattern. Testing of Configurations 67 through 70 (Appendix I) resulted in reduced drag. This testing suggested that, instead of deflecting the flow away from the BALLUTE, the ring of exhaust jets was simply added mass to the boundary layer and delayed separation. At higher velocities, however, these exhaust jets may have sufficient momentum to fulfill their design function.

3. GENERAL CONCLUSIONS

At this point, a program review yielded these general conclusions. The 80-deg BALLUTE with a 10-percent hexagonal burble fence would meet

the program's velocity and the stability goals. In all tests, the 80-deg BALLUTE deviated from a steady vertical flight path only in its response to eddies and to draft currents within the airdock. It should be noted here that the "still" air environment is a relative term. Currents and drafts up to two feet per second are common. Since drop test velocities are as low as 3.5 fps in some instances, air currents become more significant.

Preliminary work on the program review indicated that a C_D value of 0.8 would permit accomplishing the performance goals within the prescribed weight and space limitations. The hexagonal burble fence BALLUTE consistently showed C_D values above 0.9 and as high as 1.37 (drop 116), the higher values occurring at the lower velocities and Reynolds numbers.

The density used to compute the drag coefficients was derived from the barometric pressure reading for the day and for the hour. The magnitude of the drafts and thermal currents within the airdock could not be defined quantitatively and may constitute, in part, the reason for the variations in C_D values.

Although sea-level drop testing points toward good performance at mission altitudes, additional data are required to define accurately the relationship of C_D to RN. For this reason, a series of four scale models was made and tested (Configurations 62 through 66 and 72 through 85). These represent 1/10, 1/5, 1/3, and full-scale systems. Figure 25 shows drag coefficient versus Reynolds numbers for these four models recorded in the tests. Several points concerning the data are immediately obvious. In general, the larger the BALLUTE the higher the drag coefficient and - within a given size - the lower the velocity and RN the higher the drag coefficient. Just as obvious is that no trend has been established permitting prediction of system performance at altitudes above 100,000 ft. All the test data have been rechecked to ensure the validity of the drag values obtained. One factor investigated was the effect of superheating of the inflation air. To obtain full geometry, each of the BALLUTEs was inflated with the exhaust from a tank-type vacuum cleaner prior to dropping. This

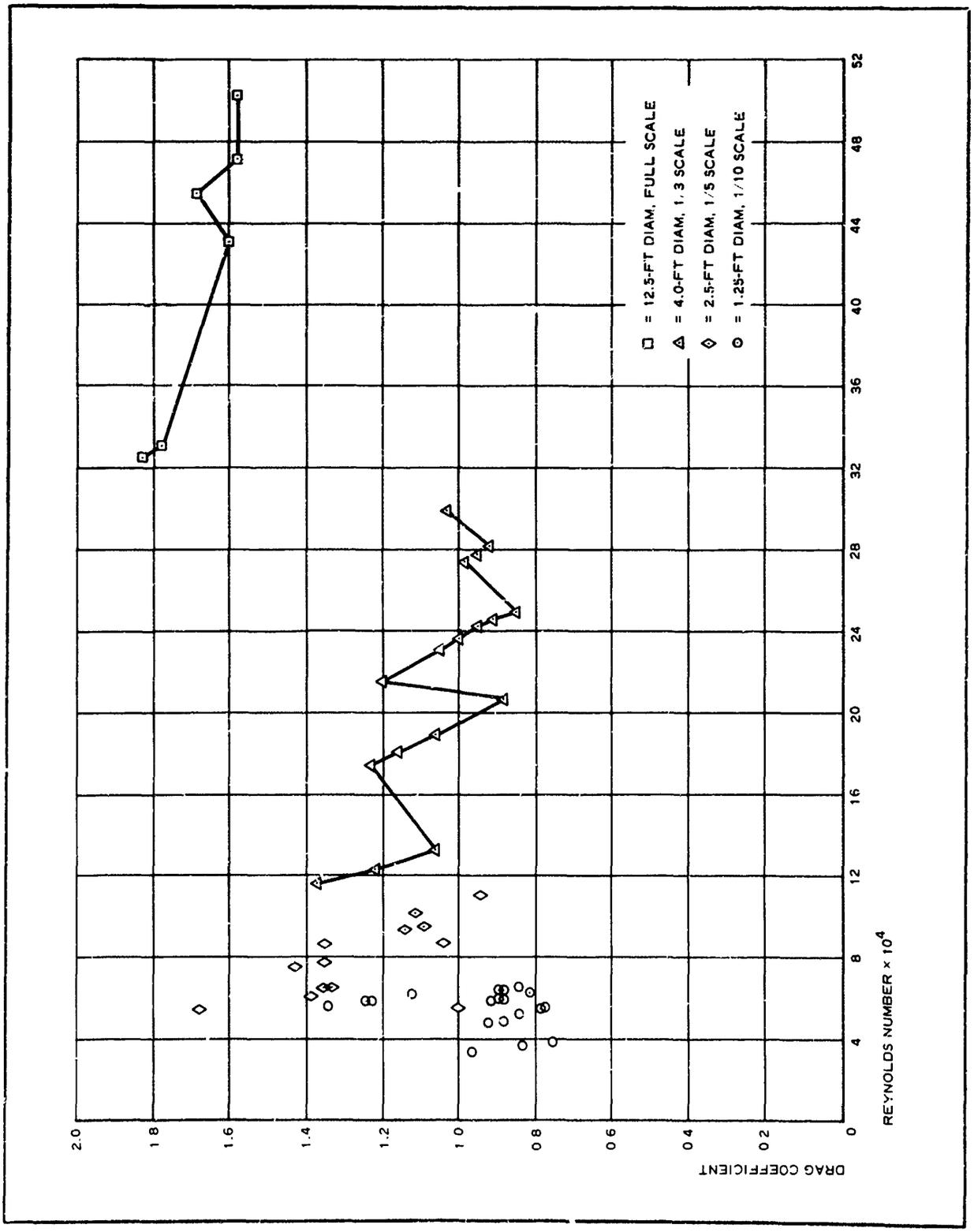

Figure 25 - Variation of C_D with Reynolds Number in Series 9 Drop Tests

warm air could have provided sufficient buoyant lift to the BALLUTE system to invalidate the C_D values. The buoyancy effect becomes especially critical in the 600-cu-ft full-scale BALLUTE.

Time-temperature checks of the inflation gas were made with the 12.5-ft-diam inflated BALLUTE. When initially inflated, the BALLUTE had internal temperatures of 5 to 7 F higher than ambient. After five minutes, the differential was less than 3 F. To define further the cooling rate, the inflation air was superheated to 30 F above ambient and allowed to cool. After 15 minutes, the differential was again less than 5 F. In the actual drop test program, the BALLUTE was inflated, dropped, and hauled back to the airdock's top without being deflated. Subsequent tests required only "topping-off" of the BALLUTE with about 5 to 10 percent of the total gas volume. Since a series of tests sometimes required several hours, the temperature differential must have been relatively small. The conclusion is that the data were affected by the lift factor, thus reducing the drag coefficients presented for the full-scale BALLUTEs. The error should not have exceeded 10 percent, which would not have substantially changed the performance picture.

Excellent stability and repeated drag coefficients greater than 1.0 show that the mission will be accomplished with the current configuration.

SECTION IV

PROTOTYPE DESIGN

1. GENERAL

After the extensive airdock drop test program was completed, the performance of the hexsymmetric BALLUTE[a] appeared sufficient to warrant freezing the design with this configuration. The stability of this BALLUTE was within the ±3-deg requirement in all the model sizes tested.

Besides stability the hexsymmetric BALLUTE yielded the highest C_D values of all configurations tested. Although the ratio of C_D values with BALLUTE size was still unexplained, the use of a $C_D = 1.2$ based on the drag efficiency of the larger BALLUTE models seemed appropriate, even though full-scale Reynolds number was not properly duplicated.

Assuming that $C_D = 1.2$, and knowing that W/C_DA required $= 0.055$ and $W = 9$, then

$$A = \frac{9}{1.2 \times 0.054}$$

$$= 136 \text{ sq ft}.$$

A hexsymmetric BALLUTE of 136 sq ft is 12-1/2 ft across the flats of the hexagon.

For eventual low-cost production, the 0.0004-in.-thick polyamide film construction was chosen for the prototype design, even though the seaming techniques had not yet been completely developed (see Figure 26).

2. RAM-AIR INLET

The method of erecting the ram-air inlet with eight beryllium-copper leaf

[a]See Series 9, Appendix I.

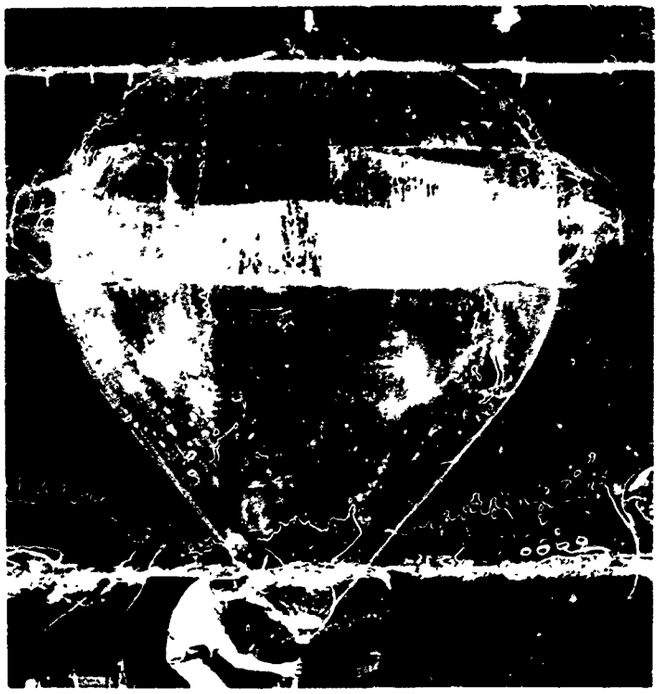

Figure 26 - Prototype 12-1/2-Ft-Diam Hexsymmetric Polyamide Film BALLUTE

springs had been checked out in two functional tests of the deployment system. The BALLUTE was ejected from its canister using the standard Arcas separation device. These tests resulted in positive erection of the ram-air inlet without damage to the adjacent film.

Some minor scortching of the BALLUTE near the apex resulted from the separation charge flash, but was not considered sufficient to warrant further action at this time.

The inlet orifice was nine inches in diameter, which would effect full inflation of the BALLUTE at about 2800-ft altitude if no auxiliary inflation were considered. The pressure ratio, however, of the atmosphere at launch and at apogee is about 8000/1. Expansion of residual air trapped within the packaged BALLUTE accounts for some portion of initial inflation.

The volume occupied by the packaged BALLUTE is

$$V_{l_T} = 122 \text{ cu in.}$$

of which the volume of the BALLUTE material is

$$V_{l_B} = 28 \text{ cu in.}$$

$$V_{l_T} - V_{l_B} = V_{l_A}$$

$$= 94 \text{ cu in.}$$

= total volume of air in the package.

Since experience indicated that 50 percent of the total gas is trapped within the BALLUTE film and 50 percent of the total gas occupies the space between the external folds of the film, the amount of trapped air

$$\frac{V_{l_A}}{2} = \frac{94}{2}$$

$$= 47 \text{ cu in.}$$

$$= 0.027 \text{ cu ft}$$

$$= V_{l_{SL}}.$$

If none of the trapped air were permitted to escape during the two-minute flight from launch to 214,000 ft, the expansion would be

P_1 at sea level = 2116 psf

P_2 at 214,000 ft = 0.26 psf

V_1 trapped air = 0.027 cu ft

$$V_2 = \frac{P_1 V_1}{P_2}$$

$$= \frac{2.116 \times 10^3 \times 27 \times 10^{-3}}{26 \times 10^{-2}}$$

= 220 cu ft.

The inflated volume of the BALLUTE is 615 sq ft. The percentage of inflation resulting from residual trapped air is

$$\frac{220}{615} = 0.36 .$$

The resultant decrease of total inflation time required increases the altitude by about 1000 ft when terminal velocity is attained.

Although the 1/3 inflation due to residual air may not impose excessive loads on the BALLUTE film during initial expansion, volume reduction can be accomplished by minute perforations in the BALLUTE film with adequate bleed ports in the BALLUTE canister.

The prototype canister therefore can be summarized as follows:

Configuration - 80 deg hexsymmetric
Diameter - 12.5 ft
Weight - 2.08 lb
C_D - 1.2
Hydraulic area - 135 sq ft
Packaged volume - 122 cu in.
Material - 0.0004-in -thick polyamide film

SECTION V

LOW-ALTITUDE DROP TEST PROGRAM

1. PURPOSE

After the airdock drop tests, the next step in the functional testing of the BALLUTE was low-altitude aircraft drops. These tests provided an intermediate performance check prior to mission-altitude flights.

Of specific interest in the low-altitude drop test program were:

1. Drag coefficients under actual flight conditions
2. BALLUTE stability in winds
3. Wind-following characteristics of the system
4. Verification of deployment sequence and of inflation rates of the full-scale system

2. TEST PROGRAM (PART I)

a. General

Part I of this program was conducted 18 January 1965 at GAC's Wingfoot Lake facilities.

The aircraft used in the tests was a Hughes Model 269A two-place helicopter. The second man in the helicopter was a GAC engineer responsible for ground-station communications, test item ejection, and photographic coverage.

Four ground stations, linked by radio transceivers, combined to obtain the test data. The tests were coordinated by a central control station, which guided the aircraft and broadcast the countdown. The trailer used for this central control station served also as a staging

area for photographic equipment, test items, and associated hardware (see Figure 27).

Two theodolite tracking stations were located as shown in Figure 27. Each of these stations was operated by two men. The instruments used were manually operated, visual theodolites. Each station used a transceiver for communication, and the theodolite readings were recorded on magnetic tape. The fourth station contained a tower-mounted anemometer with an oscillograph readout.

The flight paths of the four BALLUTEs are shown in Figure 28. Release and impact points were defined by the azimuth reading from the theodolite stations. Altitude was determined by aircraft altimeter verified by inclination readings on the theodolites.

Data sheets for the tests are given in Appendix II.

b. General Conclusions

Test No. 1 was a 1/3 scale model of the hexagonal burble fence BALLUTE that performed satisfactorily in the airdock. The drag coefficient of 1.4 obtained in test No. 1 is higher than the drag coefficient recorded previously. The highest C_D value attained with the 1/3-scale model of the hexagonal burble fence BALLUTE was 1.37, but this value was obtained at a lower Reynolds number and weight. The extreme stability of this configuration was reconfirmed.

Test No. 2 confirmed the previous data on Configuration No. 54 in the airdock.

Test No. 3 determined the efficiency of the corner reflector as a tracking aid in future high-altitude flights.

The X-band surveillance radar at Akron-Canton Airport was unable to distinguish the BALLUTE from the helicopter. Once again, the drag coefficient of 0.85 was higher than the coefficient of 0.65 in the airdock drop tests.

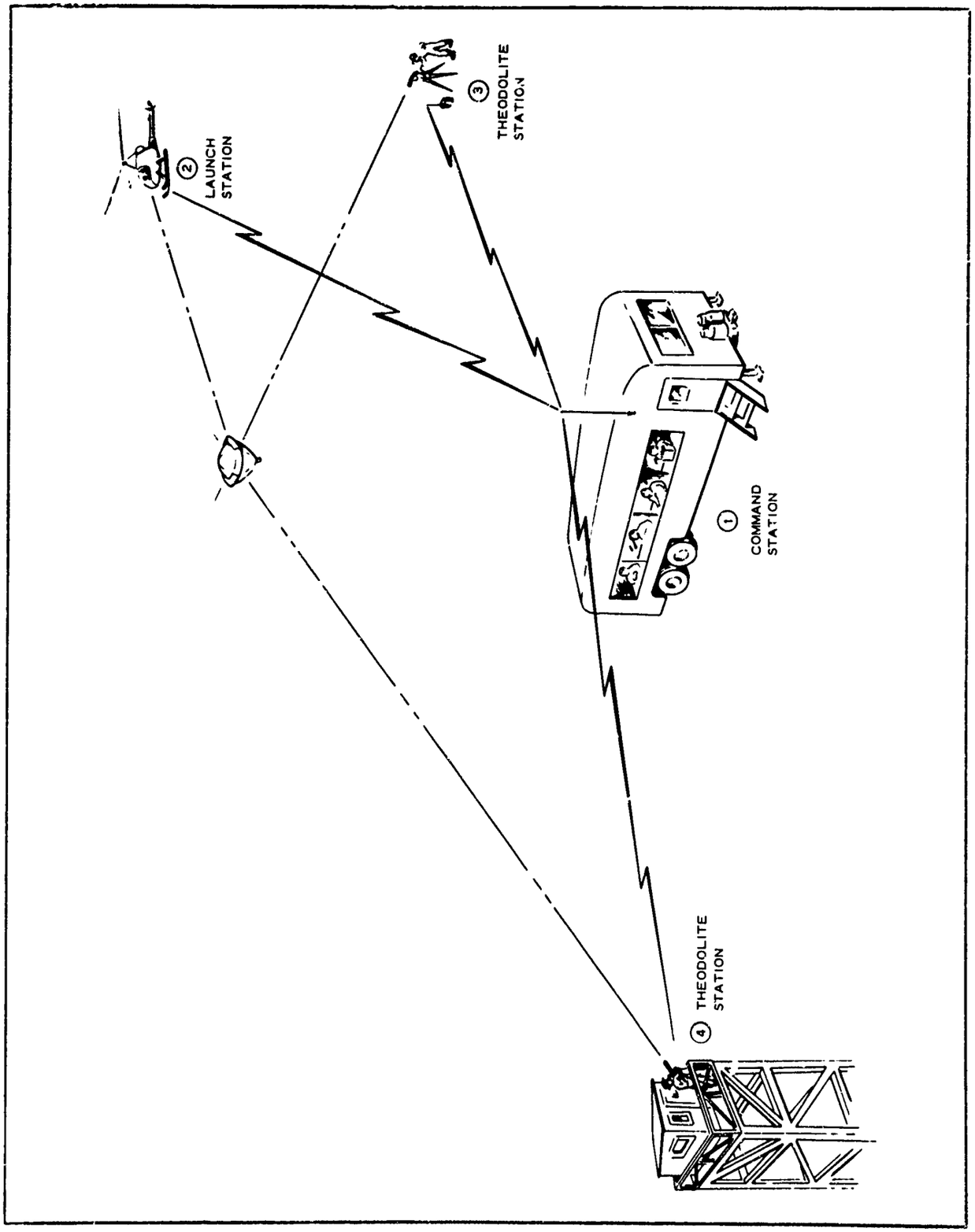

Figure 27 - Schematic of Control and Tracking Facilities

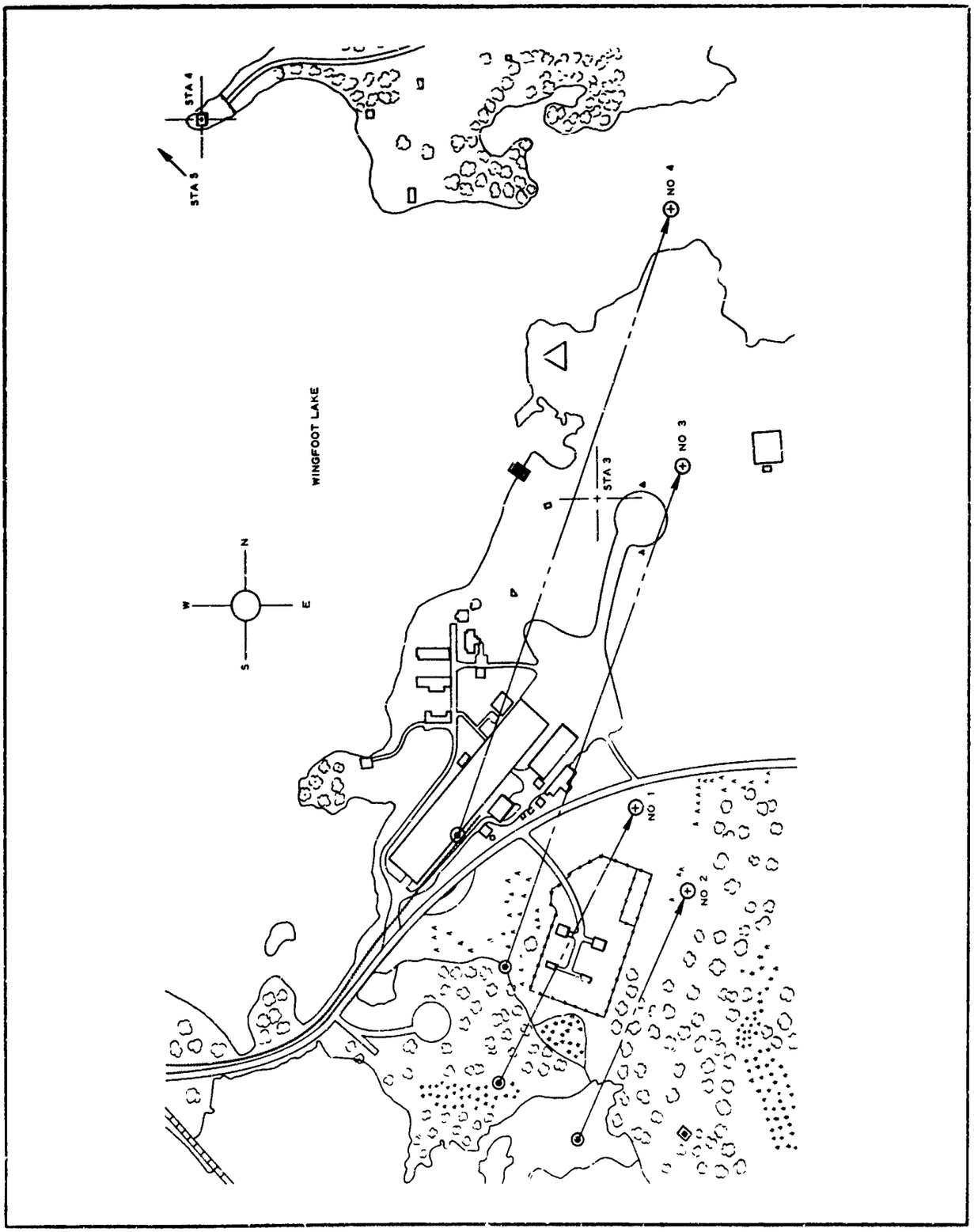

Figure 28 - Flight Paths of Test Items in Part I of Low-Altitude Drop Tests

The inlet geometry of the full-scale 12.5-ft diam BALLUTE requires 2800 to 3000 ft of free fall for full inflation. Due to low ceiling at test time, 1400 ft was the highest attainable altitude for test No. 4.

Although the full-scale BALLUTE was only about 50 percent inflated at impact, the test pointed out several important features:

1. Unfurling of the BALLUTE was immediate and smooth.
2. Orientation of the inlet normal to the air flow was quite constant.
3. The BALLUTE construction will withstand deployment and inflation dynamic pressures.
4. The flagging of the partially inflated BALLUTE was not excessive.
5. Even during the inflation period, the overall configuration is stable, although a lift factor is probably present due to asymmetry.

3. TEST PROGRAM (PART II)

The second phase of the low-altitude drop test program was conducted on 8 April 1965 at the aerial-drop facility of the Ravenna Army Ammunition Plant, Wayland, Ohio. The Ravenna site was chosen for these low-altitude drop tests because it afforded a larger impact area than the Wingfoot Lake facility for full-inflation drops from 3000 ft.

Six drops were made in the sequence given in Table 2.

All BALLUTEs[a] were constructed of 0.0004 in. nylon film and were 12-1/2 ft in diameter. The BALLUTE in test No. 1 was packed in the normal fashion, as shown in Figure 29.

[a]See BALLUTE No. 3, 4, and 5, Appendix III.

TABLE 2 - LOW-ALTITUDE DROP TESTS

Drop no.	Altitude (ft)	Payload (lb)	Type pack	Remarks
1	2200	7.0	Accordion	Payload separation
2	2200	7.0	Accordion	Aft panel rupture
3	2000	7.0	Accordion	Payload separation
4	2500	5.0	Hard twist	Incomplete inflation
5	2500	5.0	Medium twist	Aft panel rupture
6	2500	7.5	Canister	Payload separation

The package was dropped from the helicopter when the BALLUTE was partially inflated. Separation of the payload occurred immediately (Figure 30A). The separation point was just aft of the reinforced inlet area (Figure 30B).

The BALLUTE for drop No. 2 was packed or folded in the same manner

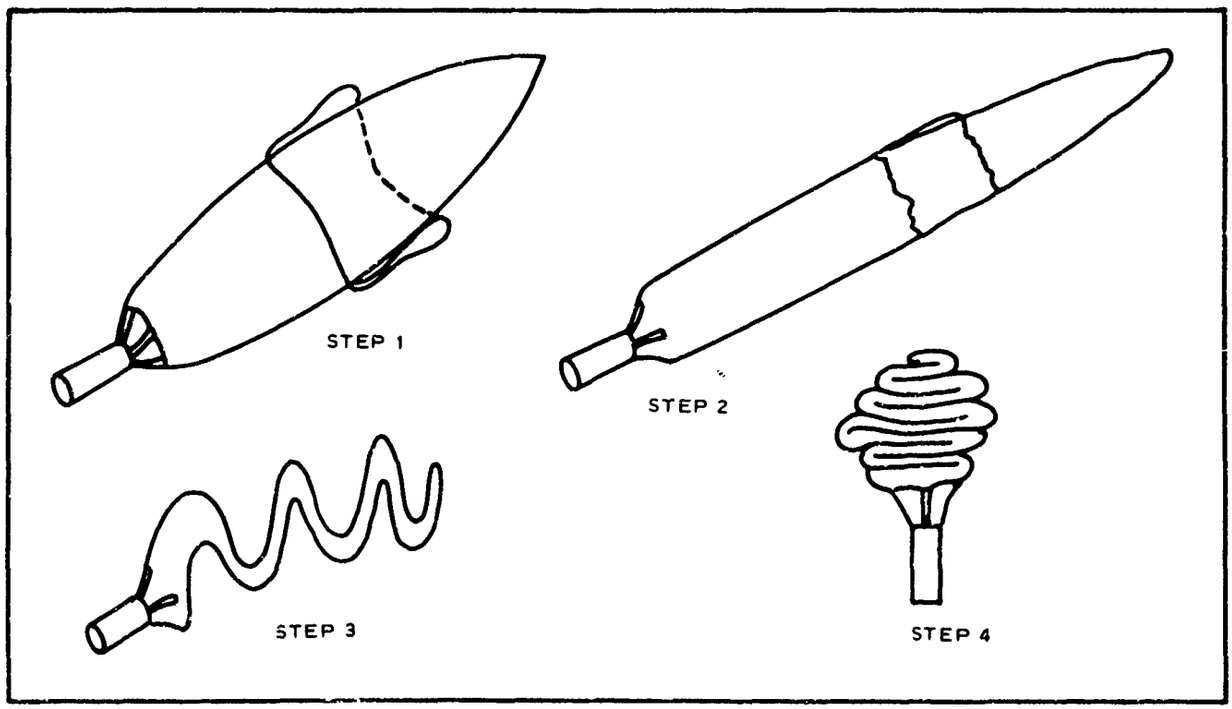

Figure 29 - Folding Procedure for BALLUTE in Test No. 1

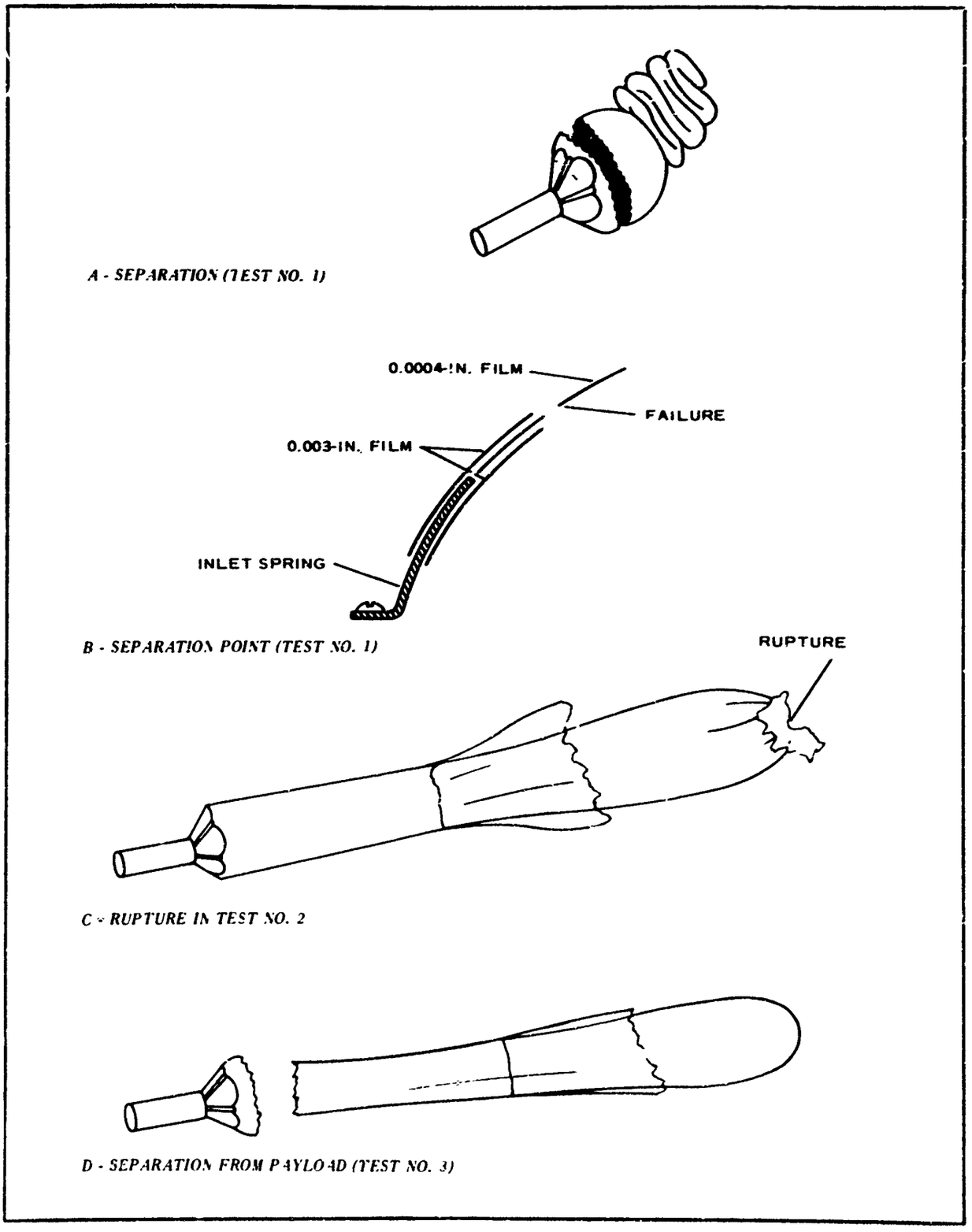

Figure 30 - Separation and Rupture Sketches

as for drop No. 1. The BALLUTE unfurled to its full length; then rupture occurred in the aft panel (Figure 30C). Unit No. 3 was folded as before, and separation of the payload occurred at film stretch similar to test No. 1 (Figure 30D).

To prevent these deployment failures the BALLUTE for test No. 4 was packaged as shown in Figure 31A. When the unit was dropped from the aircraft, the BALLUTE began to inflate and unwind simultaneously (Figure 31B). A terminal spinning condition was reached when the BALLUTE had unwound about 50 percent of its length (Figure 31C).

Test No. 6 consisted of a camera payload and BALLUTE packaged in an Arcas container (Figure 32). Separation of the payload from the BALLUTE occurred upon ejection similar to test No. 1.

The conclusions of the low-altitude drop test program (Part II) are:

1. The testing of BALLUTEs in free fall at sea level provides a conservative qualification of the system's structural integrity due to the rapid buildup of dynamic pressure, compared with the q's at mission altitudes.
2. Three failures in six tests in the forward area of the BALLUTE indicate that the structure is marginal for sea level conditions.
3. Aft film failures can be prevented by proper packaging techniques.
4. The first changes indicated are reinforcements where failures occurred.

4. TEST PROGRAM (PART III)

The purpose of the Part III tests was to ensure the adequacy of the reinforcing design changes that had been made to eliminate deployment failures.

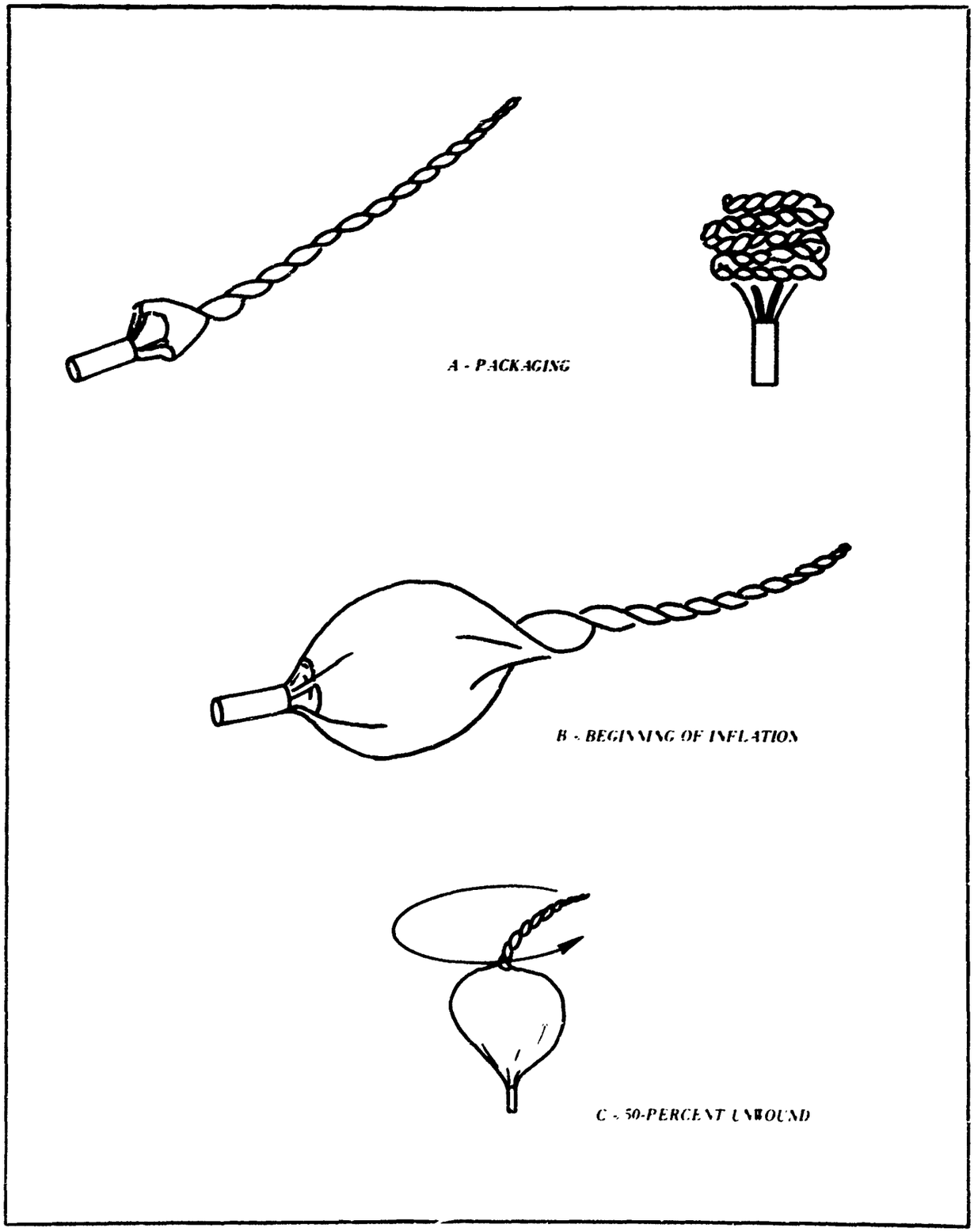

Figure 31 - Packaging and Deployment of Test No. 4

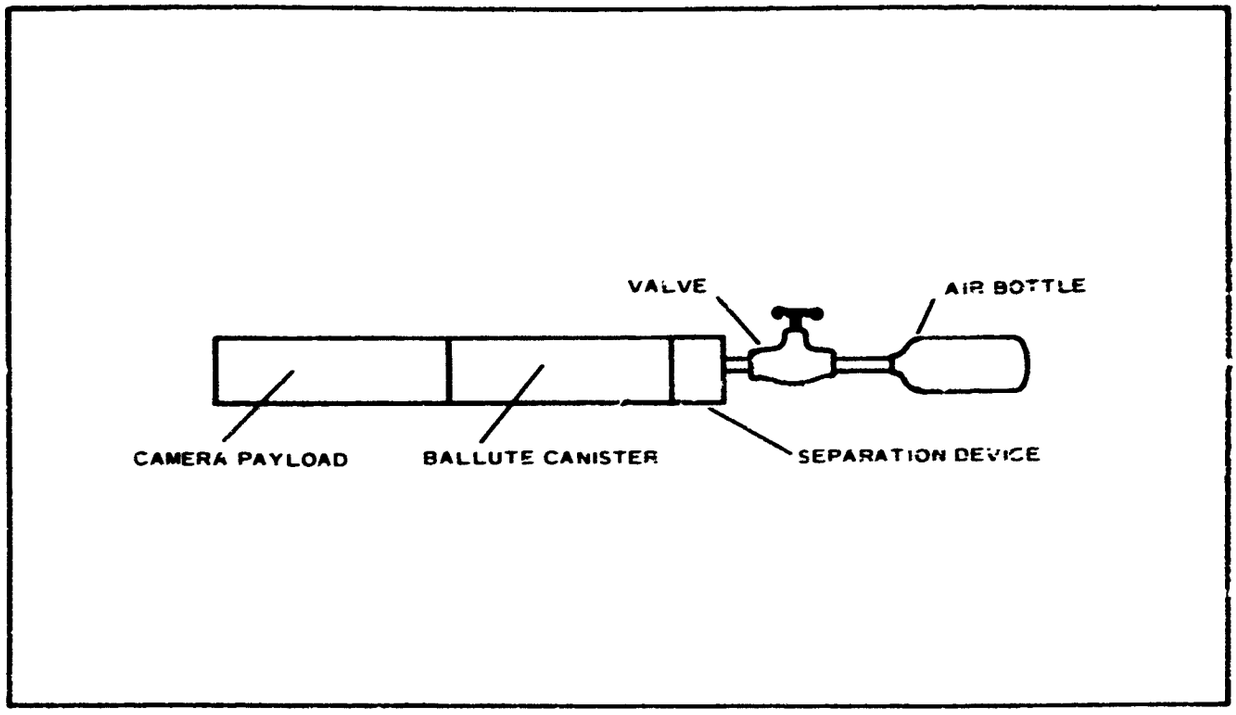

Figure 32 - Camera Payload and BALLUTE for Test No. 6

The basic film had previously been 0.0004-in.-thick polyamide film. For this strengthened redesigned configuration 0.0005-in.-thick polyester film was used for BALLUTE No. 7 (see Appendix III). BALLUTE No. 6 was constructed of the 0.0004-in.-thick polyamide film and incorporated the same reinforcements as BALLUTE No. 7, which are shown in Figure 33. The aft closure design is shown in Figure 34.

Two BALLUTEs were modified as shown in Figures 33 and 34. One of these was a refurbished 0.4-mil BALLUTE (No. 6, Appendix III) and the other a new 0.5-mil BALLUTE (No. 7, Appendix III) shown in Figure 35.

Each of these BALLUTEs was dropped three times with a five-pound payload from 800 ft in winds gusting to 30 knots. No deployment failures occurred, and inflation was normal regardless of the packing method used.

Because the maximum loading of the BALLUTE film occurs at the time of deployment, these successful tests at sea-level conditions were considered a conservative check of the system's structural integrity. The

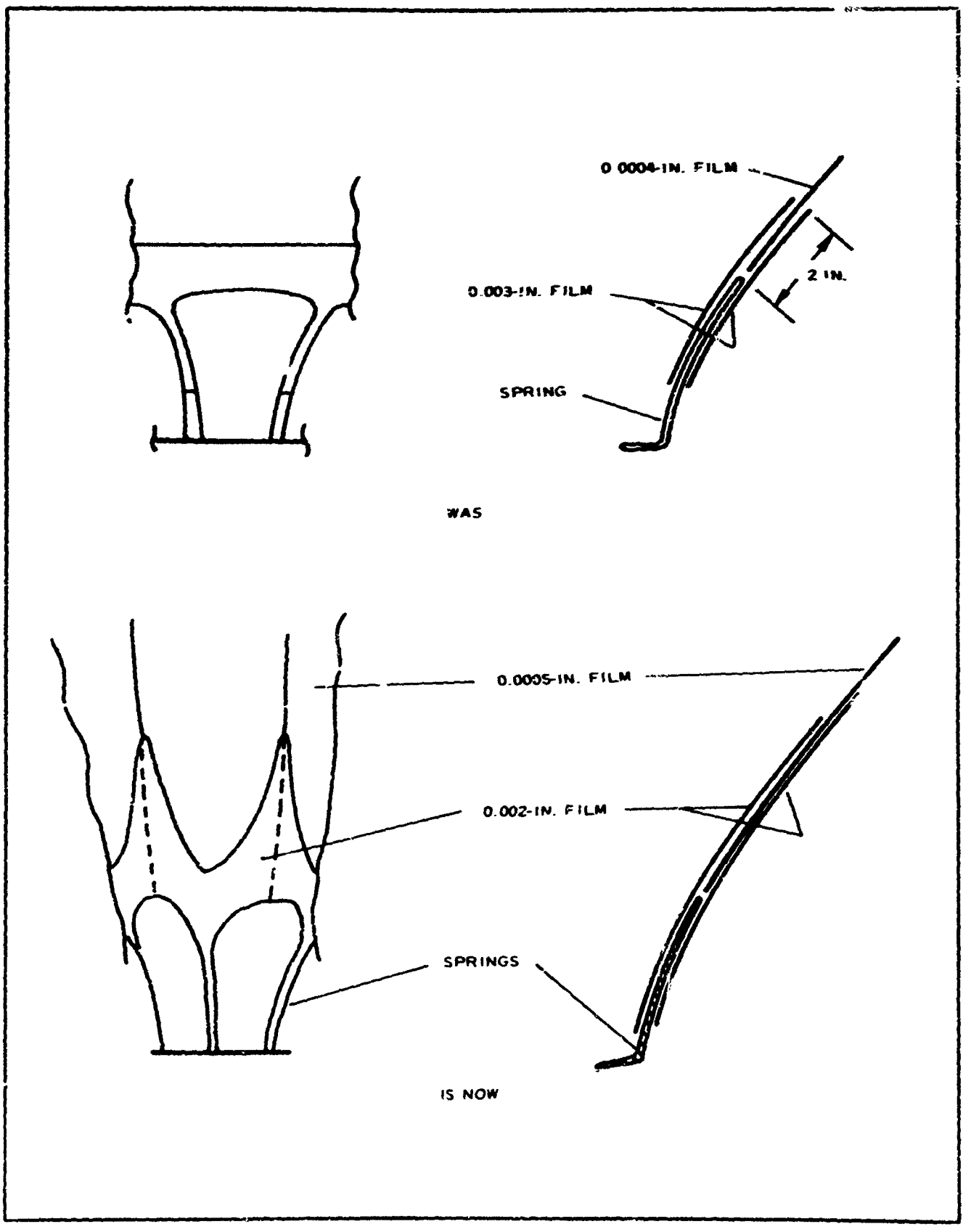

Figure 33 - BALLUTE Reinforcements

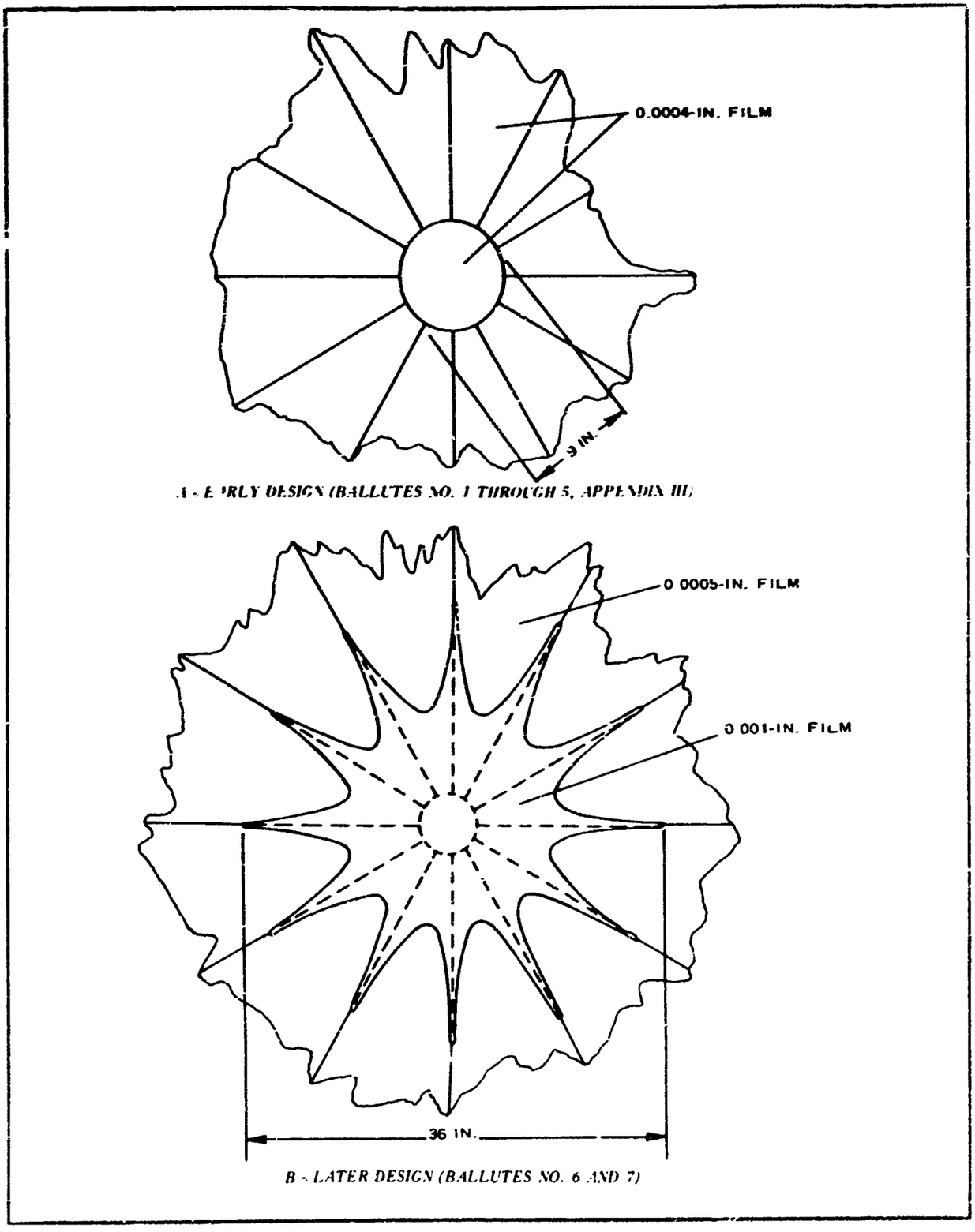

Figure 34 - Aft Closure Design

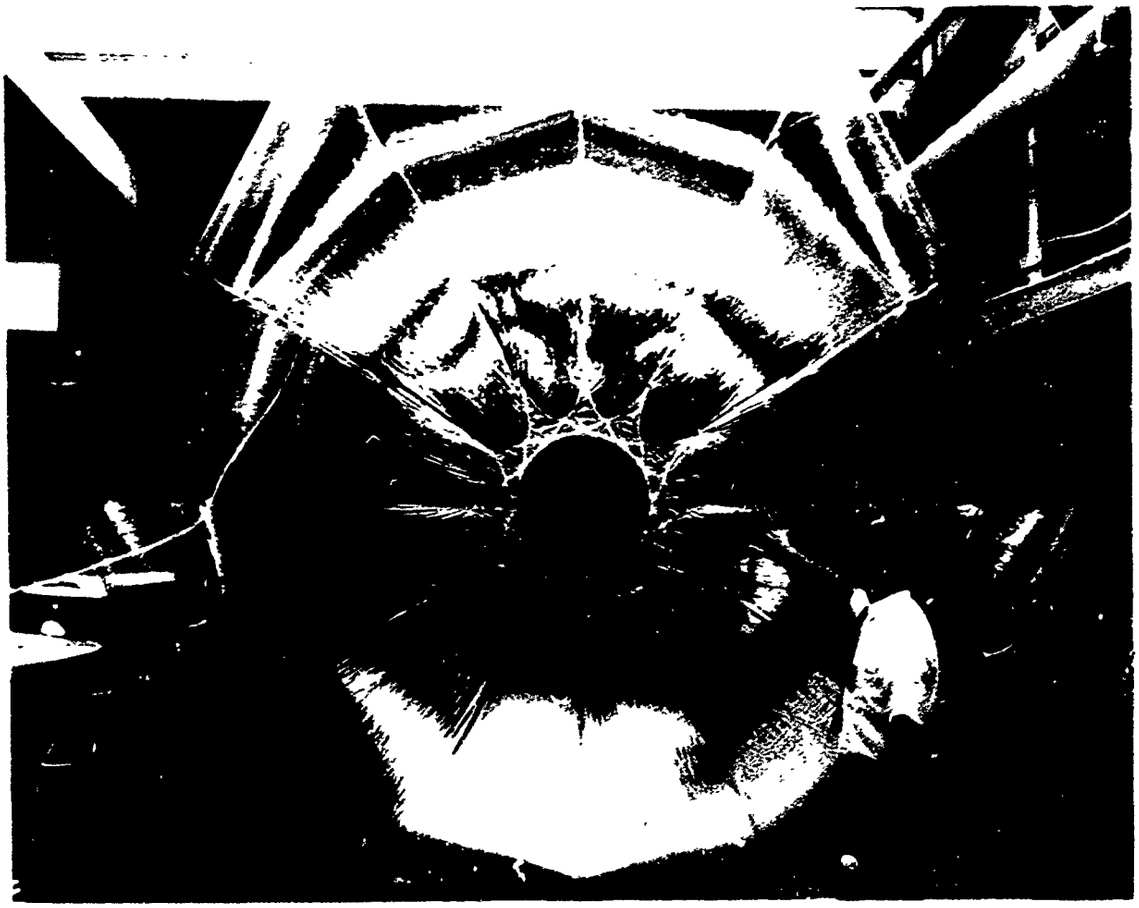

Figure 35 - Aft Construction Detail, 12-1/2-Ft Diam Hexsymmetric BALLUTE with Aluminized Gores

planned high-altitude drop test program would result in lesser deployment q's but would serve to confirm aerodynamic characteristics in the less-dense atmosphere.

SECTION VI

HIGH-ALTITUDE DROP TEST PROGRAM

1. PROGRAM OBJECTIVES

a. General

The high-altitude drop tests of the prototype BALLUTE system were designed to fill the development gap between the low-altitude drop tests and the rocket-powered flight test of the complete rocketsonde system. The specific areas of investigation and the method of data acquisition are discussed in this section.

b. Drag Efficiency

Confirmation of predicted C_D values closer to mission altitudes was to be obtained by determining descent velocities through skin-tracking radar data.

c. Stability

Both ground-based and onboard cameras were to have monitored the deviation of the descent configuration's axis from the line of flight.

d. Residual Air Effects

The rate of retardation, as determined by radar tracking and the aft-looking onboard camera, was to have provided evidence in determining the initial inflated volume attributable to residual air.

e. Ejection and Deployment

The aft-looking camera payload was to have showed any dynamics differences in the BALLUTE film during the inflation cycle, compared with dynamics differences in low-altitude inflation.

2. PROGRAM PLAN

The work statement of the contract defines the scope of the high-altitude drop test program. The effort was to have consisted of between four to six free-fall drops from altitudes of 100,000 ft or higher.

Tests were to be conducted at Holloman Air Force Base, N.M., with GFE lighter-than-air balloons, and launch and recovery operations.

Test configurations were as follows (BALLUTE No. 8, 9, 11, 12, Appendix III):

1. **Dummy payload with unpackaged BALLUTE**
2. **Camera payload with unpackaged BALLUTE**
3. **Dummy payload with canister-packed BALLUTE**
4. **Camera payload with canister-packed BALLUTE**
5. **Spare, to repeat any of tests 1 through 4**
6. **Spare, to repeat any of tests 1 through 4**

3. PROGRAM EXECUTION

a. General

During the pretest conferences at AFCRL Balloon R and D Branch, Holloman Air Force Base, modifications to the planned program were made because only two lighter-than-air ascension balloons were available. In order not to abbreviate the program, it was decided jointly to conduct at least two drop tests from each ascension balloon.

b. Flight Test No. 1

This first test was conducted on 4 May 1965. The launch configuration with the two unpackaged BALLUTE test items (No. 8 and 9, Appendix III) is shown in Figure 36. One test item was a dummy, and the other contained an aft-looking camera.

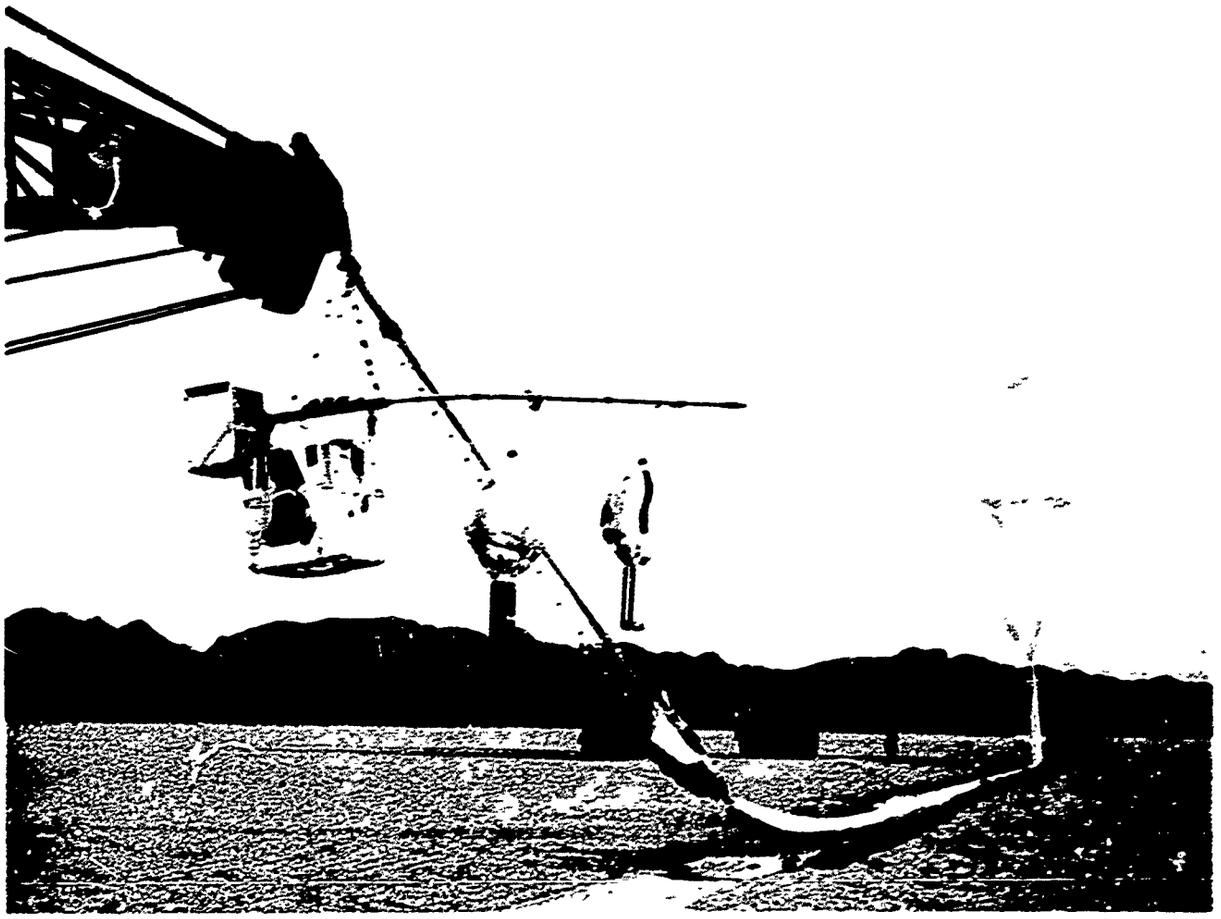

Figure 36 - Launch of High-Altitude Drop Test Showing Camera, Command Package, and Two BALLUTE Systems

The test items were to have been released at about 110,000 ft - first the dummy, followed by the camera in about five minutes.

The ascension balloon burst at an altitude of 60,000 ft, and the test items and command package descended on the recovery parachute. In attempting to obtain data, the first test item was released during this descent at about 55,000 ft. The tracking radar installation picked up several targets and tracked the largest to ground impact. The test item was not found, and it was not determined whether the item tracked was a test item or was a large fragment of the ascension balloon.

Two subsequent flights (No. 11 and 12, Appendix III) ended in failure of the ascension balloons, and no test item data were acquired.

The decision to abandon this portion of the program was made by the program monitor, with concurrence by GAC. The effort was immediately redirected to execution of the final phase, the rocket-launched flights at Cape Kennedy.

SECTION VII

ROCKET-LAUNCHED FLIGHT TESTS (PART I)

The test items used in the first two Arcas-boosted tests at Cape Kennedy used one polyamide (No. 10, Appendix III) and one polyester (No. 13, Appendix III) BALLUTE of the same configuration that was successfully tested in Part III of the low-altitude drop test program.

In each flight, the rocket ascent was normal, and apogee occurred at about 200,000 ft. Payload separation occurred at apogee on time. The descents of the payloads were tracked by radar to impact, and no deceleration attributable to the BALLUTE was noted. That BALLUTE failure occurred immediately upon deployment was evident.

Because of the lack of empirical data due to failure of the high-altitude test program, failure analysis for the rocket-launched tests must be based on a deductive review of the problem areas.

The review resulted in the following possible failure modes:

1. Film failure due to rapid inflation, which resulted from expansion of residual air
2. Film failure due to torsion, which resulted from the spin-rate differential between the rotating payload and the expanding BALLUTE
3. Tensile failure of the film due to the BALLUTE's initial drag
4. Film damage due to burning by separation charge's flash

The test program was interrupted, and a corrective redesign effort initiated.

SECTION VIII

PROTOTYPE REDESIGN

1. PURPOSE

The purpose of the prototype redesign was to construct an operational unit from which aerodynamic data might be obtained regardless of weight or of low-cost fabrication.

2. DESIGN CHANGES

To eliminate the effects of the 20-rps spin rate, a swivel assembly, shown in Figure 37, was incorporated. The swivel consisted of two needle-type thrust bearings that would permit rotational freedom for the swivel in relation to the BALLUTE, even under asymmetric loading conditions.

To eliminate excessive film loading in a concentrated area during inflating, a series of 12 meridian straps of 50-lb nylon webbing was incorporated as the main load bearing members. This network of meridian straps completely encaged the BALLUTE and provided for even drag-load distribution. The number of inlet springs was increased from 6 to 12. Each meridian strap, therefore, terminated at an inlet spring (Figure 38). The leading edge of the BALLUTE was reinforced with the same nylon webbing as shown in Figure 39.

Circumferential reinforcement of the BALLUTE was accomplished by the addition of nylon webbing at the fore and aft intersections of the gurble fence with the BALLUTE (Figure 40). The method of splicing the meridian straps at the BALLUTE's aft pole is shown in Figure 39.

The problem of residual air effects and of separation charge flash burns was handled by modification of the BALLUTE canister.

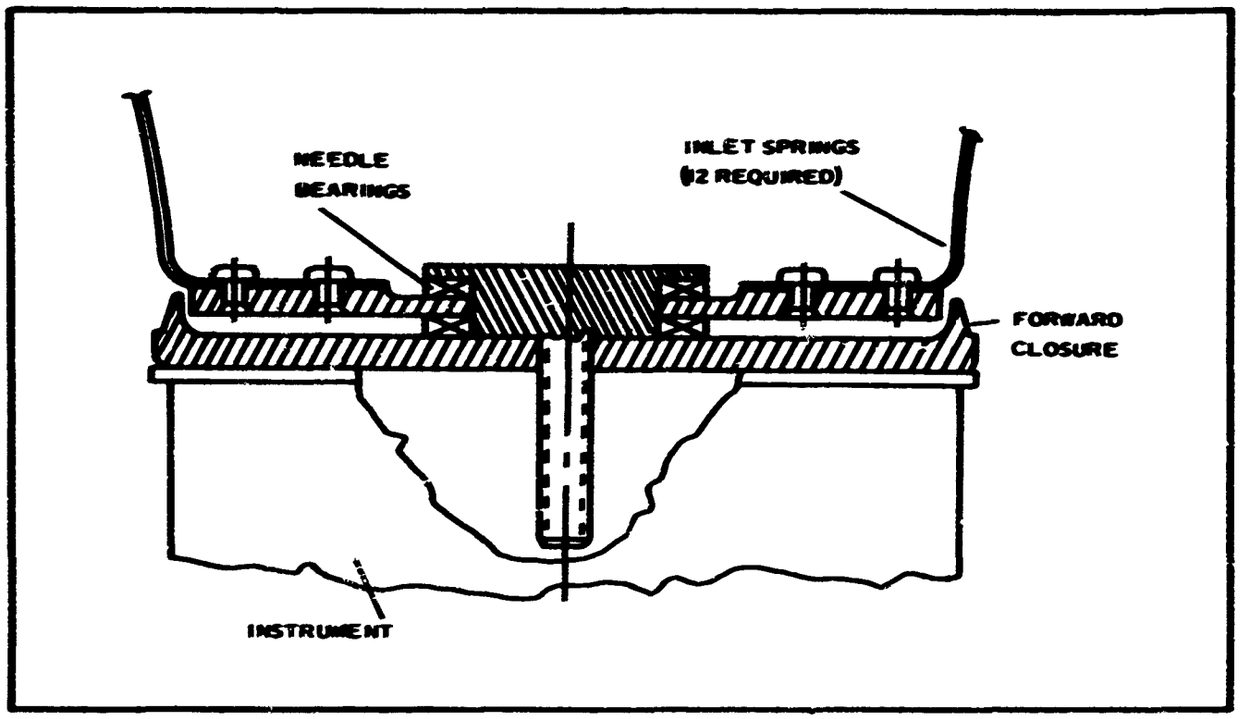

Figure 37 - Detail of Swivel Assembly

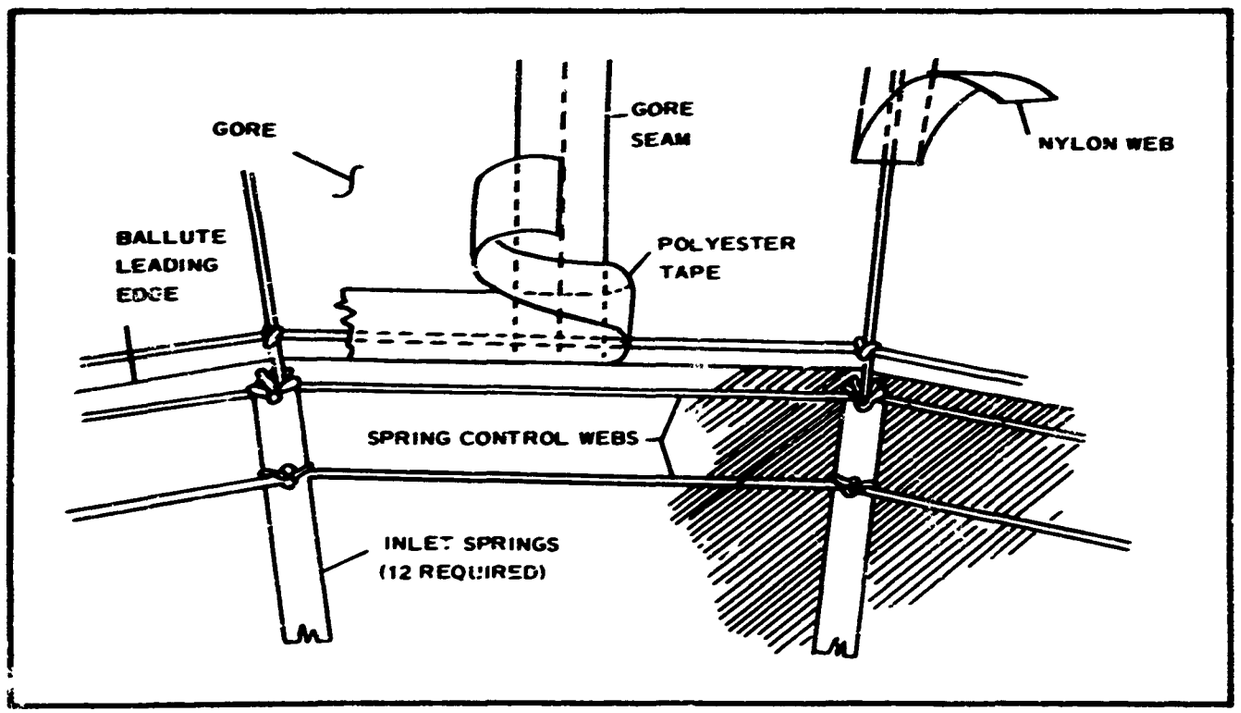

Figure 38 - Inlet Spring - BALLUTE Interface

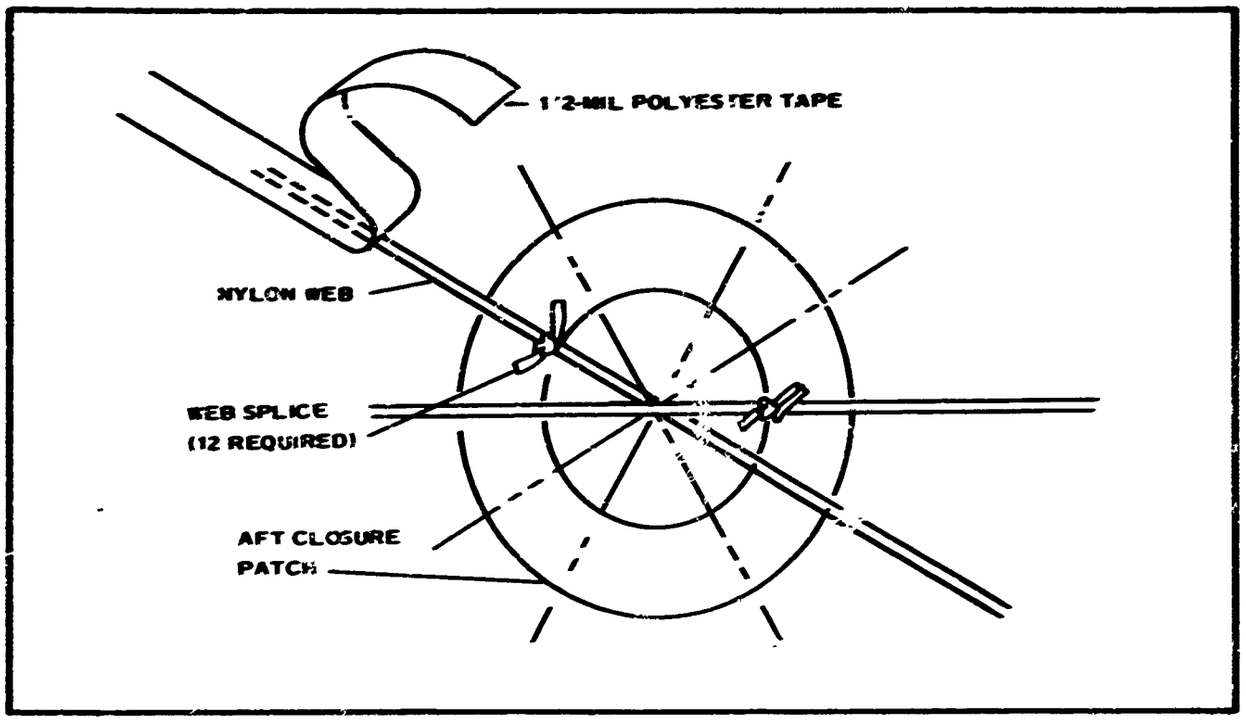

Figure 39 - Meridian Strap Splices

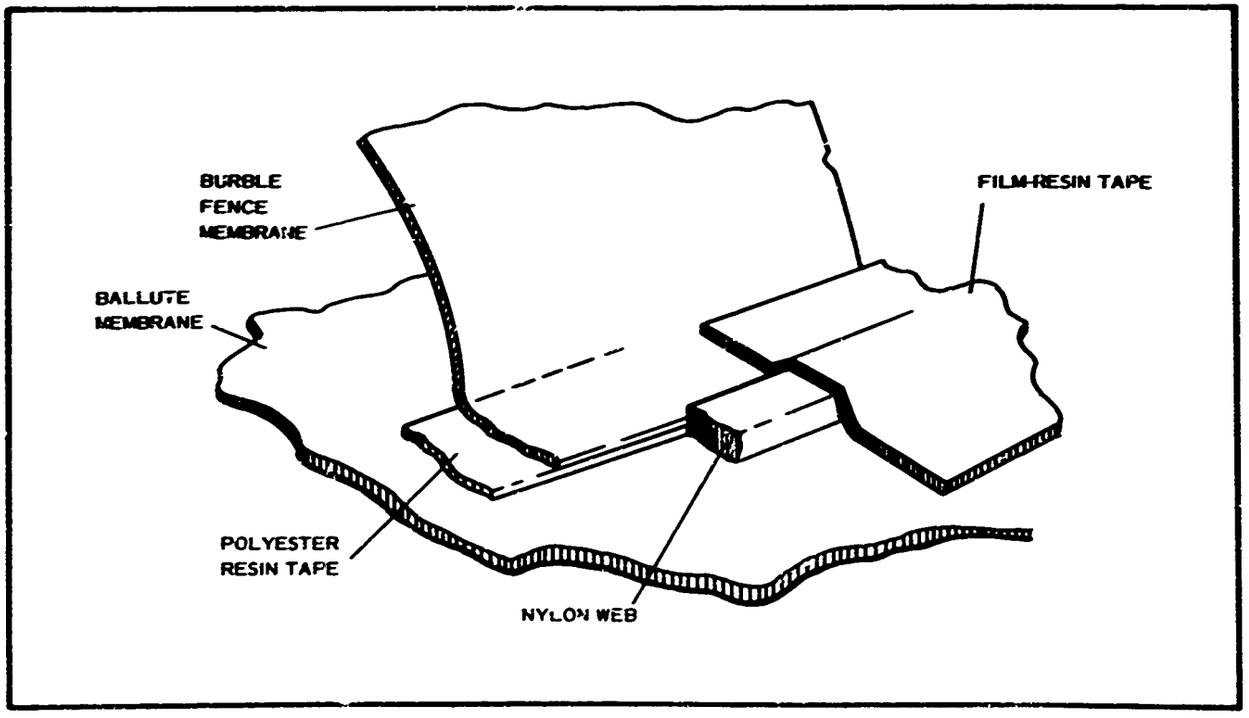

Figure 40 - Detail of Burble Fence Intersection

For the amount of trapped air to be reduced during the two-minute flight to apogee, a system of venting the canister was provided to permit evacuation of the interior when the ambient density decreased.

The standard, inner laminated fiberglass liners used in the parachute deployment system were modified for these tests. A series of 1/8-in.-diam holes was drilled one inch apart in both directions to provide air vents through the liners. In addition, a "wick" of porous fiberglass was added to both surfaces of each liner to permit maximum air passage from the BALLUTE to the ambient environment (see Figures 41, 42, and 43). Through this arrangement, the entire packaged BALLUTE was subjected to the negative pressure of the local ambient atmosphere.

The bleed holes in the canister were placed at the forward end to accomplish a secondary function - that of diverting a portion of the separation firing's incendiary effects. The ignition of the separation charge results in high-pressure, hot-gas generation behind the aft closure plate. These pressures move both the instrument and the packaged BALLUTE away from the rocket motor. When the aft closure plate passes the canister bleed holes, a portion of the hot gases will be harmlessly diverted through the canister bleed holes.

The incorporation of these changes resulted in a BALLUTE system weight of 3.12 lb. Since 3.12 lb represents a substantial weight increase, the descent velocities of the flight tests would be higher than the target descent rate. Once the aerodynamic characteristics are firmly established, a program of weight reduction and size increase can be accomplished within limitations of the existing BALLUTE canister.

Packaging of the prototype redesigned configuration is shown in Figures 44 through 53.

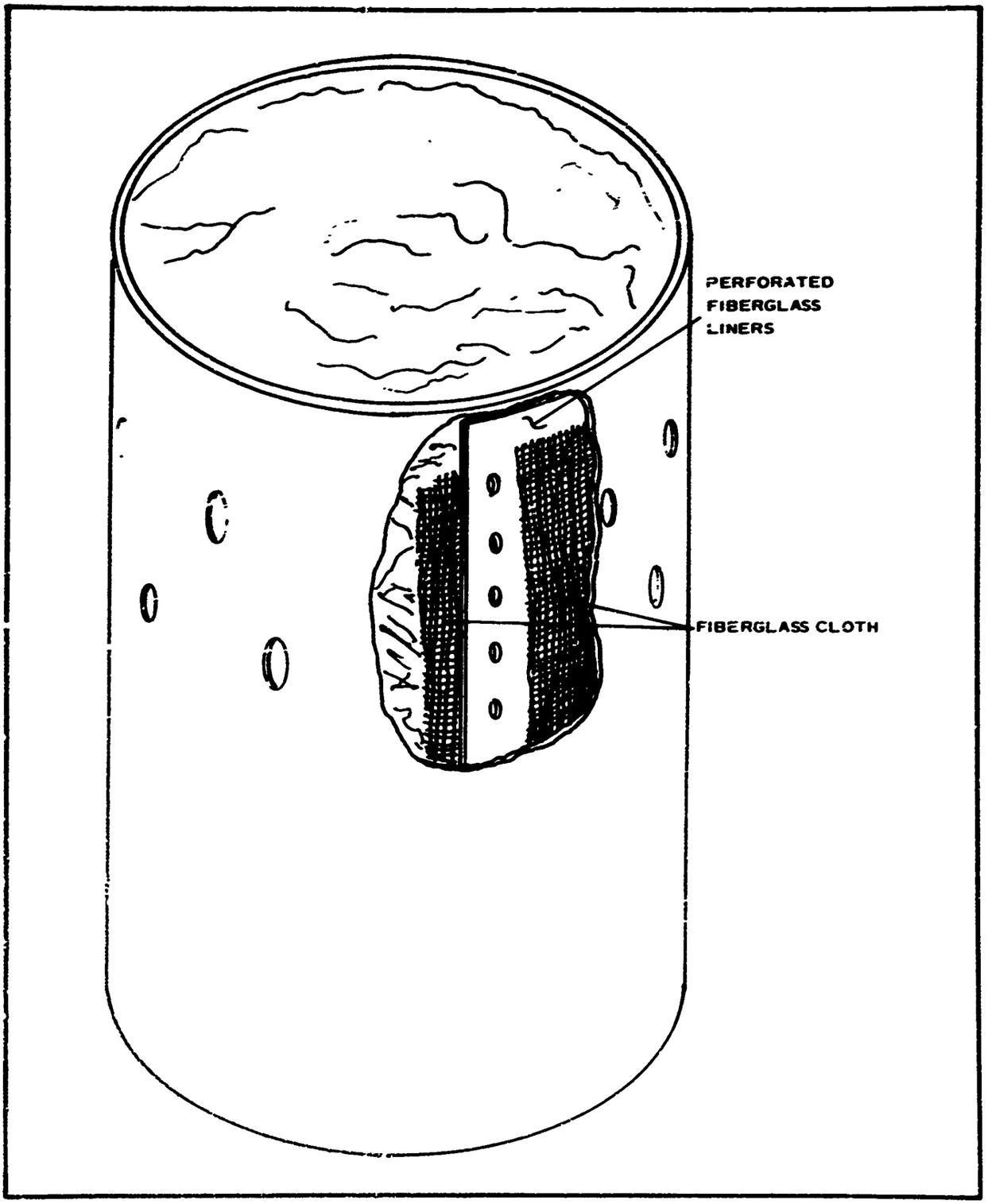

Figure 41 - Schematic of Packaged BALLUTE Showing Components of Bleed-Off System

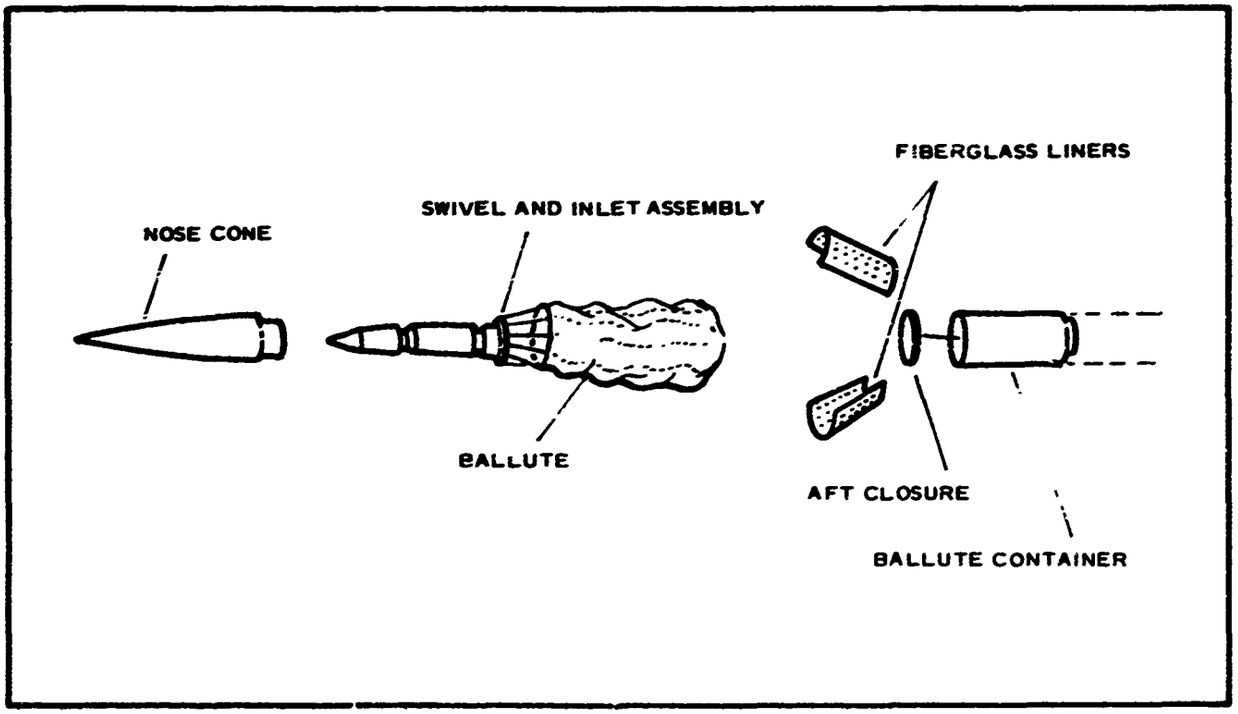

Figure 42 - BALLUTE Deployment Sequence

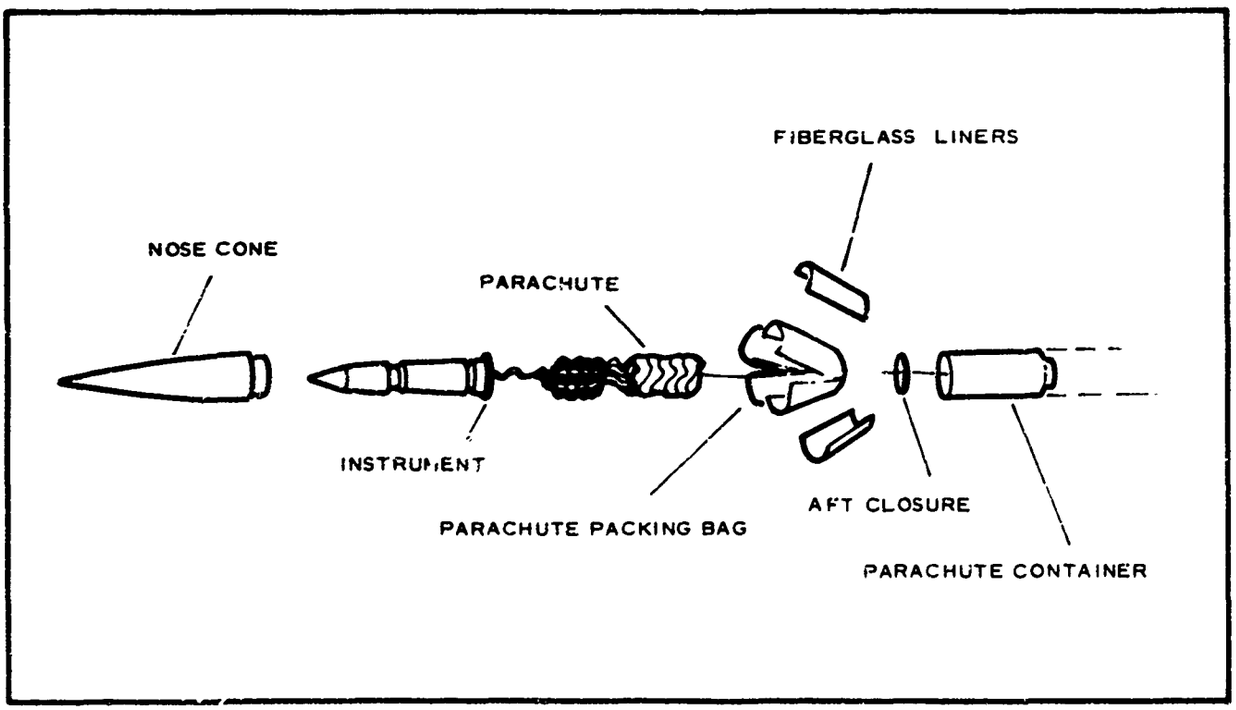

Figure 43 - Parachute Deployment Sequence

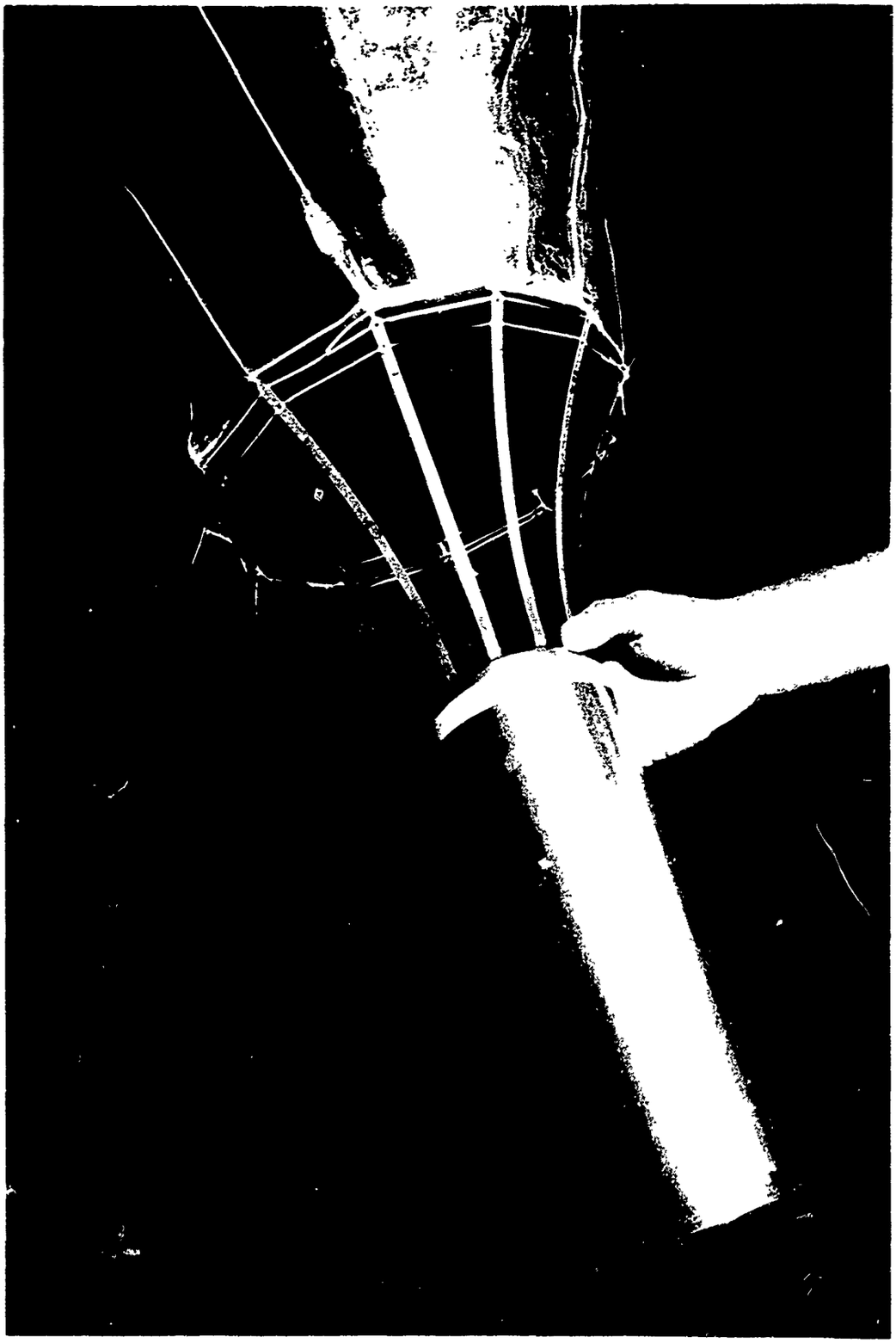

Figure 44 - Detail of BALLUTE Inlet Assembly

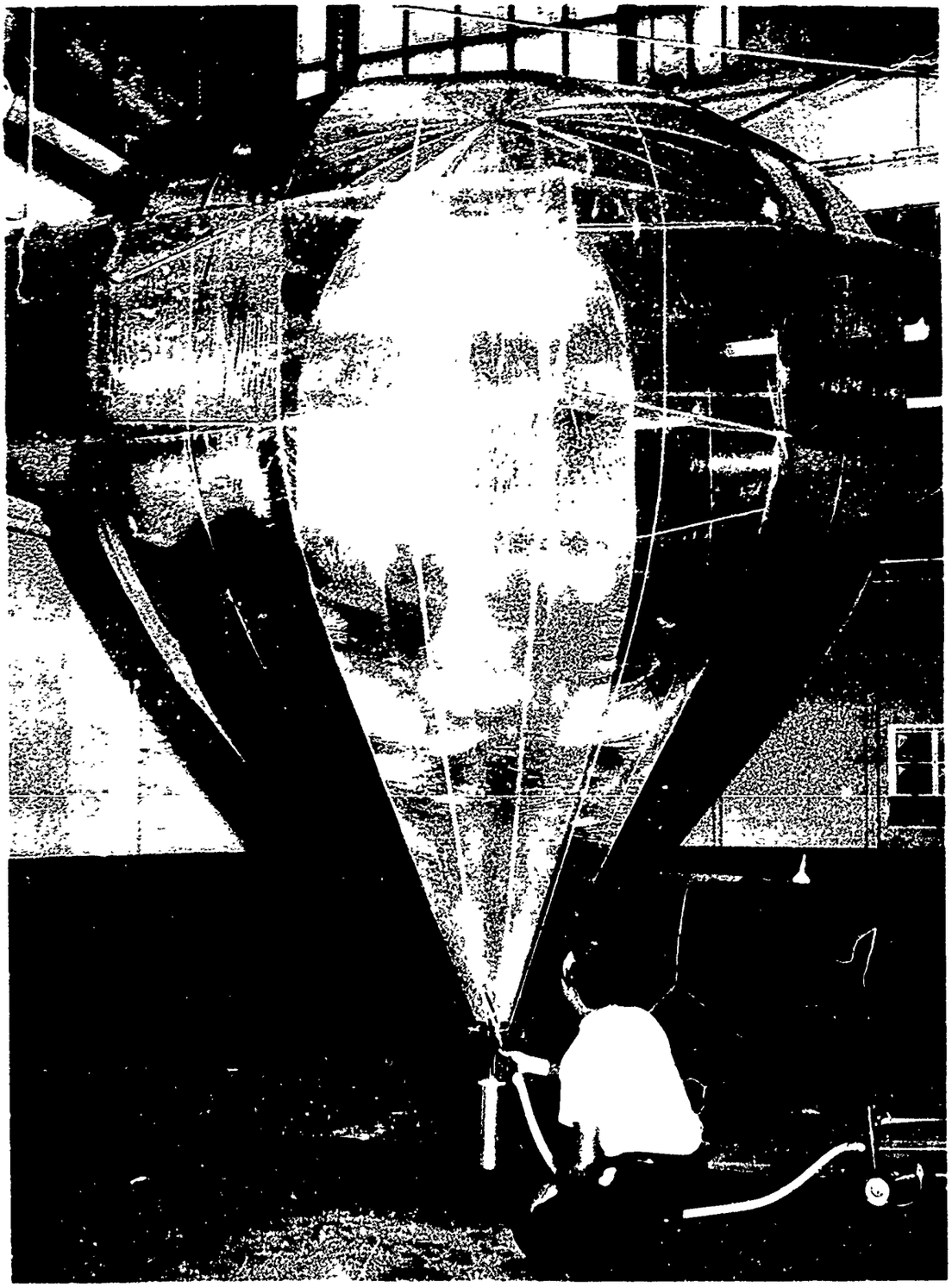

Figure 45 - Hexsymmetric BALLUTE (No. 14, 15, 16, Appendix III) with Alternate Gore Pairs Aluminized

Figure 46 - Folding the BALLUTE Prior to Vacuum Bagging

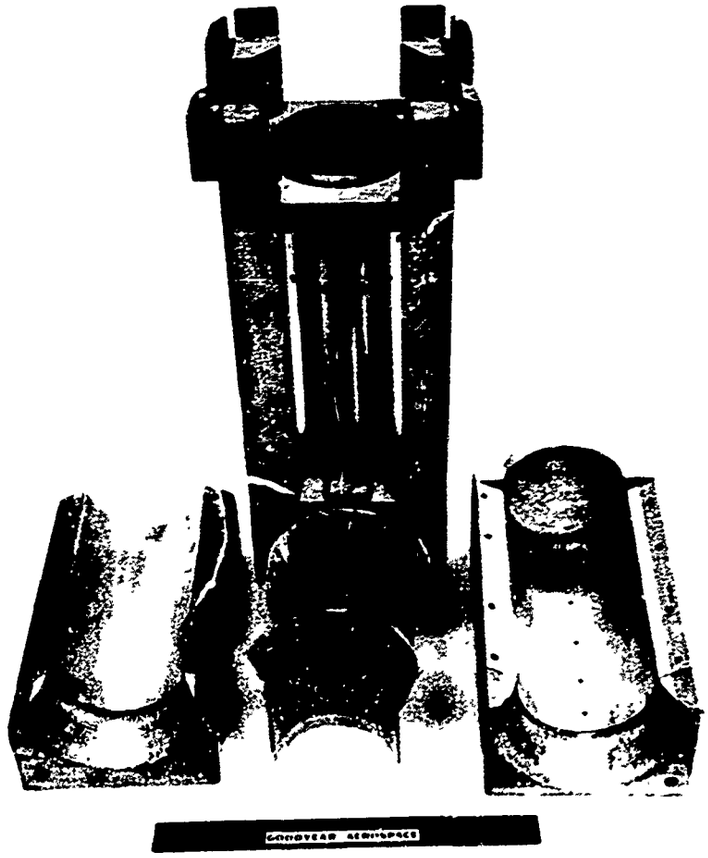

Figure 47 - BALLUTE Canister and Packing Aids

Figure 48 - BALLUTE in Vacuum Bag Prior to Insertion in Shaping Mold

Figure 49 - BALLUTE Under Vacuum in One Half of Shaping Mold

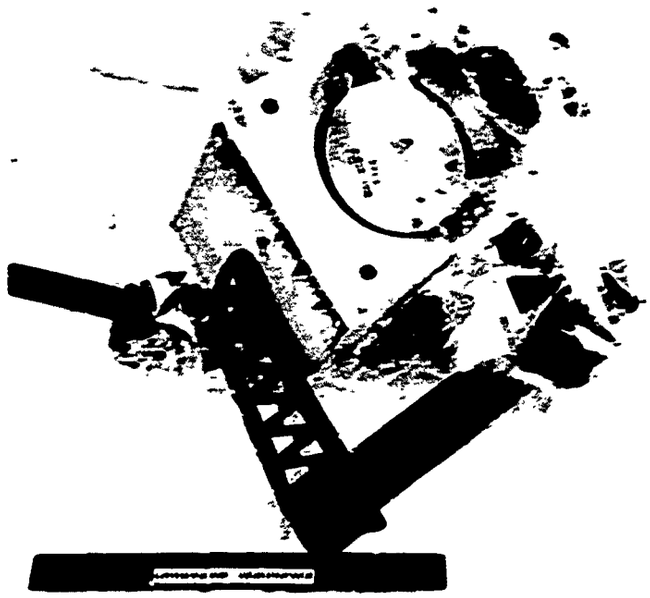

Figure 50 - BALLUTE Under Vacuum in Shaping Mold Ready for Transfer to Canister

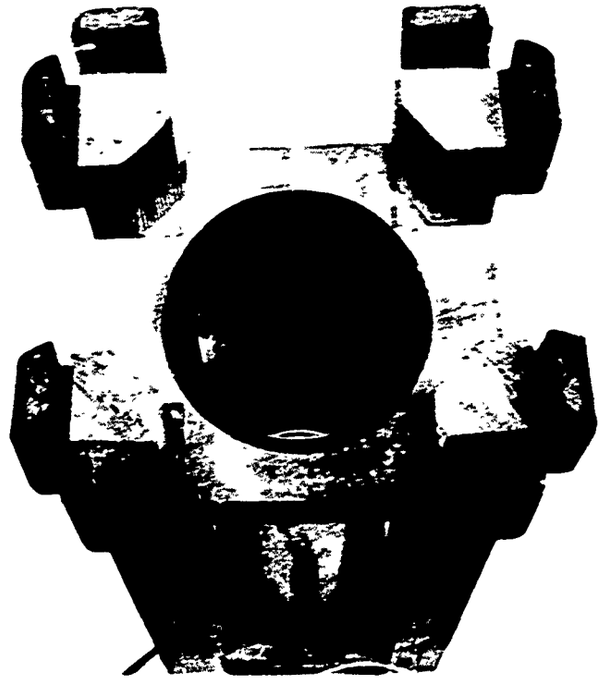

Figure 51 - BALLUTE Canister with Perforated Liners Ready to Receive BALLUTE Assembly

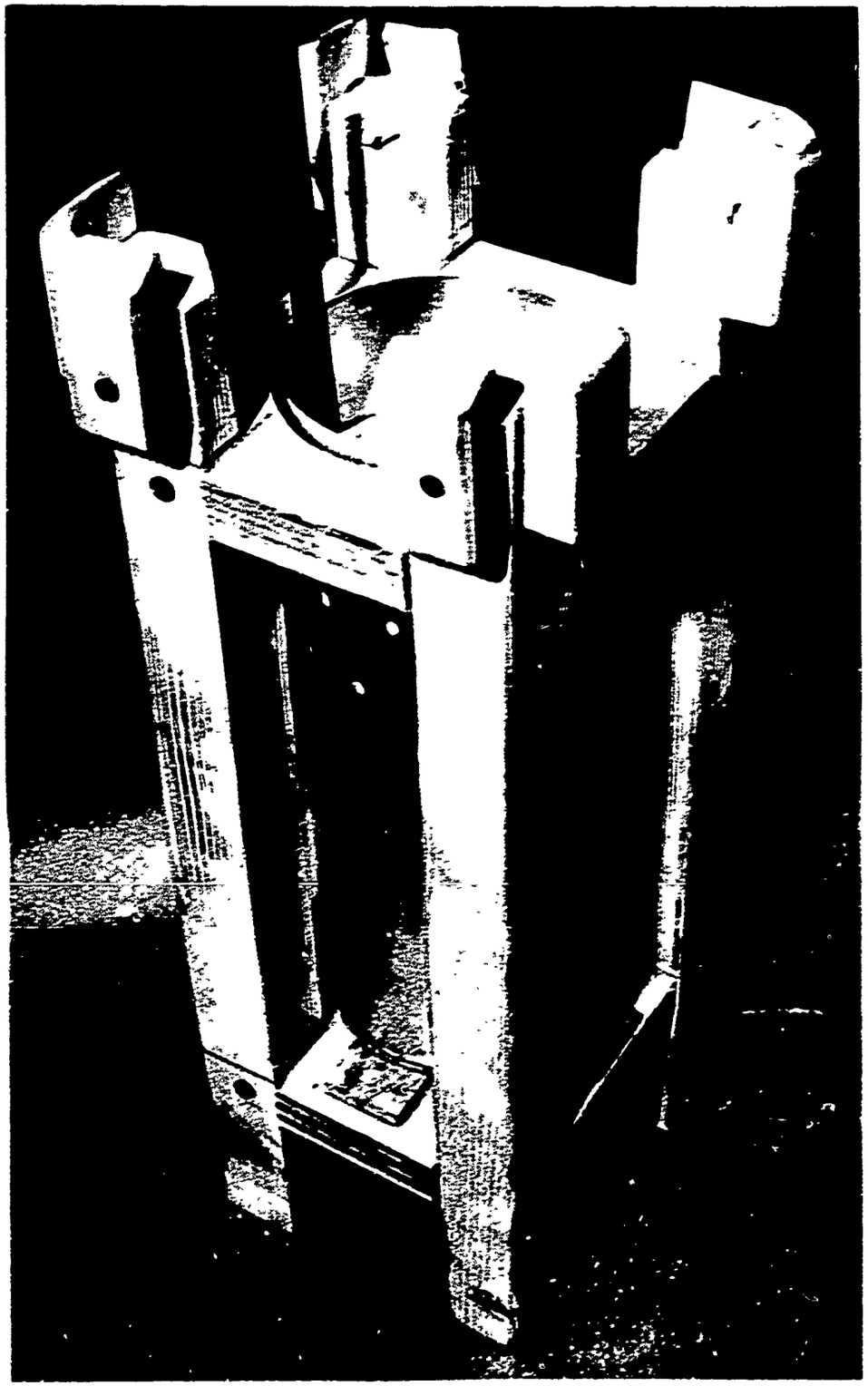

Figure 52 - Packaged BALLUTE Prior to Shear Pin Installation

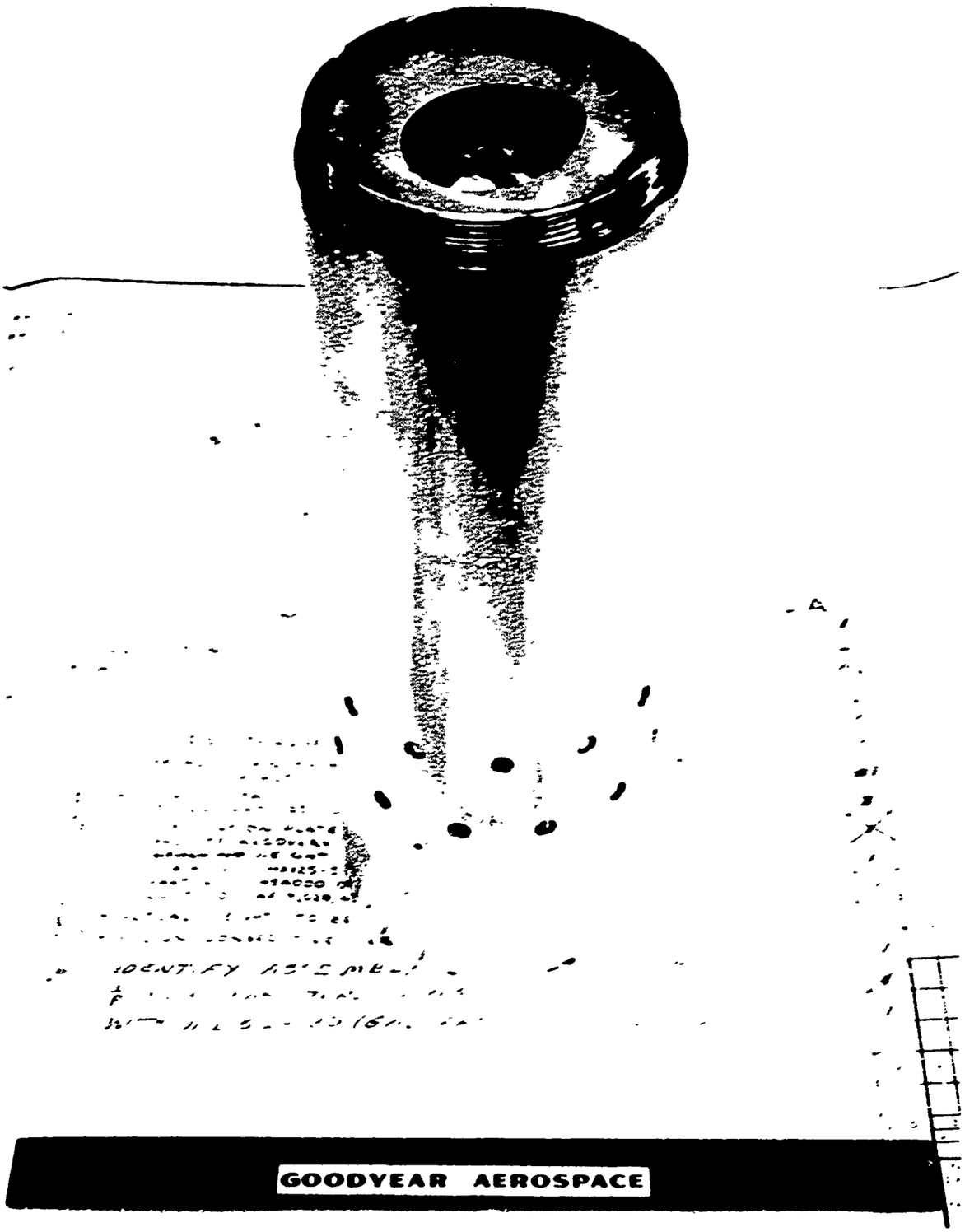

Figure 53 - Complete BALLUTE System Ready for Assembly to the Rocket Motor and Instrument

SECTION IX

ROCKET-LAUNCHED FLIGHT TESTS, PART II

1. PURPOSE

The primary objective of Part II of the rocket-launched flight tests was to obtain aerodynamic data on drag coefficients, degree of stability, and wind-sensing capability. All the forseeable structural contingencies had been reviewed, and appropriate reinforcements incorporated as described in Section VIII. All three of the units tested performed satisfactorily and produced the desired aerodynamic data. The unanticipated recovery of two systems resulted in acquiring valuable information through postflight examination of the BALLUTEs.

2. FLIGHT NO. 1 (BALLUTE NO. 14, APPENDIX III)

Data on the first rocket-launched flight are given below:

Flight no. - 4912
Date - 8 August 1965
Instrument - Arcasonde I-A
Instrument weight - 4.61 lb
BALLUTE weight - 3.12 lb
System weight - 7.73 lb

The data from this flight are based on tracking by two separate radar facilities - one an FPS-16 radar, the other an FPQ-6 installation. Figure 54 shows the vertical descent rate recorded by the FPS-16 radar. The vertical velocity fluctuates about the terminal velocity profile for a projectile with a $W/C_D A = 0.08$.

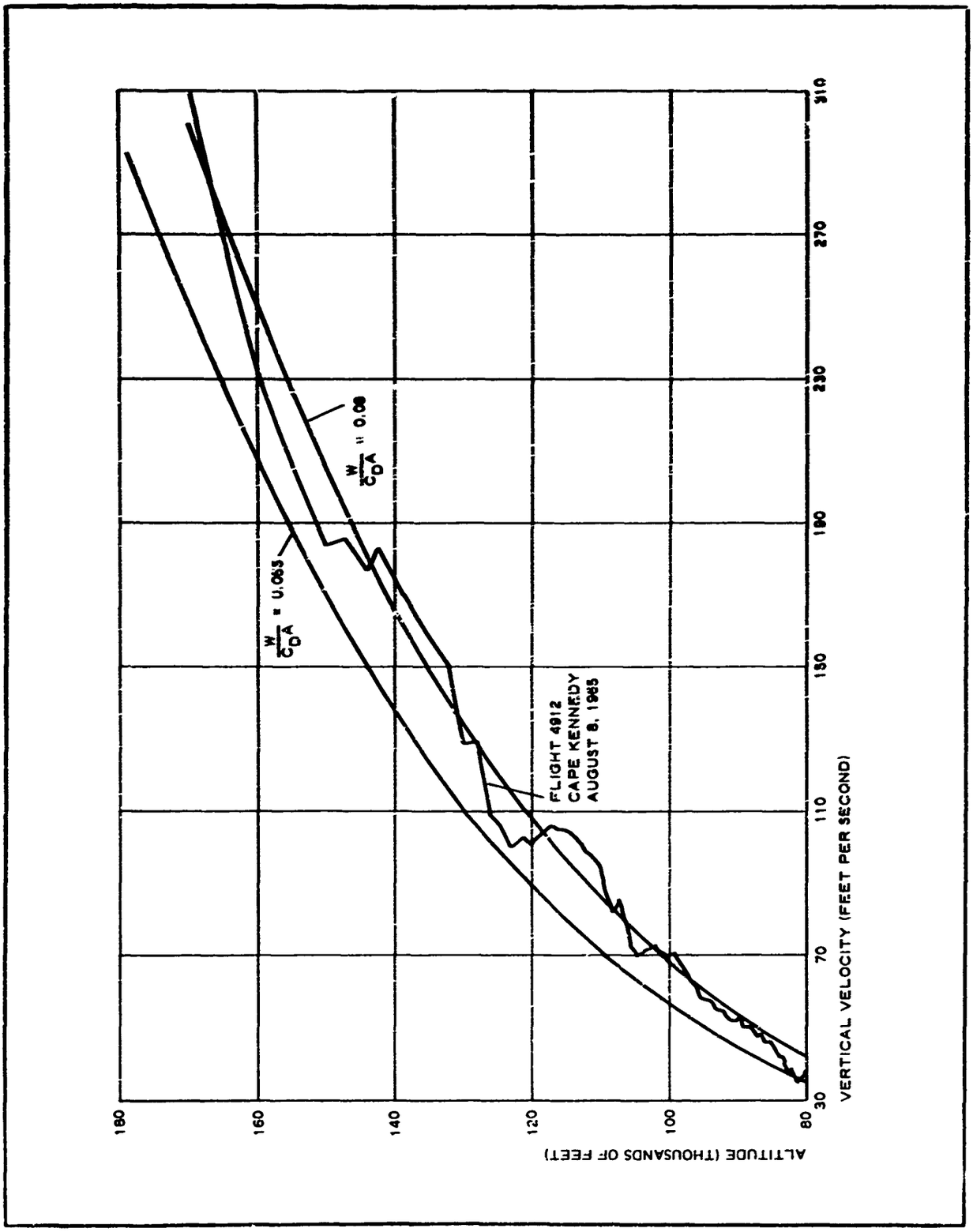

Figure 54 - Vertical Descent Velocity for Flight 4912

If

$$\frac{W}{C_D A} = 0.08 ,$$

then

$$C_D = \frac{W}{0.08\ A}$$

$$= \frac{7.73}{0.08 \times 135}$$

$$= 0.72 .$$

The density values from which the $W/C_D A$ profiles were calculated are computed by the Air Force and use the temperature data acquired during the flight. The deviations from the theoretical velocities are attributable to one or more of the following factors:

1. Radar accuracy tolerances
   a. Angular = ±0.1 mil
   b. Range = ±15 ft
2. Vertical winds
3. Local density variables

A fourth possible cause for deviating from the theoretical velocity is a variation of the $C_D A$ of the BALLUTE. In previous work, such $C_D A$ variation has never been experienced in a properly functioning BALLUTE.

Because the BALLUTE was recovered intact and evidenced no structural damage or holes that would cause partial inflation, it may be assumed that the BALLUTE was fully inflated and that the lower C_D values were due to some phenomena other than a variation in BALLUTE geometry.

The stability of the BALLUTE during the flight is verified by the clarity of the oscillograph record of the telemetered temperature data. A portion is reproduced in Figure 55. The absence of signal dropout in Figure 55 is evident when compared with the temperature record of a comparable

flight with the parachute-decelerated system (Figure 56). Such signal dropout verifies the absence of oscillation, or coning, of the instrument.

Since no baseline is available to define the wind sensitivity of the system quantitatively, the horizontal plane's changes of velocity and direction are compared with the only available parameters, vertical velocity or its resultant, dynamic pressure, or apparent W/C_DA (Figure 57). The magnitude of the horizontal excursions indicates that the system is sensitive to wind. Wind-sensing accuracy cannot be evaluated until data from some future flight can be compared with data from different sensors of known errors.

3. FLIGHT NO. 2 (BALLUTE NO. 15, APPENDIX IV)

The payload instrument used in Flight No. 2 was of the transponder variety, the Arcasonde II configuration. The payload instrument is in its final stage of development and is even more adversely affected by instability than the Arcasonde I instrument. Data on the flight are given below:

Flight no. - 4916
Date - 10 August 1965
Instrument - Arcasonde II
Instrument weight - 6.37 lb
BALLUTE weight - 3.12 lb
System weight - 9.49 lb[a]

Because the nose cone enclosed the payload thermistor for the greater portion of the flight, no usable temperature data were obtained. Temperature readings were transmitted and received by the ground station but represented the temperature inside the nose cone rather than the

[a]In Flight 4916, the nose cone remained with the instrument for 12-1/2 min after separation, or to about 90,000 ft, when it dropped off. The system weight thereafter became 8.54 lb.

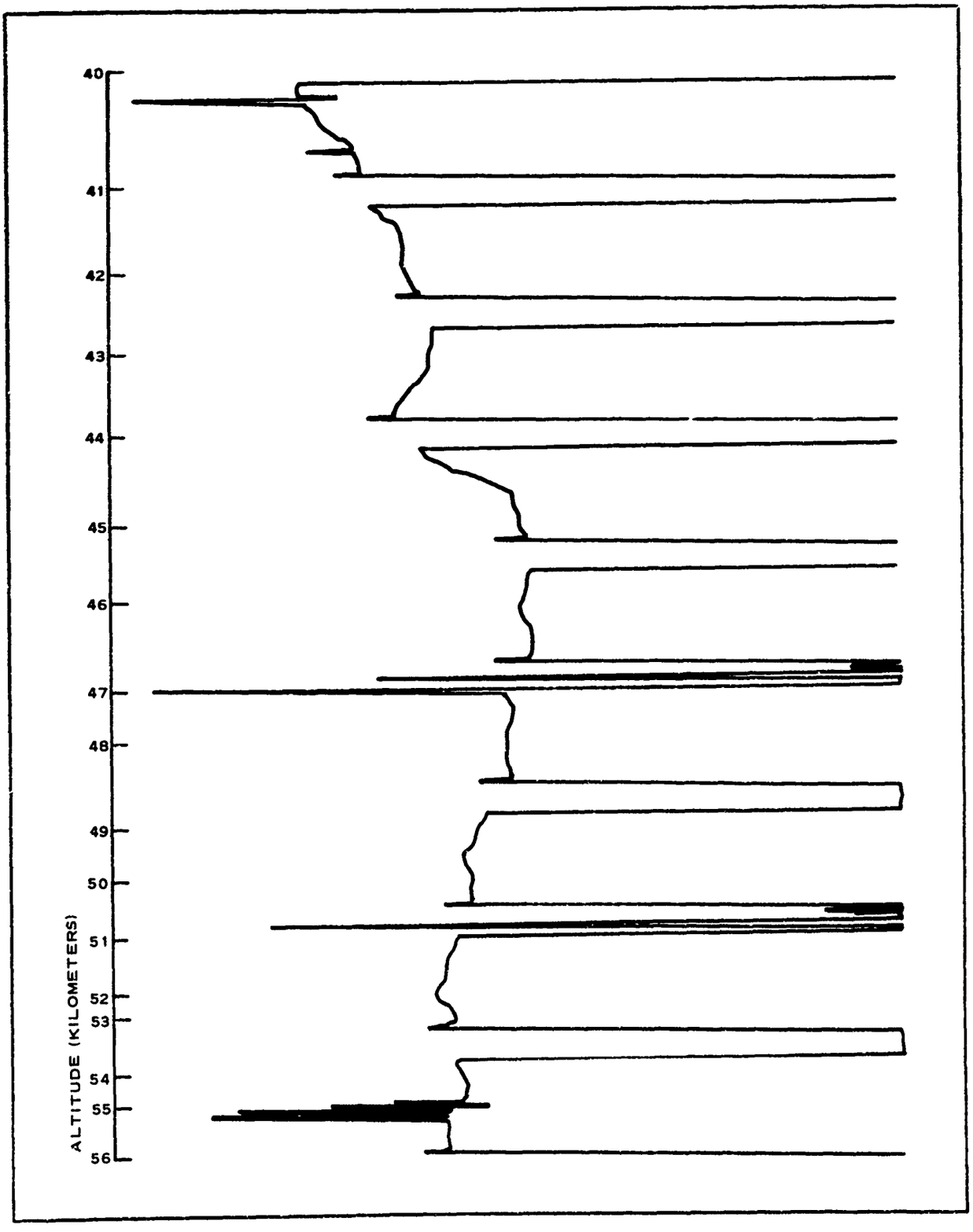

Figure 55 - Temperature Data from Flight 4912

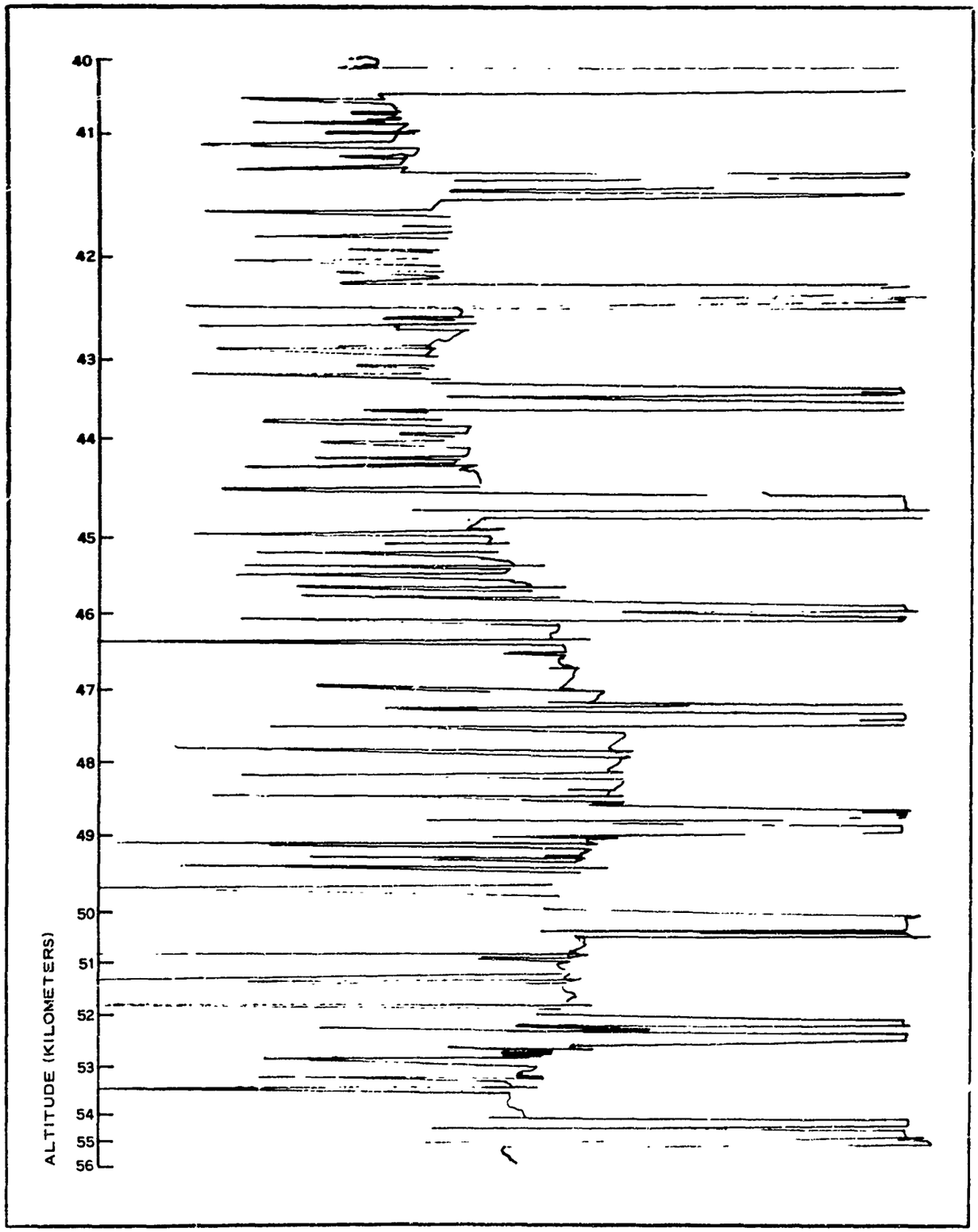

Figure 56 - Temperature Data from Typical Flight

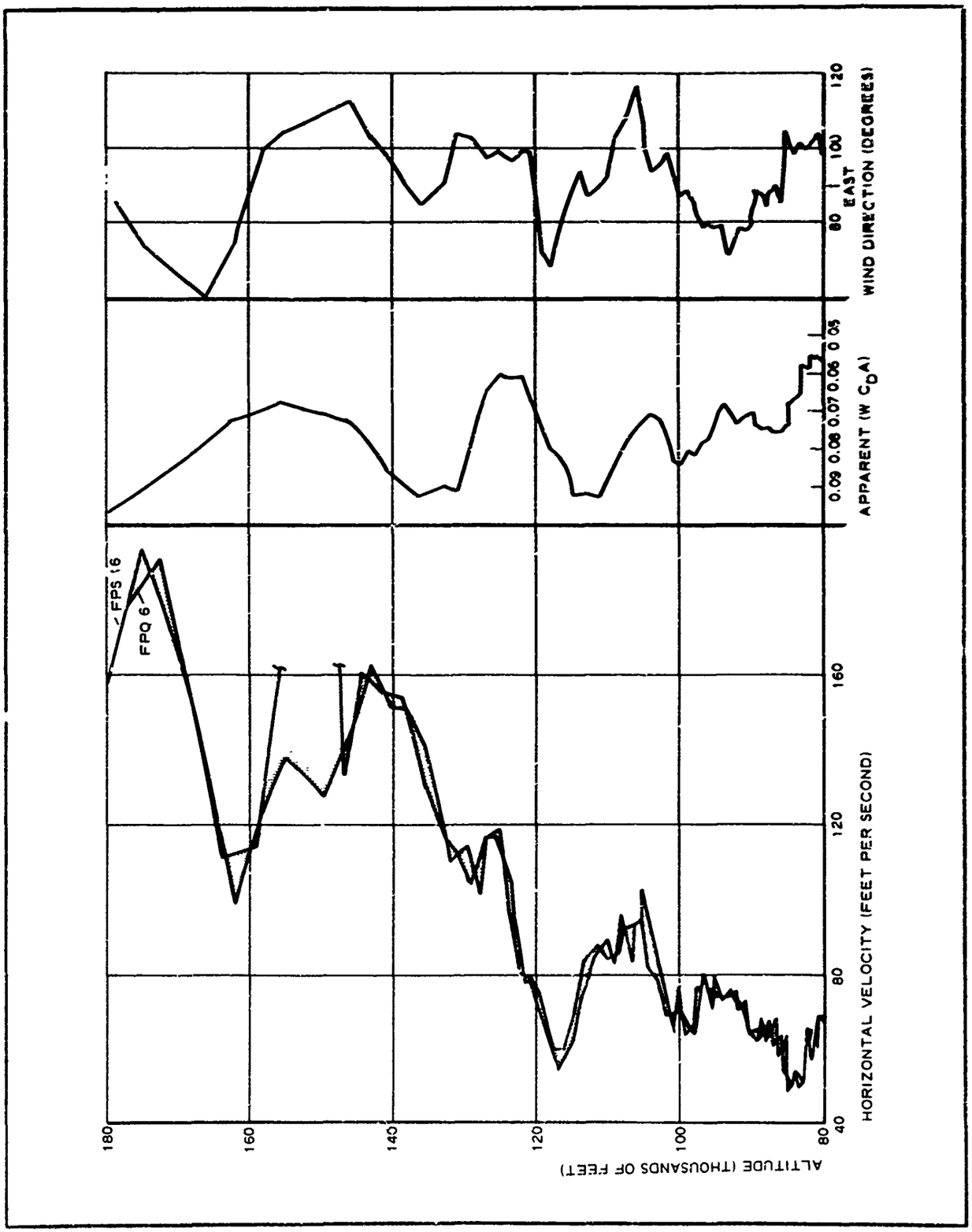

Figure 57 - Horizontal Velocity for Flight 4912

temperature of the ambient atmosphere. For this reason, the normal smoothing of the digital radar data was omitted by the Data Acquisition Group at Cape Kennedy. The vertical descent velocities presented in Figure 58 are based on 10-point smoothing of the rough radar data performed by GAC. Once again, the vertical descent velocities approximate the ballistic descent of a projectile with a $W/C_DA = 0.08$.

4. FLIGHT NO. 3 (BALLUTE NO. 16, APPENDIX III)

Data on the third flight are given below:

Flight no. - 4922
Date - 13 August 1965
Instrument - Arcasonde II
Instrument weight - 5.42 lb
BALLUTE weight - 3.12 lb
System weight - 8.54 lb

Because of the BALLUTE's success in both of the previous flights, and especially because of the extreme stability achieved, the 4th Weather Group at Cape Kennedy provided another Arcasonde II instrument for this third flight. Unstable flight was considered a deterring factor in completing development of the transponder-type system. A malfunction of either the Arcasonde II instrument or of the receiving equipment resulted in losing temperature data. Tracking of the sonde was successfully accomplished by the FPQ-6 radar. Descent velocities are shown in Figure 59. A comparison of the vertical descent rates of the system with the ballistic profile of a $W/C_DA = 0.08$ projectile shows extremely small deviations (Figure 60). Completion of three successful flights and the unexpected recovery intact of two of the systems (Flights 4912 and 4916) are considered valid demonstrations of the BALLUTE's feasibility for this mission. The two BALLUTE systems that were accidentally recovered showed burn effects from the pyrotechnic separation device.

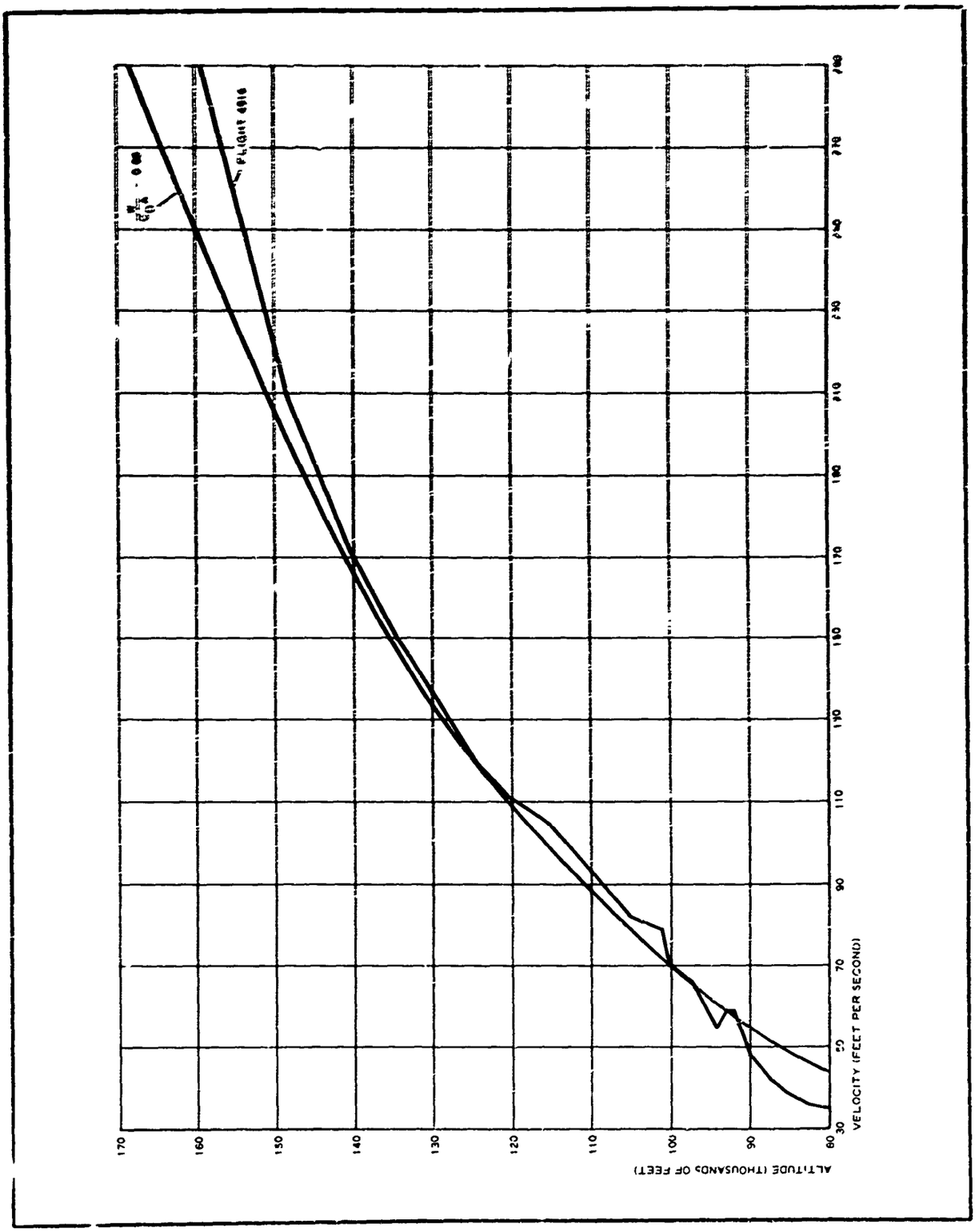

Figure 58 - Vertical Descent Velocity for Flight 4916

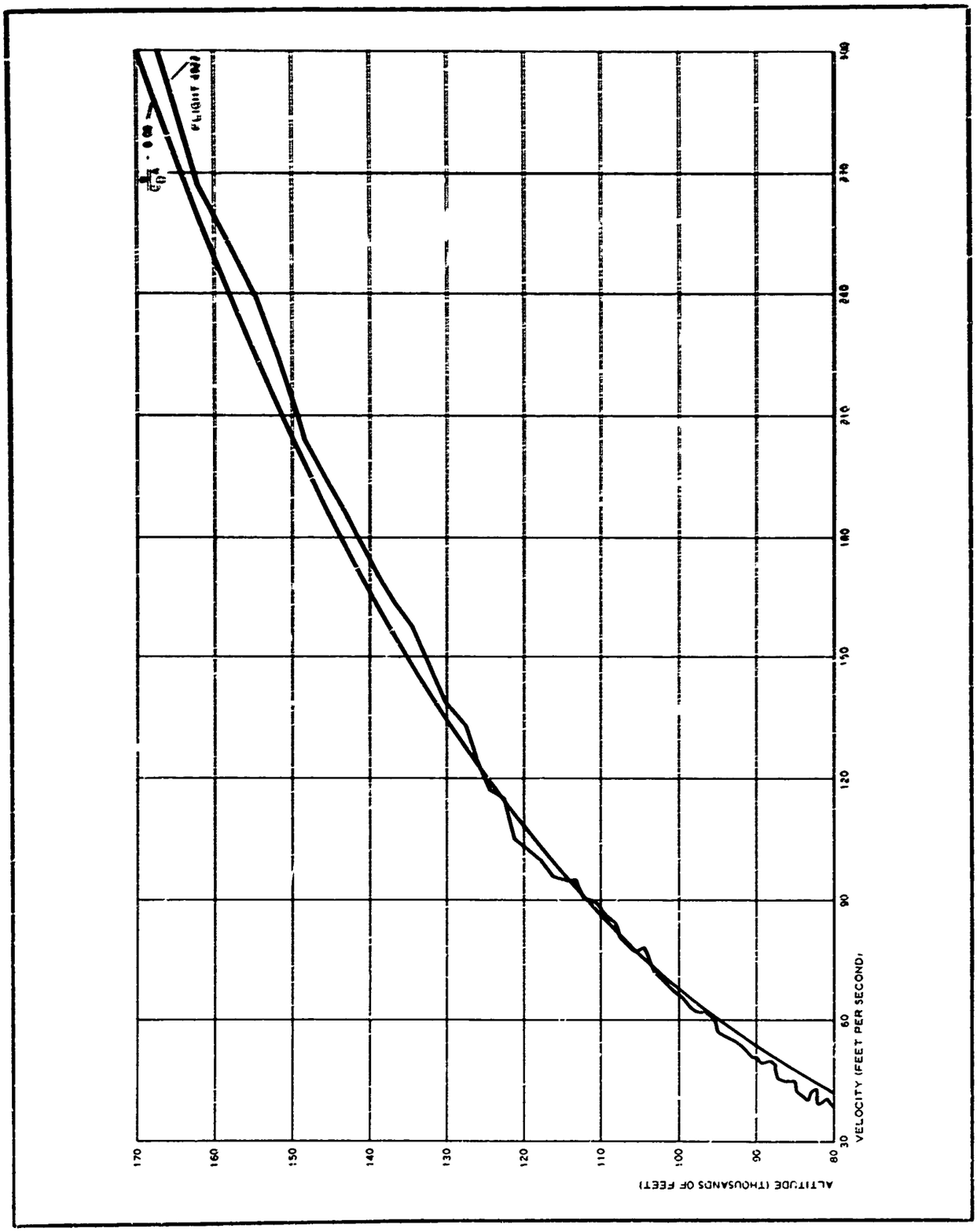

Figure 59 - Vertical Descent Velocity for Flight 4922

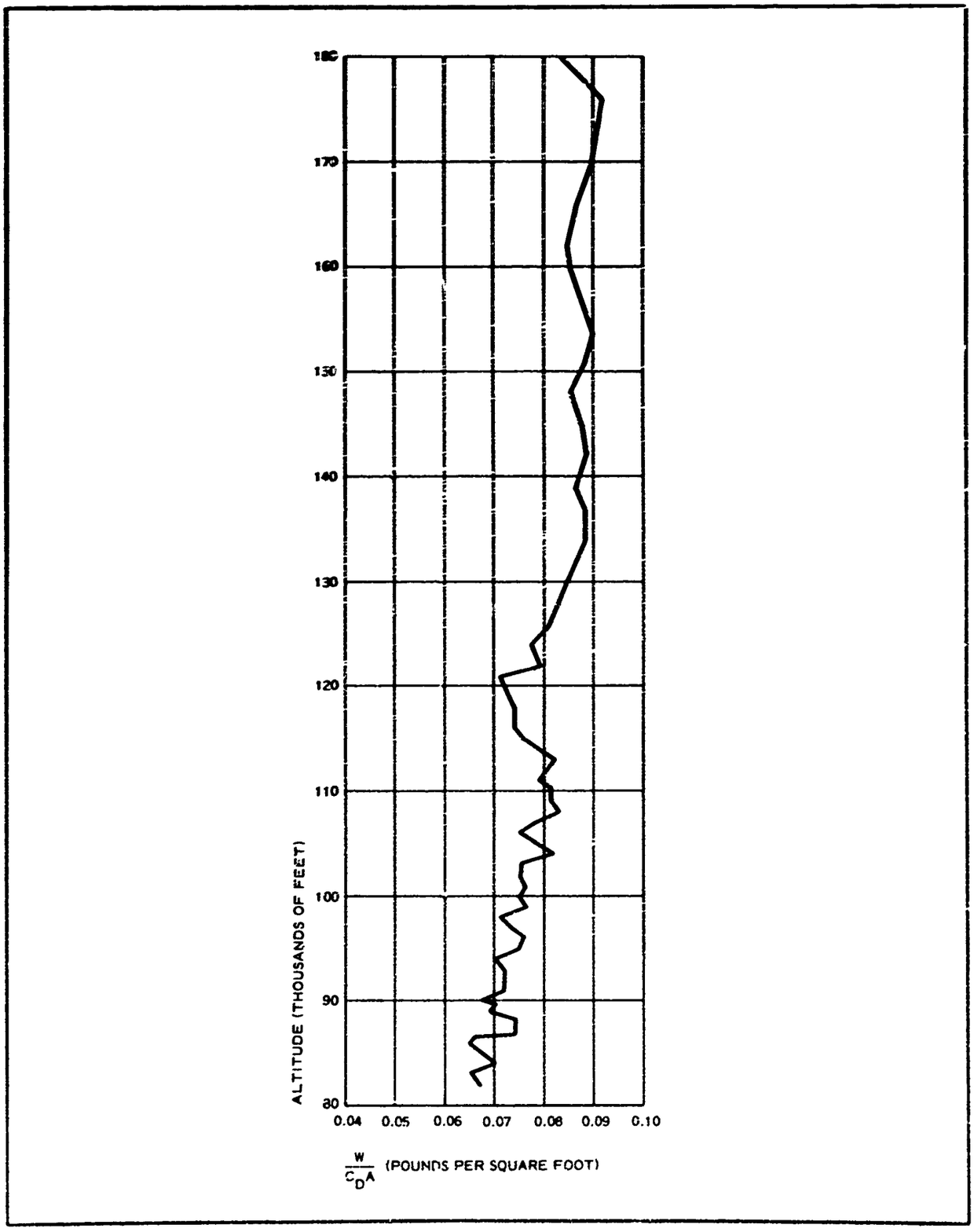

Figure 60 - Apparent Ballistic Coefficient for Flight 4922

Several holes one-in. -diam appeared on the forward conical surface of the BALLUTEs. These holes would not have affected the inflation or the performance of the BALLUTEs. The location of the holes would cause them to act as additional ram-air inlets. Critical damage could have resulted, however, from the separation charge, and preventive measures similar to the measures used with the standard parachute system should be taken (see Figures 42 and 43).

Sufficient empirical information has been obtained to permit development finalization by indicated modifications and by testing and subsequent initiation of a qualification program.

SECTION X

CONCLUSIONS AND RECOMMENDATIONS

1. GENERAL

A proper evaluation of the development program must be made regarding the design goals established at the program's beginning - that is, reliability, stability, descent rate, and production cost.

2. RELIABILITY

As a result of extensive testing of various system configurations throughout the development program, problem areas were isolated and remedial modifications incorporated, until the design represented by the last three rocket-launched flights was achieved. This final configuration proved successful each time it was tested. Although three rocket-launched flights do not provide sufficient statistical evidence to establish an accepted reliability level, these successful performances - coupled with the prior solution of many problem areas - indicate a high level of confidence in continued fail re-free flights.

3. STABILITY

By the nature of its operation, the BALLUTE is an aerodynamically stable device. Inflation is positive, geometry is constant, the coupling to the instrument is rigid, and the BALLUTE in every respect can be considered a rigid aerodynamic shape. This configuration rigidity and the ability to achieve wide variations in shape make the BALLUTE the most stable of the deployable decelerators. The almost perfect character of the temperature data achieved with the Arcasonde I-A instrument substantiates the BALLUTE's extreme stability throughout flight (see Figure 55).

4. DESCENT RATE

An overweight final configuration resulted when weight was set aside as a critical factor for the final units of the rocket-launched program to establish operational reliability. This overweight final configuration, combined with lower C_D values than indicated by sea level tests, yielded a W/C_DA = 0.08, rather than the desired 0.054.

As a result of the rocket-launched flights, two factors were firmly established, making the 0.054 ballistic coefficient readily attainable. The use of 1/4-mil film, which gives a 50-percent weight reduction of the BALLUTE, is definitely indicated. The BALLUTE size can be increased sufficiently without exceeding the existing weight and the volume restrictions.

Although the target velocity of 300 fps at 180,000 ft was not demonstrated in flight, the feasibility was definitely established.

The use of lighter gage film, coupled with weight reduction in inlet and the swivel assemblies, should permit an increase of BALLUTE size that would yield a W/C_DA of 0.054, even for the target payload weight of seven pounds.

Assuming a total system weight of nine pounds (a seven-pound payload and a two-pound BALLUTE), the BALLUTE size is determined by:

$$\frac{W}{C_DA} = 0.054 \text{ to meet the descent velocity goal}$$

and

$$C_D = 0.75, \text{ based on flight test data .}$$

Therefore,

$$A = \frac{W}{C_D \times 0.054}$$

$$= \frac{9}{0.75 \times 0.054}$$

$$= 222 \text{ sq ft ,}$$

which requires a hexsymmetric BALLUTE measuring about 16-1/2 ft across the burble fence's flats. The BALLUTE's surface area will increase about 70 percent. A film-weight reduction of one-half should accomplish the descent velocity goal, with a system weight very near to the nine-pound target.

5. PRODUCTION COST

During the materials and fabrication development study, the feasibility of semiautomated fabrication techniques was established.

The almost daily advances in the field of commercial plastic film products being made by Goodyear further enhances the cost-goal achievement. Cost reduction in both the hardware and the BALLUTE areas is required.

6. ADDITIONAL EFFORTS

Further development of the system should include the following:

1. Functional analysis of BALLUTE performance by camera payloads
2. Incremental removal of unnecessary structural reinforcements
3. Additional flight tests to establish more firmly aerodynamic coefficients
4. Simultaneous firing of instruments with BALLUTE and with parachute decelerators and chaff payloads
5. BALLUTE size increase as dictated by additional flight data
6. Preliminary design of production tooling

APPENDIX I - TABULATION OF AIRDROP TEST DATA

SERIES 1 - TOROIDAL BURBLE FENCE BALLUTE

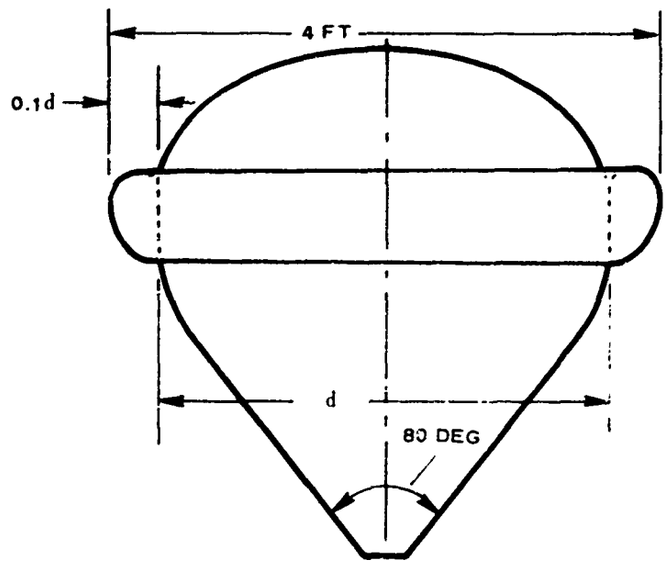

Configuration no.	Inlet diam (in.)	Gross weight (gm)	W/C_DA (mean)	Configuration no.
1	3	209	0.030	1
2	3	378	0.054	2
3	3	600	0.090	3
4	3	802	0.140	4
5	3	1003	0.171	5
12	6	301	0.040	12
13	6	400	0.067	13
14	6	600	0.092	14
15	6	800	0.156	15
16	6	1000	0.191	16

Drop no.	Configuration no.	Terminal velocity (fps)	C_D	W/C_DA	Reynolds no. $\times 10^5$	Drop no.
3	1	5.2	1.15	0.032	1.25	3
4	1	5.0	1.26	0.029	1.20	4
5	1	6.0	0.86	0.043	1.45	5
6	2	7.0	1.18	0.056	1.67	6
7	2	6.7	1.30	0.051	1.60	7
8	2	8.3	0.82	0.081	2.00	8
17	3	8.9	1.17	0.090	2.06	17
20	3	10.0	0.92	0.114	2.33	20
21	4	11.0	1.04	0.136	2.53	21
22	4	11.3	0.97	0.145	2.62	22
23	5	12.4	1.02	0.173	2.86	23
24	5	12.3	1.04	0.169	2.83	24
25	14	8.5	1.26	0.085	2.05	25
26	14	9.0	1.12	0.094	2.18	26
27	14	9.2	1.08	0.098	2.22	27
28	16	13.6	0.83	0.212	3.27	28
29	16	12.5	0.98	0.179	3.01	29
30	16	12.6	0.97	0.182	3.03	30
31	12	5.9	1.30	0.041	1.43	31
32	12	5.8	1.35	0.039	1.4	32
37	14a	9.1	1.11	0.948	2.19	37
38	14a	9.3	1.05	0.100	2.25	38
44	13	8.0	0.95	0.073	1.93	44
45	13	7.3	1.16	0.061	1.75	45
46	15	11.4	0.94	0.148	2.74	46
47	15	11.1	0.98	0.142	2.68	47
48	15	11.1	0.84	0.167	2.69	48
49	15	11.8	0.87	0.160	2.96	49
50	15	11.9	0.87	0.161	2.86	50

SERIES 2 - TUCKED-BACK BALLUTE

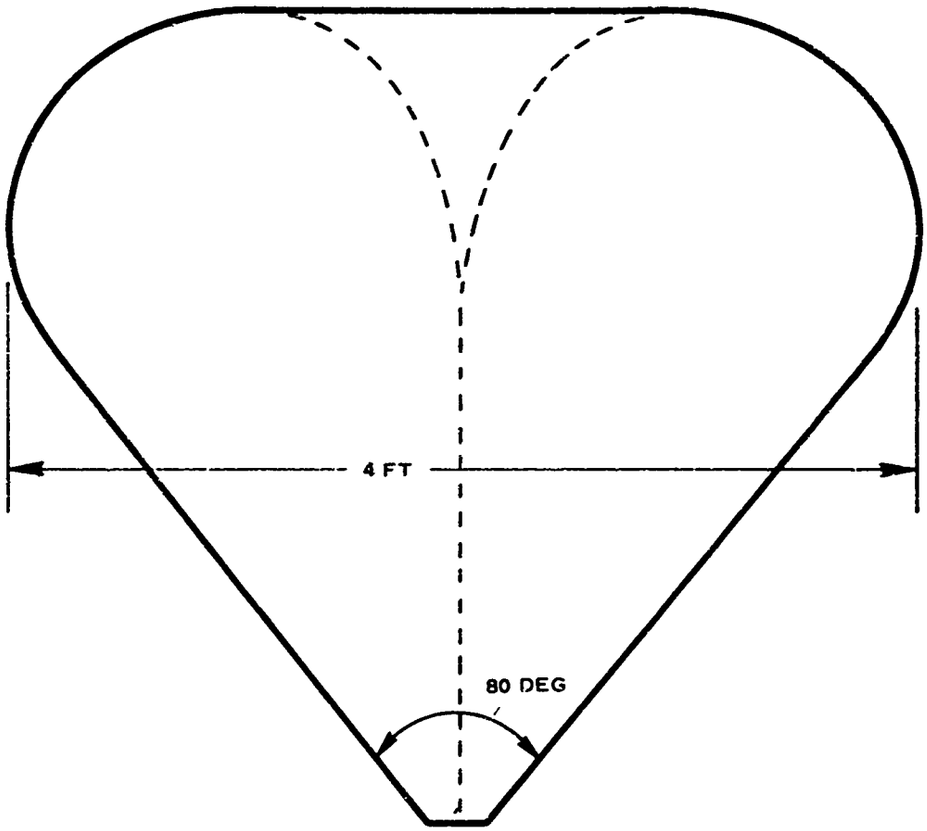

Configuration no.	Inlet diam (in.)	Gross weight (gm)	W/C_DA (mean)	Configuration no.
6	3	199	0.047	6
7	3	400	0.097	7
8	3	600	0.177	8
9	3	800	0.213	9
10	3	1000		10
17	6	300	0.062	17
18	6	400		18
19	6	600		19
20	6	800		20
21	6	1000		21

Drop no.	Configuration no.	Terminal velocity (fps)	C_D	W/C_DA	Reynolds no. $\times 10^5$	Drop no.
1	6	6.3	0.75	0.046	1.53	1
2	6	6.3	0.76	0.047	1.51	2
9	7	8.9	0.78	0.090	2.06	9
10	7	9.8	0.65	0.108	2.27	10
11	7	9.0	0.77	0.092	2.08	11
12	8	13.0	0.55	0.191	3.00	12
13	8	12.0	0.64	0.164	2.79	13
14	8	12.5	0.60	0.176	2.89	14
15	9	13.4	0.69	0.202	3.09	15
16	9	14.1	0.63	0.224	3.26	16
35	17	7.2	0.88	0.060	1.75	35
36	17	7.4	0.83	0.063	1.78	36

SERIES 3 - SIXTY-DEGREE PARTITIONED BALLUTE

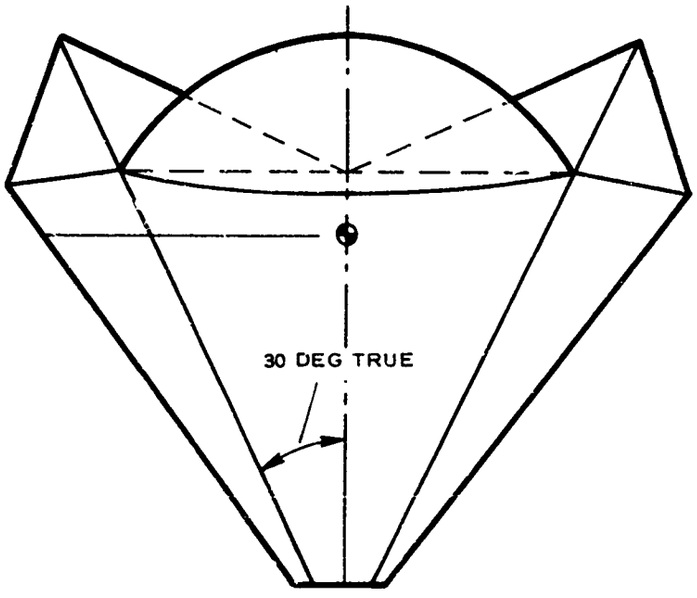

Configuration no.	Inlet diam (in.)	Gross weight (gm)	W/C_DA (mean)	Configuration no.
11	8	1354	0.233	11
22	8	301	0.048	22
23	8	401	0.070	23
24	8	599	0.106	24
25	8	800	0.137	25
26	8	1001		26

Drop no.	Configuration no.	Terminal velocity (fps)	C_D	W/C_DA	Reynolds no. $\times 10^5$	Drop no.
18	11	14.5	0.64	0.237	4.20	18
19	11	14.2	0.67	0.228	4.11	19
33	24	9.8	0.61	0.111	2.96	33
34	24	9.4	0.66	0.102	2.83	34
39	22	6.5	0.70	0.049	1.96	39
40	23	7.6	0.67	0.067	2.29	40
41	23	8.0	0.61	0.074	2.42	41
42	25	11.0	0.65	0.140	3.31	42
43	25	10.9	0.66	0.135	3.27	43

SERIES 4 - EIGHTY-DEGREE PARTITIONED BALLUTE

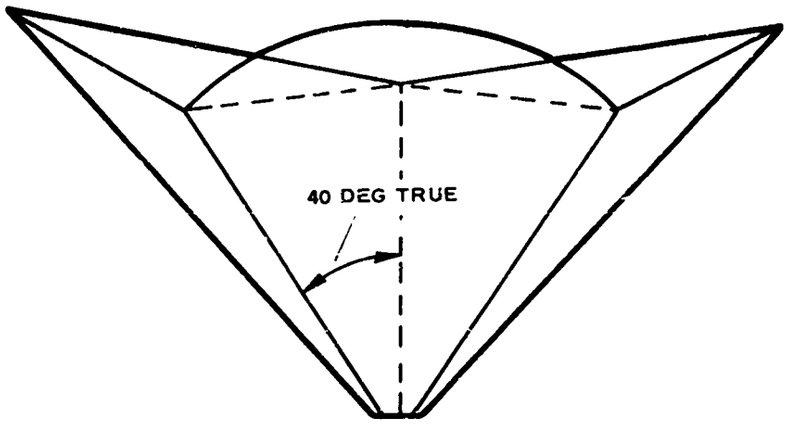

Configuration no.	BALLUTE diam (ft)	Inlet diam (in.)	Gross weight (gm)	W/C_DA (mean)	Configuration no.
27	4	6	200	0.0473	27
28	4	6	399.7	0.0955	28
29	4	6	592.7	0.142	29
30	4	6	799.2	0.1877	30
31	4	6	1000.2		31
32	1	1	9.65	0.0391	32
33	1	1	13.25	0.0495	33
34	1	1	16.85	0.062	34
35	1	1	20.45	0.0695	35
36	1	1	24.05	0.0847	36
42	1	1	6.4	0.0248	42
43	1	1	10.0		43
44	1	1	13.6		44
45	1	1	17.2		45
46	1	1	20.8	0.0736	46

Drop no.	Configuration no.	Terminal velocity (fps)	C_D	W/C_DA	Reynolds no. $\times 10^5$	Drop no.
51	27	6.48	0.623	0.048	1.65	51
52	27	6.08	0.793	0.043	1.55	52
53	27	5.74	0.793	0.038	1.47	53
54	28	8.90	0.658	0.093	2.27	54
55	28	9.26	0.608	0.100	2.36	55
56	28	8.47	0.617	0.099	2.16	56
57	28	9.92	0.546	0.112	2.53	57
58	29	10.83	0.668	0.137	2.76	58
59	29	10.83	0.668	0.137	2.76	59
60	29	10.88	0.661	0.138	2.78	60
61	30	12.70	0.684	0.188	3.24	61

Drop no.	Configuration no.	Terminal velocity (fps)	C_D	W/C_DA	Reynolds no. $\times 10^5$	Drop no.
86	27	6.64	0.618	0.049	1.68	86
89	27	6.58	0.625	0.049	1.66	89
92	27	6.31	0.683	0.044	1.60	92
94	29	11.10	0.654	0.138	2.81	94
95	29	11.41	0.618	0.146	2.89	95
97	28	9.11	0.626	0.097	2.48	97
99	28	8.98	0.644	0.094	2.44	99
62	32	5.78	0.741	0.038	0.348	62
63	32	5.80	0.736	0.039	0.350	63
64	32	5.93	0.705	0.040	0.357	64
65	33	6.53	0.795	0.049	0.394	65
66	33	6.69	0.760	0.051	0.403	66
67	33	6.47	0.810	0.048	0.390	67
69	34	7.36	0.798	0.062	0.444	69
70	34	7.36	0.798	0.062	0.444	70
71	35	7.78	0.867	0.069	0.435	71
72	35	7.78	0.867	0.069	0.435	72
73	36	8.52	0.850	0.083	0.512	73
74	36	8.75	0.803	0.088	0.485	74
75	36	8.518	0.848	0.083	0.510	75
85	42	4.70	0.765	0.025	0.271	85
88	42	4.75	0.745	0.025	0.272	88
91	46	8.20	0.812	0.075	0.472	91
93	46	8.16	0.820	0.074	0.470	93
96	46	8.00	0.851	0.072	0.461	96
103	46	7.86	0.855	0.071	0.488	103

SERIES 5 - TUCKED-BACK BALLUTE WITH INTERMITTENT FENCE

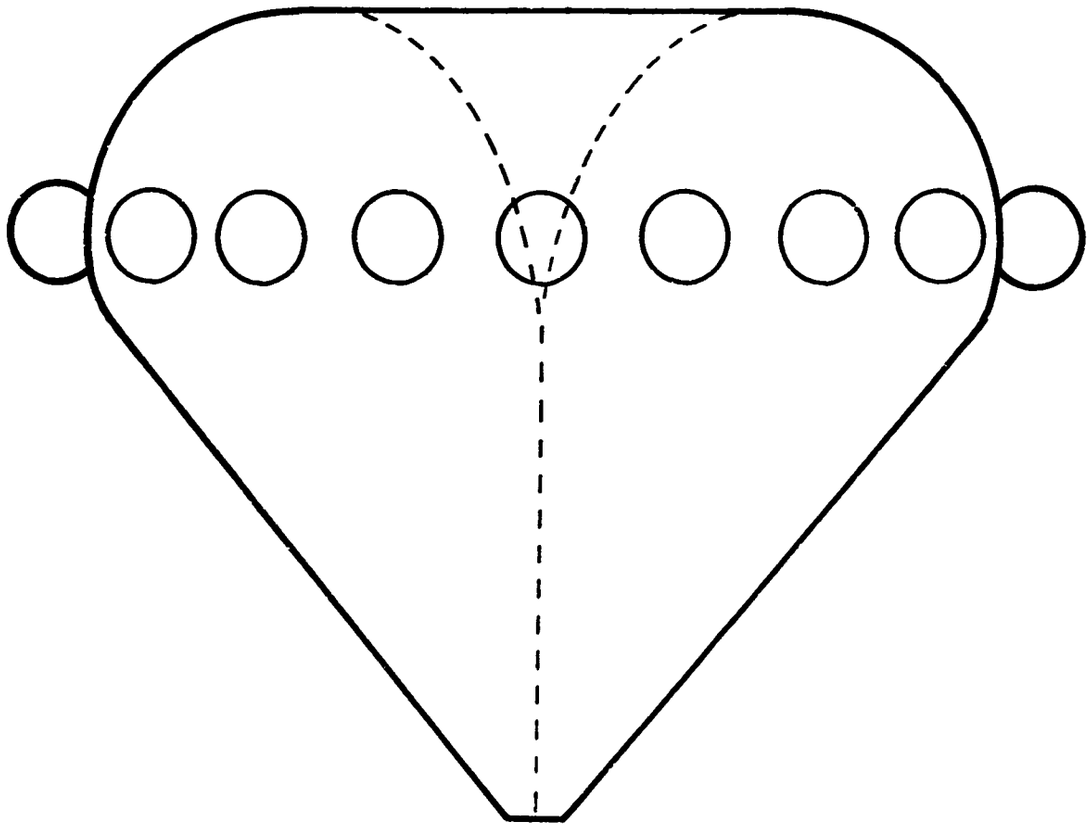

Configuration no.	Inlet diam (in.)	Gross weight (gm)	W/C_DA (mean)	Configuration no.
37	6	294.3		37
38	6	494.0	0.1405	38
39	6	693.5	0.1732	39
40	6	893.5		40
41	6	1094.5		41

Drop no.	Configuration no.	Terminal velocity (fps)	C_D	W/C_DA	Reynolds no. $\times 10^5$	Drop no.
68	39	11.90	0.695	0.162	2.925	68
76	39	12.28	0.650	0.173	3.02	76
77	39	11.90	0.695	0.162	2.93	77

Drop no.	Configuration no.	Terminal velocity (fps)	C_D	W/C_DA	Reynolds no. $\times 10^5$	Drop no.
78	39	13.00	0.580	0.196	3.20	78
79	39	13.00	0.580	0.196	3.20	79
80	38	10.59	0.625	0.129	2.60	80
81	38	10.96	0.582	0.138	2.69	81
82	38	11.32	0.545	0.148	2.78	82
83	38	11.37	0.541	0.148	2.79	83
84	38	11.37	0.541	0.148	2.79	84

SERIES 6 - ISOTENSOID BALLUTE WITH INTERMITTENT BURBLE FENCE

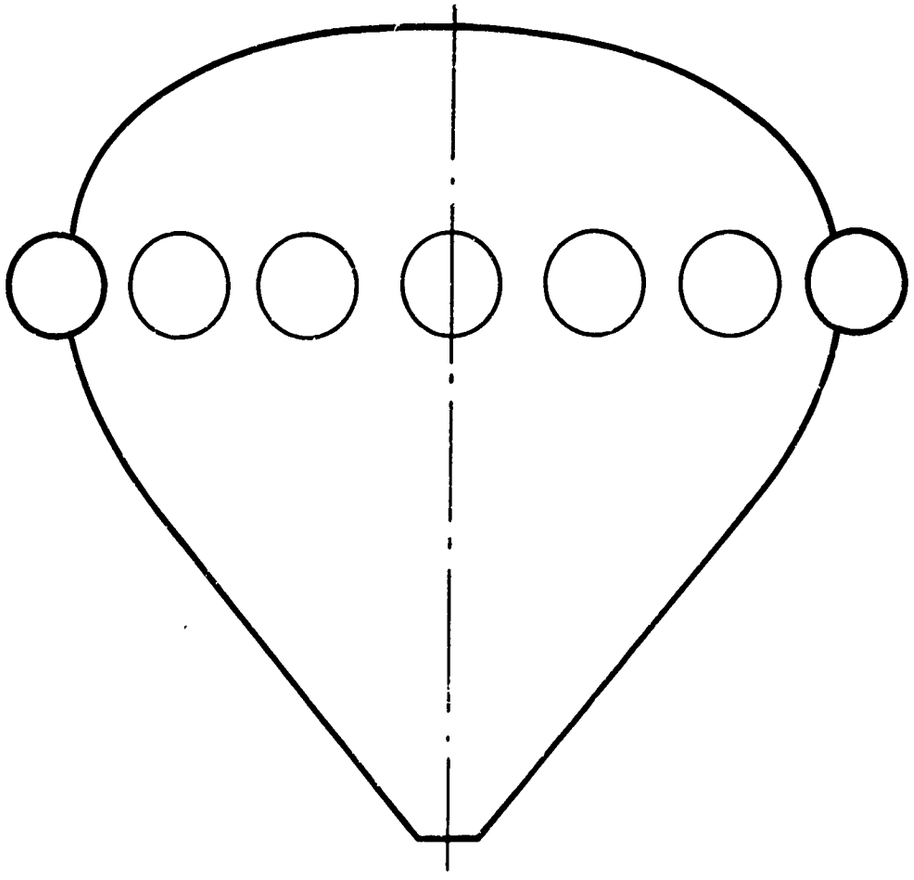

Configuration no.	Inlet diam (in.)	Gross weight (gm)	W/C_DA (mean)	Configuration no.
47	6	219.7	0.1212	47

Drop no.	Configuration no.	Terminal velocity (fps)	C_D	W/C_DA	Reynolds no. $\times 10^5$	Drop no.
90	47	11.20	0.40	0.139	2.21	90
87	47	10.75	0.430	0.129	2.12	87

SERIES 7 - ISOTENSOID BALLUTE WITH POLYAGONAL BURBLE FENCE

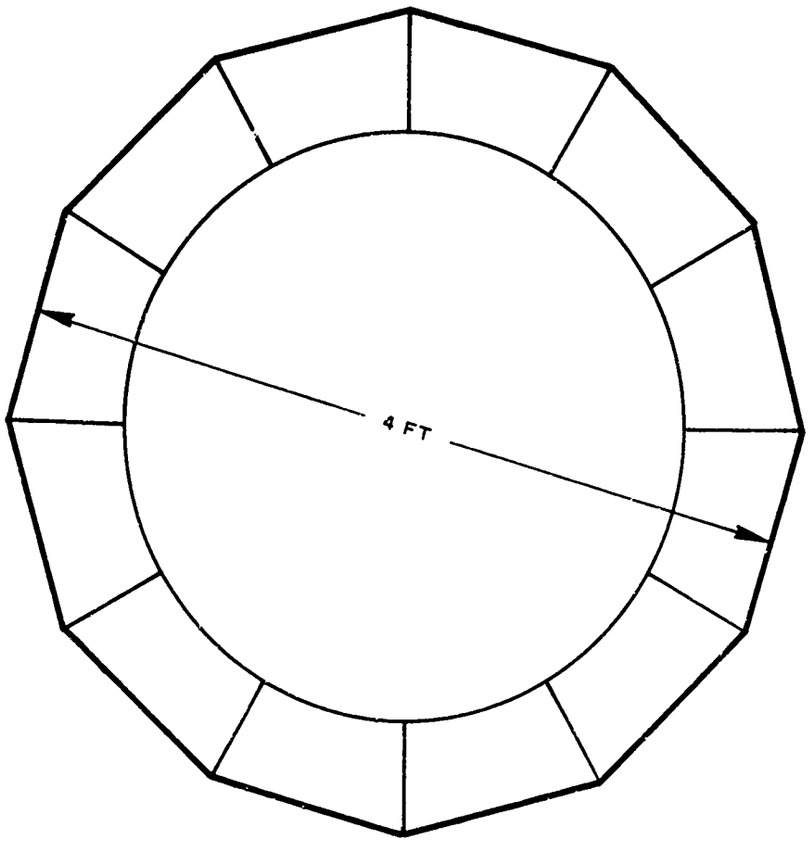

Configuration no.	Inlet diam (in.)	Gross weight (gm)	W/C_DA (mean)	Configuration no.
52	6	199.0	0.065	52
53	6	427.2		53
54	6	627.2	0.1675	54
55	6	828.7		55
56	6	1026.2		56

Drop no.	Configuration no.	Terminal velocity (fps)	C_D	W/C_DA	Reynolds no. $\times 10^5$	Drop no.
101	54	*	*	*	*	101
102	54	*	*	*	*	102
98	52	7.48	0.586	0.065	1.82	98
100	54	12.01	0.714	0.168	2.93	100

*No data.

SERIES 8 - ISOTENSOID BALLUTE WITH HEXAGONAL BURBLE FENCE AND CONES

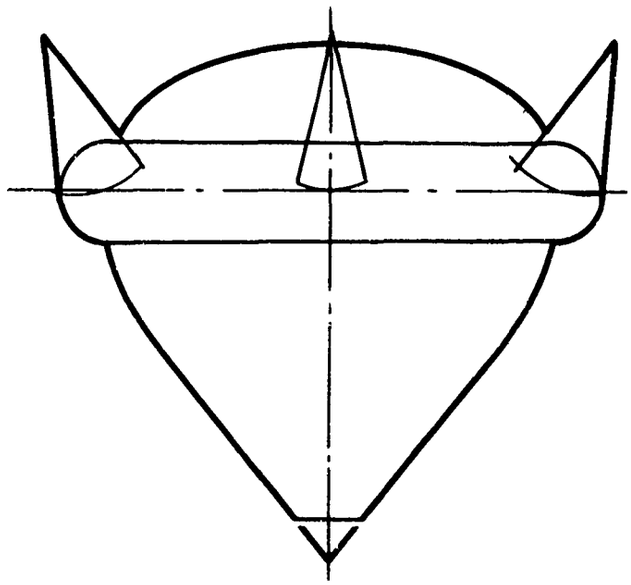

Configuration no.	Inlet diam (in.)	Gross weight (gm)	W/C_DA (mean)	Configuration no.
57	6	199	0.022	57
58	6	404	0.046	58
59	6	604	0.090	59
60	6	803.5		60
61	6	1000		61

Drop no.	Configuration no.	Terminal velocity (fps)	C_D	W/C_DA	Reynolds no. $\times 10^5$	Drop no.
104	57	4.66	1.462	0.022	1.12	104
105	57	4.70	1.435	0.022	1.01	105
106	57	4.80	1.38	0.023	1.15	106
107	58	7.03	1.305	0.029	1.09	107
108	58	6.32	1.610	0.040	1.52	108
109	58	6.98	1.32	0.049	1.67	109
110	58	*	*	*	*	110
111	59	9.26	1.12	0.086	2.22	111
112	59	9.26	1.12	0.086	2.22	112
113	59	9.76	1.01	0.095	2.34	113
114	59	9.76	1.01	0.095	2.34	114
115	59	9.38	1.10	0.087	2.25	115

*No data.

SERIES 9 - HEXSYMMETRIC BALLUTE

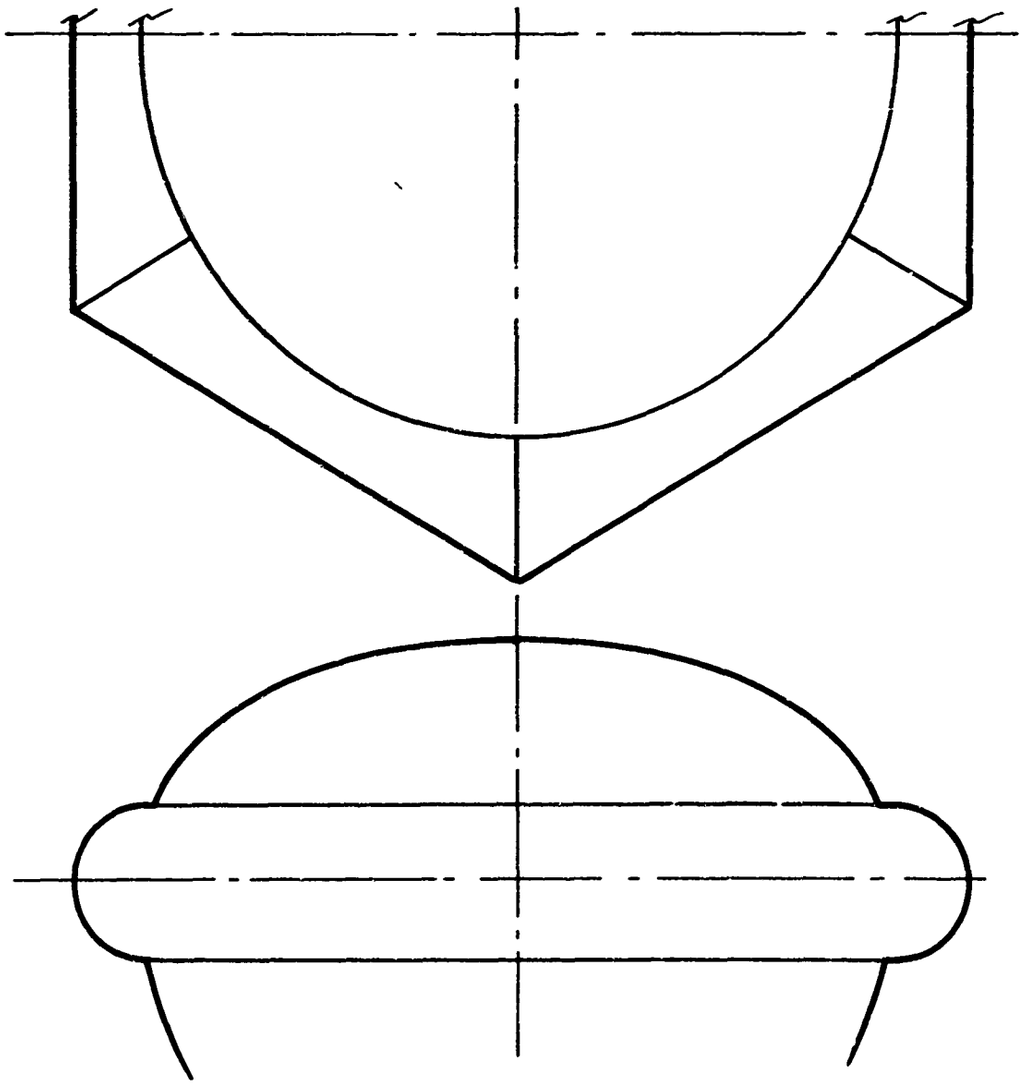

Configuration no.	BALLUTE diam (ft)	Inlet diam (in.)	Gross weight (gm)	$W/C_D A$ (mean)	Configuration no.
62	4	6	201	0.026	62
63	4	6	409	0.061	63
64	4	6	602.5	0.098	64
65	4	6	798.5	0.133	65
66	4	6	994	0.153	66

Configuration no.	BALLUTE diam (ft)	Inlet diam (in.)	Gross weight (gm)	W/C_DA (mean)	Configuration no.
72	1.25	2	9.5	0.019	72
73	1.25	2	20.3	0.040	73
74	1.25	2	31.1	0.058	74
75	2.50	3.5	26.7	0.011	75
76	2.50	3.5	50.0	0.016	76
77	2.50	3.5	70.0	0.023	77
78	2.50	3.5	100.0	0.037	78
79*	12.50	9	3.78 lb	0.016	79
80*	12.50	9	4.78 lb	+	80
81*	12.50	9	5.78 lb	0.027	81
82*	12.50	9	6.78 lb	+	82
83*	12.50	9	7.78 lb	0.036	83
84*	12.50	9	8.78 lb	+	84
85*	12.50	2	41.9	0.056	85

*See BALLUTE No. 1, Appendix III.

+No data.

Drop no.	Configuration no.	Terminal velocity (fps)	C_D	W/C_DA	Reynolds no. $\times 10^5$	Drop no.
116	62	4.45	1.37	0.023	1.16	116
117	62	5.05	1.06	0.030	1.32	117
118	62	4.71	1.22	0.026	1.23	118
119	63	7.90	0.88	0.074	2.06	119
120	63	6.90	1.16	0.056	1.80	120
121	63	6.68	1.23	0.053	1.74	121
122	63	7.22	1.06	0.061	1.89	122
123	64	8.83	1.05	0.091	2.31	123
124	64	9.02	1.00	0.096	2.36	124

Drop no.	Configuration no.	Terminal velocity (fps)	C_D	W/C_DA	Reynolds no. $\times 10^5$	Drop no.
125	64	8.23	1.20	0.080	2.15	125
126	64	9.27	0.95	0.101	2.42	126
127	64	9.75	0.85	0.113	2.50	127
128	64	9.43	0.91	0.106	2.46	128
129	65	10.79	0.92	0.138	2.82	129
130	65	10.55	0.98	0.129	2.75	130
131	65	10.63	0.95	0.133	2.78	131
132	66	11.46	1.03	0.153	2.99	132
145	72	4.07	0.75	0.021	0.378	145
146	75	2.96	1.00	0.011	0.550	146
147	76	4.33		0.023	0.805	147
148	72	3.88	0.83	0.019	0.360	148
149	76	3.47	1.35	0.015	0.645	149
150	72	3.60	0.96	0.016	0.334	150
151	73	5.84	0.78	0.043	0.542	151
152	76	3.51	1.33	0.015	0.653	152
153	73	5.87	0.77	0.043	0.545	153
154	77	4.11	1.35	0.021	0.765	154
155	73	5.61	0.84	0.039	0.521	155
156	77	4.70	1.04	0.028	0.873	156
157	77	4.01	1.43	0.020	0.745	157
158	74	6.76	0.89	0.057	0.628	158
159	74	6.97	0.84	0.061	0.647	159
160	75	*	*	*	*	160
161	62	6.68	0.58	0.055	1.99	161
162	74	6.80	0.88	0.058	0.630	162
163	78	5.91	0.94	0.043	1.10	163
164	74	*	*	*	*	164
165	78	5.42	1.11	0.037	1.01	165
166	79	3.50	1.83	0.015	3.24	166

Drop no.	Configuration no.	Terminal velocity (fps)	C_D	W/C_DA	Reynolds no. $\times 10^5$	Drop no.
167	79	3.55	1.78	0.016	3.3	167
168	81	4.63	1.60	0.027	4.3	168
169	81	4.63	1.60	0.027	4.3	169
170	83	5.41	1.58	0.036	5.02	170
171	74	7.38	0.81	0.063	0.616	171
172	78	5.12	1.35	0.030	0.856	172
173	74	7.08	0.88	0.058	0.591	173
174	78	5.58	1.14	0.036	0.934	174
175	74	7.04	0.89	0.057	0.588	175
176	78	5.70	1.09	0.037	0.953	176
177	64	*	*	*	*	177
178	85	6.98	1.22	0.056	0.583	178
179	76	3.57	1.39	0.015	0.596	179
180	85	6.92	1.24	0.055	0.578	180
181	76	3.25	1.68	0.012	0.544	181
182	85	6.64	1.34	0.051	0.554	182
183	76	3.56	1.39	0.015	0.595	183
184	85	7.27	1.12	0.061	0.607	184
185	74	6.95	0.91	0.056	0.581	185
186	73	5.72	0.88	0.038	0.478	186
187	73	5.58	0.92	0.038	0.466	187
188	83	5.64	1.58	0.037	4.71	188
189	83	5.44	1.69	0.034	4.54	189

*No data.

SERIES 10 - VENTED HEXSYMMETRIC

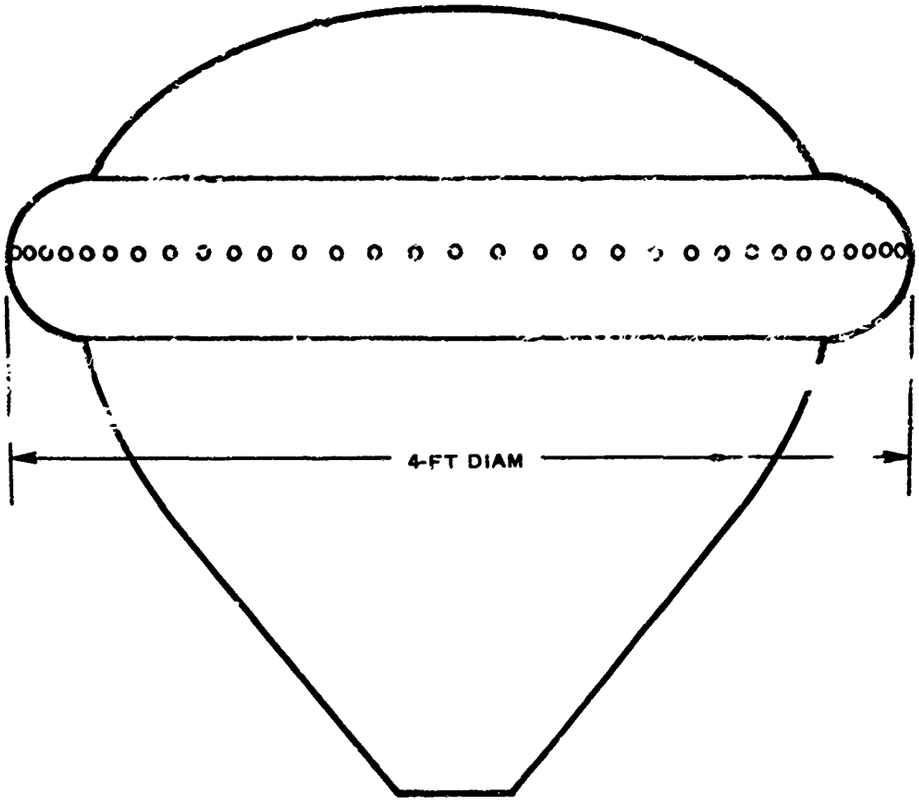

Configuration no.	Inlet diam (in.)	Gross weight (gm)	W/C_DA (mean)	Configuration no.
67	6	201	0.031	67
68	6	409	0.067	68
69	6	602.5	0.110	69
70	6	798.5	0.138	70

Drop no.	Configuration no.	Terminal velocity (fps)	C_D	W/C_DA	Reynolds no. $\times 10^5$	Drop no.
133	69	9.6	0.88	0.109	2.51	133
134	69	10.2	0.78	0.123	2.66	134
135	69	8.6	1.09	0.088	2.24	135

Drop no.	Configuration no.	Terminal velocity (fps)	C_D	W/C_DA	Reynolds no. $\times 10^5$	Drop no
136	69	9.7	0.86	0.112	2.53	136
137	69	9.4	0.92	0.104	2.46	137
138	69	10.2	0.78	0.123	2.64	138
139	70	10.8	0.92	0.138	2.92	139
140	70	10.8	0.92	0.138	2.82	140
141	67	5.0	1.08	0.030	1.31	141
142	67	5.1	1.03	0.031	1.33	142
143	68	7.4	1.00	0.065	1.93	143
144	68	7.6	0.95	0.068	1.98	144

APPENDIX A - DROP TEST DATA SHEETS

TEST NO. 1

Date	January 18, 1965	
Time	11:26	
Test item	Gross weight	1.76 lb
	BALLUTE type	Hexagonal burble fence
	BALLUTE diameter	4 ft
	Projected area	13.85 sq ft
	Comparable airdock configuration	No. 65
	Similar airdock configuration	No. 62 to 66
Test conditions	Release altitude	600 ft
	Mean wind velocity	8.1 mph
	Mean wind heading	200 deg
	Temperature	30 F
	Density	2.42×10^{-3}
	Pressure	28.6 in Hg
Test data	Descent time	70 sec
	Vertical distance	600 ft
	Descent rate	8.6 fps
	Range	1170 ft
	Horizontal rate	16.7 fps (11.4 mph)
Performance	Inflation	Rapid and complete
	Stability	No oscillation
	Wind following	No visible angle of attack
Calculated data	Dynamic pressure	0.09
Comparison	C_D airdock	0.95
	C_D Wingfoot Lake	1.4

TEST NO. 2

Date	January 18, 1965	
Time	12:50	
Test item	Gross weight	1.76 lb
	BALLUTE type	10 percent toroidal fence
	BALLUTE diameter	4 ft
	Projected area	11.50 sq ft
	Comparable airdock configuration	
	Similar airdock configuration	52 to 56
Test conditions	Release altitude	1170 ft
	Mean wind velocity	7.5 mph
	Mean wind heading	200 deg
	Temperature	30 F
	Density	2.4×10^{-5}
	Pressure	28.6 in Hg
Test data	Descent time	87 sec
	Vertical distance	1140 ft
	Descent rate	13.1 fps
	Range	1029 ft
	Horizontal rate	11.8 ips (8.1 mph)
Performance	Inflation	Rapid and complete
	Stability	No oscillations
	Wind following	No angle of attack
Calculated data	Dynamic pressure	0.207
Comparison	C_D airdock	0.7
	C_D Wingfoot Lake	0.74

TEST NO. 3

Date	January 18, 1965	
Time	13:12	
Test item	Gross weight	1.76 lb
	BALLUTE type	Partitioned with corner reflector
	BALLUTE diameter	5 ft
	Projected area	19.64 sq ft
	Comparable airdock configuration	29
	Similar airdock configuration	27 to 30
Test conditions	Release altitude	1400 ft
	Mean wind velocity	13 mph
	Mean wind heading	200 deg
	Temperature	31 F
	Density	2.41×10^{-3}
Test data	Descent time	150 sec
	Vertical distance	1400 ft
	Descent rate	9.34 fps
	Range	2013 ft
	Horizontal rate	9.1 mph
Performance	Inflation	Very rapid and complete
	Stability	Excellent
	Wind following	No angle of attack
Calculated data	Dynamic pressure	0.105
Comparison	C_D airdock	0.65
	C_D Wingfoot Lake	0.85

TEST NO. 4

Date	January 18, 1965	
Time	13:28	
Test item*	Gross weight	4.5 lb
	BALLUTE type	Hexagonal burble fence
	BALLUTE diameter	12.5 ft
	Projected area	135.3 sq ft
	Comparable airdock configuration	80
	Similar airdock configuration	79 to 84
Test conditions	Release altitude	1400 ft
	Mean wind velocity	10 mph
	Mean wind heading	200 deg
	Temperature	31 F
	Density	2.4×10^{-3}
Test data	Descent time	110 sec
	Vertical distance	1400 ft
	Descent rate	12.72 fps
	Range	2496 ft
	Horizontal rate	15.5 mph
Performance	Inflation	60 percent at impact
	Stability	Low frequency flagging
	Wind following	Lift due to sail effect
Calculated data	Dynamic pressure	0.195
Comparison	C_D	0.17 (partial inflation)

*See BALLUTE No. 2, Appendix III.

APPENDIX III - SUMMARY OF 12-1/2-FT-DIAMETER HEXSYMMETRIC BALLUTE CHARACTERISTICS

Characteristics of the 12-1/2-ft-diameter BALLUTEs tested are summarized in Table 3.

TABLE 3 - SUMMARY OF 12-1/2-FT-DIAMETER HEXSYMMETR

BALLUTE no.	Serial no.	Material		Seam type	Aluminization	Mer str
		Type	Gage (in.)			
1	HX-125-4-1	Polyamide	0.0004	1/8 in. band	None	None
2	HX-125-4-2	Polyamide	0.0004	1/8 in. band	None	None
3	HX-125-4-3	Polyamide	0.0004	1/8 in. band	None	None
4	HX-125-4-4	Polyamide	0.0004	1/8 in. band	None	None
5	HX-125-4-5	Polyamide	0.0004	1/8 in. band	None	None
6	HX-125-4A-1	Polyamide	0.0004	1/8 in. band	None	None
7	HX-125-5-1	Polyester	0.0005	Butt and tape	All gores	None
8	HX-125-4A-2	Polyamide	0.0004	1/8 in. band	None	None
9	HX-125-4A-3	Polyamide	0.0004	1/8 in. band	None	None
10	HX-125-4A-4	Polyamide	0.0004	1/8 in. band	None	None
11	HX-125-5A-1	Polyester	0.0005	Butt and tape	All gores	None
12	HX-125-5A-2	Polyester	0.0005	Butt and tape	All gores	None
13	HX-125-5A-3	Polyester	0.0005	Butt and tape	All gores	None
14	HX-125-5B-1	Polyester	0.0005	Butt and tape	Alternate gore pairs	0.08 in nylon ta
15	HX-125-5B-2	Polyester	0.0005	Butt and tape	Alternate gore pairs	0.08 in nylon ta
16	HX-125-5B-3	Polyester	0.0005	Butt and tape	Alternate gore pairs	0.08 in nylon ta

A

METER HEXSYMMETRIC BALLUTE CHARACTERISTICS

luminization	Meridian straps	Inlet springs	Swivel assembly	Weight (lb)	Test program
one	None	6	None	2.08	Airdock
one	None	6	None	2.08	Low altitude, Part 1
one	None	6	None	2.08	Low altitude, Part 2
one	None	6	None	2.08	Low altitude, Part 2
one	None	6	None	2.08	Low altitude, Part 2
one	None	6	None	2.11	Low altitude, Part 3
l gores	None	6	None	2.50	Low altitude, Part 3
ne	None	6	None	2.11	High-altitude drop test
ne	None	6	None	2.11	High-altitude drop test
ne	None	6	None	2.11	Rocket launched, Part 1
l gores	None	6	None	2.50	High-altitude drop test
l gores	None	6	None	2.50	High-altitude drop test
l gores	None	6	None	2.50	Rocket launched, Part 1
ternate gore irs	0.08 in. woven nylon tape	12	Figure 37	3.12	Rocket launched, Part 2
ternate gore irs	0.08 in. woven nylon tape	12	Figure 37	3.12	Rocket launched, Part 2
ternate gore irs	0.08 in. woven nylon tape	12	Figure 37	3.12	Rocket launched, Part 2

UNCL SSIFIED
Security Classification

DOCUMENT CONTROL DATA - R&D

(Security classification of title, body of abstract and indexing annotation must be entered when the overall report is classified)

1. ORIGINATING ACTIVITY (Corporate author) Goodyear Aerospace Corporation Akron, Ohio	2a. REPORT SECURITY CLASSIFICATION UNCLASSIFIED 2b. GROUP

3. REPORT TITLE
Development of BALLUTE for Retardation of Arcas rocketsondes

4. DESCRIPTIVE NOTES (Type of report and inclusive dates)
Final report Scientific Period covered: May 1964 to Dec 1965

5. AUTHOR(S) (Last name, first name, initial)
Graham, John J. Jr.

6. REPORT DATE 20 December 1965	7a. TOTAL NO. OF PAGES 129	7b. NO. OF REFS 1
8a. CONTRACT OR GRANT NO. AF19(628)-4194 b. PROJECT AND TASK NO. 6682-06 c. DOD ELEMENT 65402154 d. DOD SUBELEMENT 676682	9a. ORIGINATOR'S REPORT NUMBER(S) GER-12317 9b. OTHER REPORT NO(S) (Any other numbers that may be assigned this report) AFCRL-65-877	

10. AVAILABILITY/LIMITATION NOTICES Qualified requestors may obtain copies of this report from DDC. Other persons or organizations should apply to the Clearinghouse for Federal Scientific and Technical Information (CFSTI), Sills Building, 5285 Port Royal Road, Springfield, Virginia 22151.

11. SUPPLEMENTARY NOTES	12. SPONSORING MILITARY ACTIVITY Hq. AFCRL, OAR (CRE) United States Air Force L.G. Hanscom Field, Bedford, Mass.

13. ABSTRACT

Goodyear Aerospace Corporation has completed a design and development program for a BALLUTE[a] retardation system for Arcas rocket-launched meteorological instruments. Various BALLUTE configurations were fabricated, tested, and evaluated in four stages: airdock drop tests; low-altitude helicopter drop tests; high-altitude balloon-borne drop tests; and rocket-launched flight tests at Cape Kennedy. The program culminated in three successful rocket-launched flights of the final configuration which, because of the high stability of the system, yielded telemetered temperature data of unprecedented quality. The BALLUTE system that meets the design goals of reliability, stability, descent rate, and cost will be made of fractional mil plastic film, will be about 16-1/2 ft in diameter, and will weigh about two pounds. Further development and system qualification testing are recommended prior to incorporation of the BALLUTE into the operational sounding system.

[a] TM, Goodyear Aerospace Corporation, Akron, Ohio.

DD FORM 1 JAN 64 1473

UNCLASSIFIED
Security Classification

14. KEY WORDS	LINK A		LINK B		LINK C	
	ROLE	WT	ROLE	WT	ROLE	WT
BALLUTE (BALLoon-parachUTE)						
Arcas rocket						
Retardation device						
Parachute						
Deceleration						
Stabilization						
Recovery						
Rocketsonde						
Radiosonde						
Meteorology						
Meteorological sounding						
Meteorological instruments						

INSTRUCTIONS

1. ORIGINATING ACTIVITY: Enter the name and address of the contractor, subcontractor, grantee, Department of Defense activity or other organization *(corporate author)* issuing the report.

2a. REPORT SECURITY CLASSIFICATION: Enter the overall security classification of the report. Indicate whether "Restricted Data" is included. Marking is to be in accordance with appropriate security regulations.

2b. GROUP: Automatic downgrading is specified in DoD Directive 5200.10 and Armed Forces Industrial Manual. Enter the group number. Also, when applicable, show that optional markings have been used for Group 3 and Group 4 as authorized.

3. REPORT TITLE: Enter the complete report title in all capital letters. Titles in all cases should be unclassified. If a meaningful title cannot be selected without classification, show title classification in all capitals in parenthesis immediately following the title.

4. DESCRIPTIVE NOTES: If appropriate, enter the type of report, e.g., interim, progress, summary, annual, or final. Give the inclusive dates when a specific reporting period is covered.

5. AUTHOR(S): Enter the name(s) of author(s) as shown on or in the report. Enter last name, first name, middle initial. If military, show rank and branch of service. The name of the principal author is an absolute minimum requirement.

6. REPORT DATE: Enter the date of the report as day, month, year, or month, year. If more than one date appears on the report, use date of publication.

7a. TOTAL NUMBER OF PAGES: The total page count should follow normal pagination procedures, i.e., enter the number of pages containing information.

7b. NUMBER OF REFERENCES: Enter the total number of references cited in the report.

8a. CONTRACT OR GRANT NUMBER: If appropriate, enter the applicable number of the contract or grant under which the report was written.

8b, 8c, & 8d. PROJECT NUMBER: Enter the appropriate military department identification, such as project number, subproject number, system numbers, task number, etc.

9a. ORIGINATOR'S REPORT NUMBER(S): Enter the official report number by which the document will be identified and controlled by the originating activity. This number must be unique to this report.

9b. OTHER REPORT NUMBER(S): If the report has been assigned any other report numbers *(either by the originator or by the sponsor)*, also enter this number(s).

10. AVAILABILITY/LIMITATION NOTICES: Enter any limitations on further dissemination of the report, other than those imposed by security classification, using standard statements such as:

(1) "Qualified requesters may obtain copies of this report from DDC."

(2) "Foreign announcement and dissemination of this report by DDC is not authorized."

(3) "U. S. Government agencies may obtain copies of this report directly from DDC. Other qualified DDC users shall request through

_____."

(4) "U. S. military agencies may obtain copies of this report directly from DDC. Other qualified users shall request through

_____."

(5) "All distribution of this report is controlled. Qualified DDC users shall request through

_____."

If the report has been furnished to the Office of Technical Services, Department of Commerce, for sale to the public, indicate this fact and enter the price, if known.

11. SUPPLEMENTARY NOTES: Use for additional explanatory notes.

12. SPONSORING MILITARY ACTIVITY: Enter the name of the departmental project office or laboratory sponsoring *(paying for)* the research and development. Include address.

13. ABSTRACT: Enter an abstract giving a brief and factual summary of the document indicative of the report, even though it may also appear elsewhere in the body of the technical report. If additional space is required, a continuation sheet shall be attached.

It is highly desirable that the abstract of classified reports be unclassified. Each paragraph of the abstract shall end with an indication of the military security classification of the information in the paragraph, represented as *(TS), (S), (C), or (U).*

There is no limitation on the length of the abstract. However, the suggested length is from 150 to 225 words.

14. KEY WORDS: Key words are technically meaningful terms or short phrases that characterize a report and may be used as index entries for cataloging the report. Key words must be selected so that no security classification is required. Identifiers, such as equipment model designation, trade name, military project code name, geographic location, may be used as key words but will be followed by an indication of technical context. The assignment of links, rules, and weights is optional.